Characterization of Ventral Mesencephalic neuron enriched culture in vitro: Correlation to Parkinson's disease

A thesis submitted for the degree of

Doctor of Philosophy

By

V Satish Bollimpelli

Department of Biotechnology and Bioinformatics
School of Life Sciences
University of Hyderabad
Hyderabad-46, Telangana, INDIA

August, 2015

Enrolment Number: **09LTPH14**

University of Hyderabad
School of Life Sciences
Department of Biotechnology & Bioinformatics
Hyderabad- 500046, (Telangana), India

DECLARATION

I, **V Satish Bollimpelli**, hereby declare that this thesis entitled "**Characterization of Ventral Mesencephalic neuron enriched culture in vitro: Correlation to Parkinson's disease**." Submitted by me under the guidance and supervision of **Prof. Anand K. Kondapi** is a bonafide research work which is also free from plagiarism. I also declare that it has not been submitted previously in part or in full to this University or any other University or Institution for the award of any degree or diploma. I hereby agree that my thesis can be deposited in Shodganga/INFLIBNET.

A report on plagiarism statistics from the University Librarian is enclosed.

Date:

Name : V Satish Bollimpelli

Signature of the student :

Regd. No : 09LTPH14

Signature of the Supervisor:

University of Hyderabad
School of Life Sciences
Department of Biotechnology & Bioinformatics
Hyderabad- 500046, (Telangana), India

CERTIFICATE

This is to certify that thesis entitled "**Characterization of Ventral Mesencephalic neuron enriched culture in vitro: Correlation to Parkinson's disease"** submitted by **Mr. V Satish Bollimpelli** bearing Regd. No **09LTPH14** in partial fulfillment of the requirements for the award of Doctor of Philosophy in **Biotechnology** is a bonafide work carried out by him under my supervision and guidance which is a plagiarism free thesis.

The thesis has not been submitted previously in part or in full to this or any other University or Institution for the award of any degree or diploma.

Prof. Anand K. Kondapi
Supervisor

Head, Department of Biotechnology and Bioinformatics

Dean, School of Life Sciences

ACKNOWLEDGEMENTS

Firstly, I would like to express my sincere gratitude and respect to my supervisor, Prof. Anand K Kondapi for his continuous support, motivation and freedom he has given me during my research. His advices on both research as well as on my career have been priceless.

I thank the former and present Dean, SLS, & former and present Heads of the Department of Biotechnology for allowing me to use the general and department facilities.

I thank my Doctoral committee members, Dr. M Venkataramana and Dr. N Prakash Prabhu for their valuable advices.

I thank the entire faculty of SLS for the help and guidance during this research tenure.

A special mention of my seniors- Dr. Bhaskar & family, Dr Anil & family Dr.Kishore & family and Dr.Upendhar for their indelible love and warmth.

I would also like to extend this special mention to my room-mate Siva for his constant support and love which made my stay memorable.

I thank all my lab mates- Dr. Kannapiran, Dr. Uday, Dr. Preethi, Dr Balakrishna, Srinivas, Sarada, Farhan, Hari, Sonali, Lakshmi, Kiran, Akhila and Prachi for creating a friendly atmosphere in the lab.

I thank my labmate Mr Prashanth for his timely support whenever I needed something in lab.

I thank my labmates Kurumurthy, Jagadeesh, Prashanth and Pankaz for their cheerful nature which made my days in lab very enjoyable & memorable.

I must thank the lab attenders- Srinivas (paper work), Bhanu & Chandra Mohan (for taking care of animal room).

I wish to thank Ms. Nalini for her amicable assistance in confocal microscopy; Mr. Srinivas Murthy for help in paper work.

I sincerely thank CSIR for the fellowship. I thank the funding bodies, DBT and DST for funding my work through periodic grants. The infrastructure developed under various programs including UGC-UPE, X plan, CREBB and DST-FIST is duly acknowledged.

I am extremely fortunate to have a very sweet family. Rather than saying thanks I would like to share this achievement and happiness with them. My family- Parents: Mr Prabhakara Rao & Mrs Annapurna; Brother: Suresh; Wife: Devi; and My greatest Love: My grand ma.

Last but not the least; I thank THE GOD almighty for guiding me all through and for his generous blessings.

- *Satish*

Index

Abbreviations

AD	: Alzheimer's disease
AFM	: Atomic force microscopy
ALS	: Amyotrophic lateral sclerosis
ANOVA	: Analysis of Variance
Apo E2/3	: Apolipoprotein isoforms 2 and 3
APP	: Amyloid precursor protein
Ara C	: Cytosine Arabinoside
BSA	: Bovine serum albumin
CAG	: Cytosine Adenine Guanine
cDNA	: complementary DNA
CMH2DCFDA	: Chloro methyl derivative of 2,7 dichlorodihydrofluorescein
DA	: Dopamine
DAPI	: 4',6-diamidino-2-phenylindole
DIV	: Day in vitro
DJ-1	: Protein deglycase
DLS	: Dynamic light scattering
DMEM F-12	: Dulbecco's modified eagle medium/nutrient mixture F-12
DMSO	: Di methyl sulfoxide

DNA	:	Deoxy ribo nucleic acid
EDTA	:	Ethylene diamine tetraacetic acid
FBS	:	Fetal bovine serum
FE-SEM	:	Field emission scanning electron microscope
HBSS	:	Hanks balanced salt solution
HD	:	Huntington's disease
HEPES	:	4-(2-hydroxyethyl)-1-piperazineethanesulfonic acid
HPLC	:	High performance liquid chromatography
HRP	:	Horse radish peroxidase
LRRK2	:	Leucine rich repeat kinase 2
LDH	:	Lactate de hydrogenase
MAO-B	:	Mono amine oxidase-B
MAP-2	:	Microtubule associated protein-2
MPTP	:	1-methyl-4-phenyl-1,2,3,6-tetrahydropyridine
MTT	:	3(4,5-dimethylthiazol-2-yl)2,5diphenyltetrazolium bromide
NADH	:	Dihydronicotinamide adenine dinucleotide
NMDA	:	N-Methyl-D-Aspartate
NTC	:	No Template Control
OD	:	Optical density
6-OHDA	:	6 hydroxy dopamine

PAGE	:	Poly acrylamide gel electrophoresis
PBS	:	Phosphate buffered saline
PD	:	Parkinson's disease
PDI	:	Poly dispersity index
PDL	:	Poly D Lysine
PEG	:	Poly ethylene glycol
PINK1	:	PTEN induced putative kinase 1
PS1,2	:	Presenilins 1 and 2
PVDF	:	Poly vinylidene fluoride
q-RT PCR	:	Quantitative real time polymerase chain reaction
RIPA	:	Radio immuno precipitation assay
RNA	:	Ribo nucleic acid
ROS	:	Reactive oxygen species
SCA	:	Spinocerebellar ataxia
SNPc	:	Substantia nigra pars compacta
SOD1	:	Superoxide dismutase 1
TBST	:	Tris-buffered saline and tween 20
TH	:	Tyrosine hydroxylase
UCHL1	:	Ubiquitin c-terminal hydrolase
VM	:	Ventral mesencephalon

Chapter-1
Introduction

Aging

Aging, in its broadest sense reflects all the changes that take place over a period of life. These irreversible and deleterious changes effect normal physiological functions and eventually lead to death. These changes manifest from molecular to cellular and to organismic level. Few common characteristics that were reported with mammalian aging are biochemical changes in tissues/organs, increased vulnerability to disease and increased mortality (Troen 2003). The diseases that are seen with increasing frequency with aging are known as aging associated diseases. They are different from aging process itself, as not all aged people experience all age associated disorders. They differ from person to person due to genetic and environmental factors. The process of aging affects organs and tissues with both high proliferation and quiescence. This include reduction in muscle mass (Sarcopenia), loss of bone mass (Osteoporosis), diminished musculoskeletal mobility, anaemia in haematopoietic system, cardiovascular diseases and altered immune system resulting in diseases like rheumatoid arthritis (Sahin and Depinho 2010). Convergence of aging and cancer biology was also reported (Finkel, Serrano et al. 2007). Although many theories of aging were proposed, none of them were successful due to complex multifactorial nature of aging. Few of the important causes behind aging were found to be DNA

damage, reduction in telomere length, increase in ROS levels, Protein damage, accumulation of insoluble mis-folded protein aggregates etc. (Holliday 2004).

Brain Aging

Brain is no exception to this complex phenomenon of aging. During this process, brain undergoes many structural, chemical and functional changes. Structural changes include region specific reduction of cerebral volume (Raz, Lindenberger et al. 2005). Signals are transmitted in brain through chemical messengers called neurotransmitters and they include dopamine, glutamate, serotonin, acetyl choline etc. Synthesis, binding sites and receptors of these neurotransmitters undergo changes during aging. (Mobbs and Hof 2009; Yamamoto, Suhara et al. 2002; Kaiser, Schuff et al. 2005). Memory function that are associated with medial temporal lobe and frontal lobes were known to be affected by age related process (Hof and Morrison 2004; Craik and Salthouse 2000). It was also reported that inflammation in hypothalamus of brain releases systemic age related hormones (Zhang, Li et al. 2013). The above mentioned changes are not pathological and considered to be part of healthy aging. Aging associated brain diseases comes into the picture when brain cells (glial and neuron) fail to respond adaptively to increases in metabolic, ionic and oxidative stresses and thereby leading to accumulation of damaged DNA, protein and membranes (Mattson and Magnus 2006). The size and location of these cells, disease specific protein metabolism, stress resistant mechanisms and signal transduction pathways determine the neuronal

vulnerability. In aging, neuronal death may be activated by some gene specific mutations and/or environmental factors such as dietary elements and toxicants. The nervous system may adapt to these changes or succumb to them leading to neuronal death.

Fig 1.1: Factors leading to neuronal death in aging (Mattson and Magnus 2006)

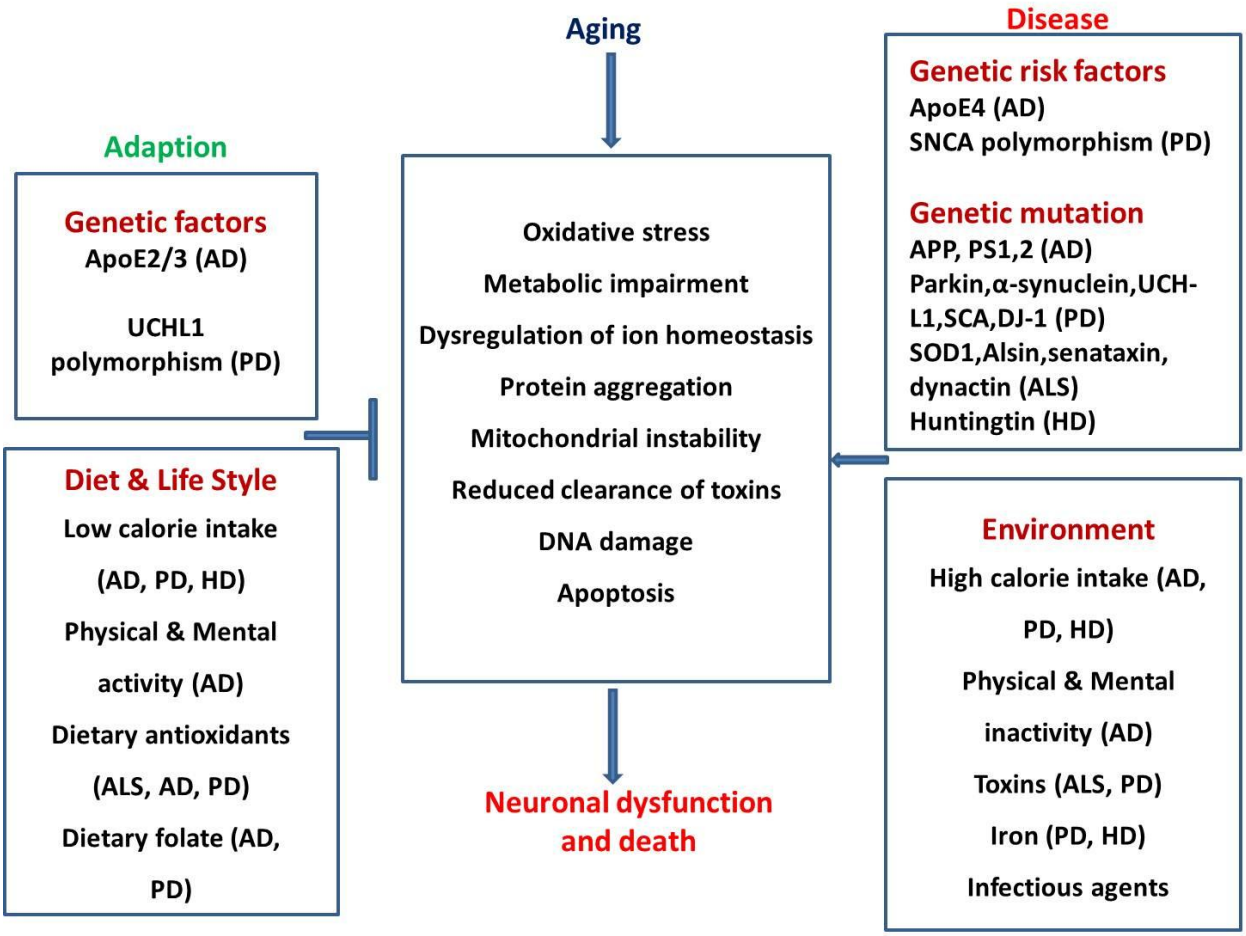

Neurodegenerative Diseases

Neurodegenerative diseases are a diverse group of disorders marked by progressive degeneration of structure and/or function of specific neurons in central nervous system or peripheral nervous system. They share a common predisposing factor i.e aging of brain. There is a high probability of developing neurodegenerative diseases like Alzheimer's disease (AD), Parkinson's disease (PD), Huntington's disease (HD) and amyotrophic lateral sclerosis (ALS) after sixth decade of life. These diseases affect different regions of the brain. They start in specific areas of brain and later other regions also get affected. Even within these regions, injury of selective neuronal classes can be observed.

Fig 1.2: Neurodegenerative diseases and the specific regions in brain they affect.

(Mattson and Magnus 2006)

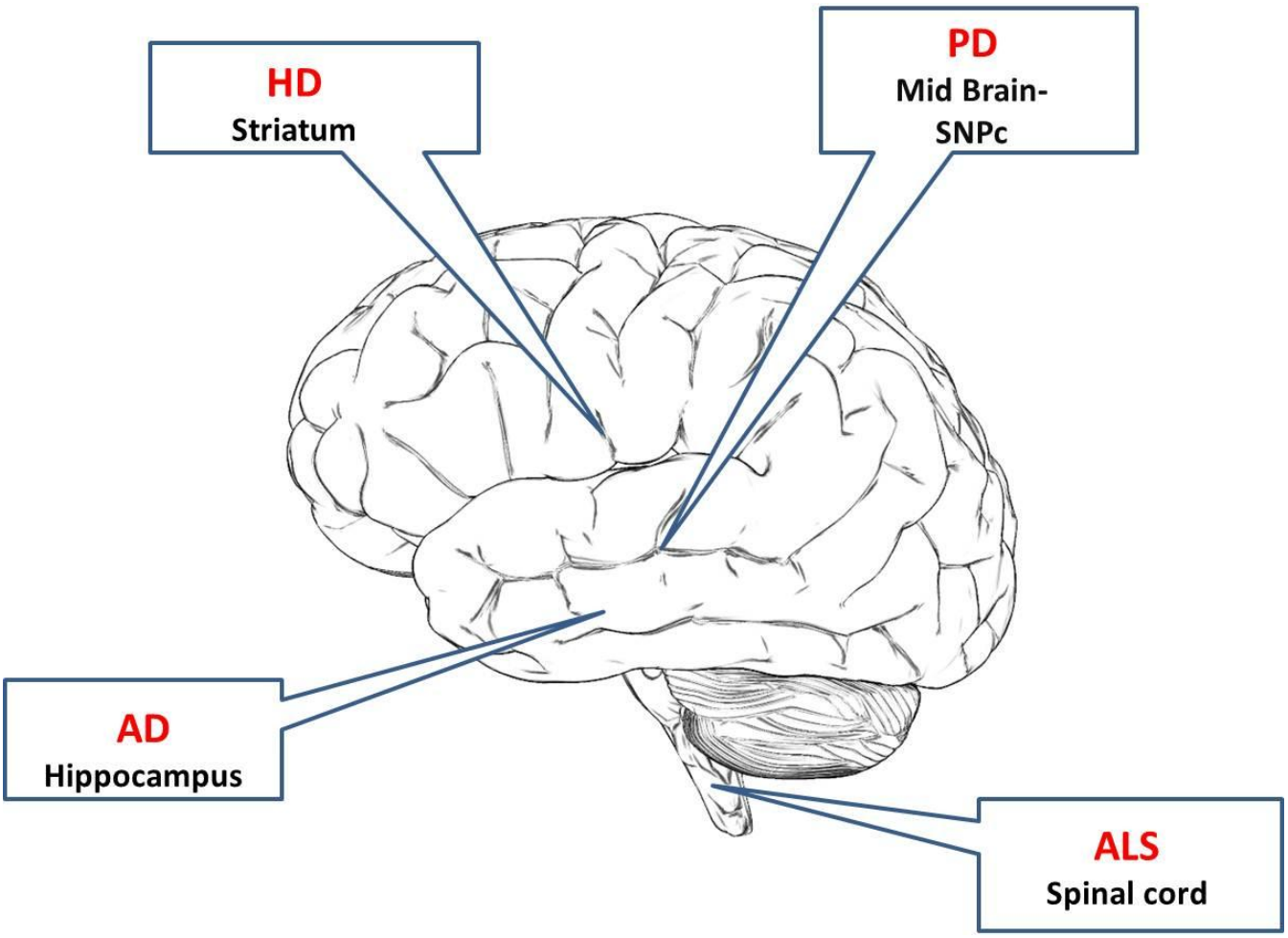

AD

AD is characterized by dementia that begins with poor memory and gradually advances leading to incapacitation. It is often accompanied by delirium. The pathological hallmarks of AD are neuritic plaques resulted by accumulation of amyloid beta peptide and neurofibrillary tangles due to hyper phosphorylation of microtubule associated Tau protein in neuronal cells (De-Paula, Radanovic et al. 2012). The etiology of AD is still unclear. It is of both familial and sporadic forms. The current treatment strategies being employed are inhibiting acetylcholinesterase, using antagonists of NMDA receptors and antidepressants to deal with associated depression.

HD

HD is a rare neurodegenerative disorder characterized by motor, cognitive and psychiatric disturbances. It is also associated with unwanted choreatic movements. The average age of onset of symptoms is 30 to 50 years (Roos 2010). The hallmark feature of HD is elongated stretch of 36 or more CAG tri nucleotide repeats on Huntington gene in the short arm of chromosome 4p16.3. The longer the CAG trinucleotide repeats, the early will be the onset of disease. As of now there is no cure. However, symptoms can be treated by dopamine receptor blocking and depleting

agents. The most common cause of death in these cases is due to pneumonia, followed by suicide (Roos 2010).

ALS

ALS also known as Charcot disease is characterized by muscle atrophy resulting in difficulty in speaking, swallowing and eventually breathing (Rowland and Shneider 2001). The main cause of this neurodegenerative disorder is motor neuronal death. However, the mechanisms responsible for this loss of motor neurons still remain elusive (Lunn, Sakowski et al. 2014). It is present in both familial and sporadic form. The onset of this disease is usually at the age of 60's and in case of familial form it is around 50's (Kiernan, Vucic et al. 2011). Although there is no cure, Riluzole remains the only evidence based drug for this disease (Miller, Mitchell et al. 2012).

PD

PD is a progressive neurodegenerative disease characterized by movement disorder that results mainly because of dopaminergic (DA) neuronal death in substantia nigra pars compacta (SNPc) region of mid brain (Lang and Lozano 1998). Symptoms associated with this disease are bradykinesia, rigidity, resting tremor and postural instability. The pathological hallmarks are proteinaceous aggregates termed as lewy bodies and dystrophic neurites of surviving neurons (Forno 1996). PD is both sporadic and familial in nature, while its specific etiology is still elusive. Both forms of

PD tend to share important feature like parkinsonism with nigrostriatal DA degeneration (Hardy, Cookson et al. 2003). DA neurons in SNPc secrete neurotransmitter DA and death of these neurons leads to dearth of DA in nigrostriatal pathway culminating in PD.

Oxidative stress, mitochondrial dysfunction and misfolded protein aggregation play a key role in pathogenesis of PD (Moore, West et al. 2005). Post mortem studies of PD patient's brains showed a significant amount of oxidative damage to DNA, Proteins and lipids (Jenner 2003). It is believed that this oxidative stress might have compromised the integrity of vulnerable DA neurons. Reports also suggest mitochondrial complex-I dysfunction in PD patients (Schapira, Cooper et al. 1990).

Fig 1.3: Common pathways underlying PD pathogenesis integrating mitochondria and ubiquitin proteasome system (Moore, West et al. 2005)

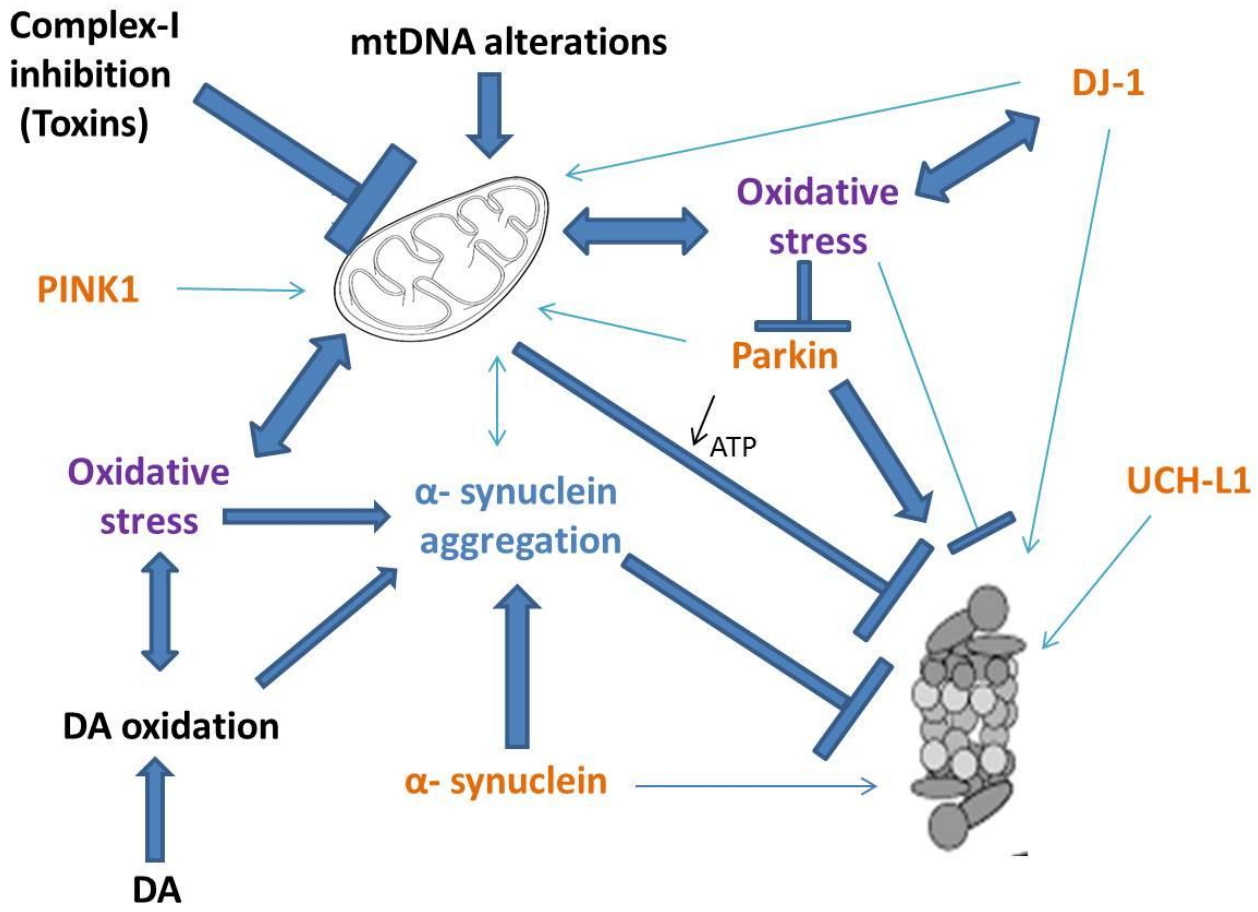

Despite of this knowledge regarding pathology of PD, its etiology still remains unknown.

PD models

The major impediment for developing neuroprotective therapies against PD is limited understanding on key molecular processes that initiate neurodegeneration. Both *in-vitro* and *in-vivo* models have been instrumental in unraveling the molecular cascade of cell death in DA neurons. Predominantly PD models are neurotoxin based models while others being models based on manipulation of PD genes like LRRK2, Parkin, DJ-1, PINK1 and α-synuclein (Dawson, Ko et al. 2010). Among the neurotoxins used to induce DA neurodegeneration, MPTP, 6-OHDA, paraquat and more recently rotenone have received the most attention. Animal models simulate disease conditions better than cellular models. However, cellular models are of more use in dissecting a complex and multifactorial processes in a disease like PD into simpler events. The classical *in-vitro* models are correct choice for preliminary studies on molecular roles of new drugs, toxins and single genetic factors. They may be far form replicating complexity of PD but can provide valuable insights for validation in animal models and/or in human specimens. Studies in cellular models can be based on targeting molecular/biochemical events or on unbiased transcriptomic or proteomic analysis (Alberio, Lopiano et al. 2012). Cellular models may be categorized into cell line model, stem cell model or primary cell culture model. We have used both primary cell culture model and cell line model for our studies.

PD treatment

At present there is no cure for PD. However, medications against symptoms may provide some relief. The treatment varies depending on state of disease. The main family of drugs that are being currently used for treating motor symptoms in PD are Levodopa, dopamine agonists (both ergot and non-ergot types), MAO-B inhibitors, NMDA receptor inhibitors and anti-cholinergics (Gazewood, Richards et al. 2013). Important unwanted aspects in PD medical therapy are behavioral problems like psychosis, hallucinations and impulse control problems. Most importantly these drugs do not exhibit neuroprotective effects.

Curcumin

Curcumin is isolated from the roots of turmeric (*curcuma longa*). It's a polyphenol and active ingredient of turmeric (Joe, Vijaykumar et al. 2004). Curcumin had been reported to have neuroprotective role in various models of AD (Yang, Lim et al. 2005). Curcumin mediated neuroprotection in various models of PD was also reported (Zbarsky, Datla et al. 2005; Rajeswari 2006; Wang, Du et al. 2009). Curcumin can target multiple pathways and could be of great therapeutic potential against PD.

Fig 1.4: Curcumin probable targets during neuroprotection in PD

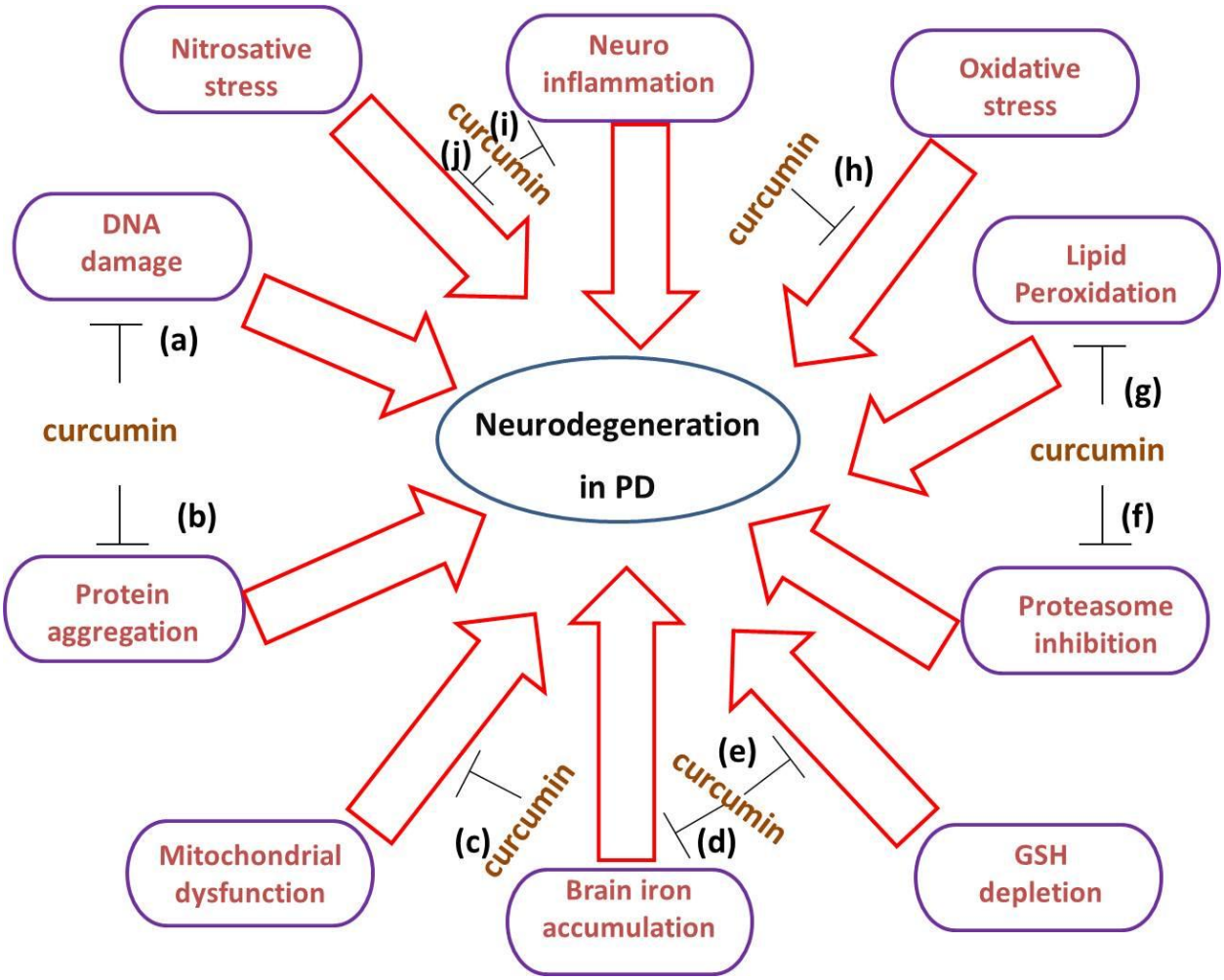

(a) Hegde, Hegde et al. 2010; (b) Pandey, Strider et al. 2008; (c) Mythri, Harish et al. 2011; (d) Jiao, Wilkinson et al. 2009; (e) Dale and Russell 1956; (f) Ali and Rattan 2006; (g) Zhu, Chen et al. 2004; (h) Jagatha, Mythri et al. 2008; (i) Thaloor, Miller et al. 1999; (j) Mythri, Harish et al. 2011.

Nanotechnology approach in PD treatment

Nanotechnology is the science that deals with design, synthesis and characterization of materials on a nano scale with certain functional organization. These nanoparticles are aimed at biological molecular interactions in cells and tissues. The blood brain barrier protects and isolates central nervous system from rest of the body creating a unique biochemical and immunological environment. This barrier obstructs entry of not only the pathogens but also drugs into the brain. For a drug to cross this blood brain barrier and target a specific group of cells in brain, it needs to be engineered to make things happen together.

Several nano technology approaches have been developed to date to address different aspects of complex PD etiology. For example, PEGylated immunoliposomes were used as gene therapy carrier for delivery of Tyrosine hydroxylase (TH) expressing plasmids in a murine model of PD disease (Zhang, Calon et al. 2003). Delivery of neurotrophic factor expressing plasmid mediated by polyplexes was also successfully tested in a rat PD model (Gonzalez-Barrios, Lindahl et al. 2006). Since the relationship between onset of PD and oxidative stress was well established antioxidant nanoparticles are being increasingly tested to scavenge ROS. For example the ability of polyhydroxylated fullerenes to scavenge ROS was successfully tested in a PD cellular model (Cai, Jia et al. 2008).

Rationale

PD is a progressive neurodegenerative movement disorder that is associated with aging and characterized by DA neuronal death in SNPc region of Ventral Mesencephalon (VM) (Lang and Lozano 1998). Due to its complex pathophysiology and multifactorial nature, etiology of PD still remains elusive. Both *in-vitro* and *in-vivo* models of PD are being used to address different aspects of PD. We have chosen *in-vitro* cellular model comprising of rat primary VM neurons to deal with rotenone induced neurotoxicity in PD. Rotenone is a flavonoid, usually present in pesticides and one of the environmental factors that induces PD like features both *in-vitro* and *in-vivo* (Betarbet, Sherer et al. 2000; Chaves, Melo et al. 2010). VM cells comprise of both post-mitotic neuronal cells and mitotic glial cells. These glial cell were reported to have both neuroprotective and neuodegenerative activities (Rappold and Tieu 2010). In order to avoid this ambivalence nature of glial cells in our studies, we have established VM neuron enriched culture devoid of glial cells. Adult neurogenesis was reported in aging population suggesting the presence of both immature and mature neurons in aging brain (Tatsunori, Kazunobu et al., 2011). As PD occur at higher frequency during aging it would be interesting to see the effect of rotenone in both immature and mature neurons. Hence, we have characterized the VM neuron enriched culture in terms of maturity, which can also be used for further studies on VM neuronal development. Since PD is known to have complex pathophysiology,

whole transcriptome analysis was done to identify novel genes that are regulated in rotenone induced PD.

Most of the current approaches in PD treatment are aimed at restoring DA levels, which provide only symptomatic relief but not neuroprotection. Therefore we have chosen curcumin, which has antioxidant, anti-inflammatory properties and so can be of great therapeutic value in offering neuroprotection in PD. The receptors of lactoferrin play a role in iron uptake by cells and earlier it was reported that expression of lactoferrin receptors increased in mesencephalon of patients with PD (Faucheux, Nillesse et al. 1995). Adding to this, transcytosis of lactoferrin through blood brain barrier by receptor mediated endocytosis was also reported (Fillebeen, Descamps et al. 1999). We have hypothesized that encapsulation of curcumin with this lactoferrin protein provides the target specificity alongside with general advantages of nanoparticles like optimum size for cellular uptake and improved intracellular localization.

Objectives:

Based on the above observations, the following objectives were framed.

a). Establishment of enriched rat primary VM neurons as an in *vitro* culture model.

b). Investigating rotenone induced neurotoxicity in cellular models of VM neurons and SK-N-SH cell line.

c). Evaluating neuroprotective effect of curcumin-loaded lactoferrin nano particles against rotenone induced neurotoxicity.

Chapter-2

Materials & Methods

2.1 Materials:

All chemicals are from Sigma unless specified.

2.1.1 Animals

Pregnant female Wistar rats were procured from National Institute of Nutrition, Hyderabad, India and maintained at the animal house facility according to norms of Institutional animal ethical committee (IAEC), University of Hyderabad. (Proposal number LS/IAEC/AKK/10/1).

2.1.2 Cell line

SK-N-SH, a neuroblastoma cell line was procured from National Center for Cell Science (NCCS), Pune, India.

2.1.3 Primary antibodies

Mouse anti-rat MAP-2 monoclonal antibody (IF 1: 500) (ab11267), Rabbit anti-rat Nestin polyclonal antibody (Immunofluorescence (IF 1: 200) (ab27952), Mouse anti-rat α synuclein monoclonal antibody (ab78155) was obtained from Abcam, MA, USA; Mouse anti-Topoisomerase IIβ monoclonal antibody (IF 1: 1000, WB 1: 1000) (611493) was from Becton Dickinson biosciences, NJ, USA. Rabbit anti-rat Tyrosine Hydroxylase polyclonal antibody (IF 1:1000, WB 1: 1000) (OPA1-04050) was from Thermo Scientific.

2.1.4 Secondary antibodies

Goat anti-rabbit HRP conjugated antibody (1: 5000) (ab6721), goat anti-mouse HRP conjugated antibody (1: 5000) (ab97023) were obtained from Abcam, USA; Alexa Fluor 594 goat anti-rabbit antibody (A11037), Alexa Fluor 488, goat anti-mouse antibody (A11029) were from Invitrogen, NY, USA. alexa fluor antibodies were used at 1: 200 dilutions.

2.2 Methodology:

2.2.1 Isolation and culture of VM neurons

The preparation of VM neurons was based on a previously described method (Roger and Alan 2000). Anesthetized pregnant Wistar rats (E14) were decapitated and embryonic pups were removed aseptically by a 'C' section. SNc tissue from embryonic mesencephalon was collected and washed with Hank's Balanced Salt Solution (HBSS) at 4^0C and incubated in 2ml of pre-warmed 2.5mg/ml trypsin solution (Gibco, NY, USA) for 15 min at room temperature. After trypsinization, the tissue was resuspended in 2 ml of pre warmed DNAse (10µg/ml) and the solution was centrifuged at 1200g for 4 min. Then Supernatant was removed and the tissue was triturated with 0.1- 0.2ml triturating solution (1mg/ml BSA, 10µg/ml DNAse 1, 0.5 mg/ml soybean trypsin inhibitor in HBSS / piece of VM tissue). The suspension was placed on ice and triturated using a fire-polished glass pipette with minimal

number of strokes to obtain a suspension of single cells. Three pipettes of decreasing tip diameters were used and the entire suspension was passed through each pipette tip 2-4 times and triturated slowly without any air bubbles. VM neurons were plated in the presence of Dulbecco's Modified Eagle Medium/Nutreint mixture F-12 (DMEM F-12) containing 10% fetal bovine serum, (Gibco, NY, USA). Cultures were incubated in a humidified atmosphere of 5% CO_2 at 37°C. 1 x 10^6 cells were seeded in 1ml of medium per well in a 12 well plate coated with 0.1mg/ml Poly-D- Lysine (PDL) (Sigma chemical co, MO, USA). For other culture dishes, cells were seeded proportionally. Cultures were maintained by replacing half the volume of medium every alternate day. 2μM arabinosylcytosine (Ara C, mitotic inhibitor) (Sigma chemical co, MO, USA) was added to cultures from second day of culture to suppress the proliferation of mitotic non neuronal cells and replenished every alternate day. In rotenone and curcumin treated cultures, the compounds were dissolved in culture grade DMSO (Sigma chemical co, MO, USA). Rotenone was added to the cultures in a single shot at specified concentrations and at specified time points and treated for 48 hrs.

2.2.2 SK-N-SH Cell culture

Neuroblastoma cell line SK-N-SH was procured from National Center for Cell Science, Pune, India. Cells were cultured in DMEM medium supplemented with 2mM glutamine (Gibco, NY, USA), Pen strep antibiotic (1X) (50 units/ml pencillin,

50ug/ml streptomycin) (Gibco, NY, USA) and 10% heat-inactivated fetal bovine serum (Gibco, NY, USA). Culture was maintained at 37ºC, 5% CO2 and 95% humidity. Medium was changed after every 3 days. For all experiments, soluble curcumin (sol curcumin), nano curcumin and rotenone were freshly prepared in DMSO.

2.2.3 Cell viability assays

2.2.3.1 MTT assay

In vitro neuronal cell viability was quantified by measuring reduction of MTT (3-(4,5-dimethylthiazol-2-yl)-2,5-diphenyltetrazolium bromide) (Sigma chemical Co, MO, USA) to purple insoluble formazan crystals by the mitochondrial dehydrogenases of live cells. Briefly, neurons were seeded in PDL coated 96 well plates in triplicate at a density of 0.1 x 10^6 cells per well in 200 µl of complete medium. On the day of assay, 20 µl of MTT (5 mg/ml) was added to each well and incubated for 4h at 37 °C in 5% humidified CO_2 atmosphere. The plates were then centrifuged at 1500 rpm for 20 min at room temperature and the medium was carefully aspirated. DMSO was added to dissolve the formazan crystals and absorbance was then measured at 570 nm using a Tecan multilabel reader- INFINITE 200 PRO (Tecan, Mannedorf, Switzerland) with DMSO as blank. Neuronal cell viability was derived from optical density (OD) of the formazan crystals and expressed as percent viable cells in the treated cultures

compared to the respective negative controls (control was considered to be of 100% viability).

2.2.3.2 Trypan blue exclusion assay

Number of viable neuronal cells was quantified by trypan blue dye exclusion principle of viable cells. VM neurons were seeded in PDL coated 24 well plates in triplicates at a density of 0.5 x 10^6 cells per well in 500 µl of complete medium. On the day of assay, 500 µl of 1X trypsin (Gibco, NY, USA) was added to each well and incubated for 5min (until all the cells got into suspension) at room temperature. Cell suspensions from each well were collected individually and were centrifuged at 1200 rpm for 5min at 4ºC. Each of those cell pellets were suspended in 0.2ml of HBSS and 10µl of each of these cell suspensions were added to 10µl of 0.4% trypan blue solution (w/v) (Sigma chemical co, MO, USA) making a dilution factor of 2. The cell suspension was immediately loaded on to a hemocytometer and the number of viable cells was counted.

2.2.3.3 Lactate dehydrogenase release assay

Activity of lactate dehydrogenase (LDH) released into the medium was quantified based on the principle of pyruvate reduction to lactate, mediated by β-NADH. After treatment with rotenone over a range of concentrations, 50 µl of medium from each sample was added to 0.15 mg/ml β-NADH solution separately in a 96 well plate at

room temperature. To these wells, 22.7mM of pyruvate was added to initiate the reaction. Oxidation of NADH to NAD+ was measured by recording the absorbance at 570 nm using a Tecan multilabel reader- INFINITE 200 PRO (Tecan, Mannedorf, Switzerland). The change in LDH release was calculated by subtracting control from the treated sample. Taking the untreated cells as controls LDH values were calculated based on activity of standard solution of LDH 500U/L.

2.2.4 Immunofluorescence

Adherent VM cultures grown on PDL coated cover slips were washed with phosphate buffered saline containing 4% sucrose (PBS+sucrose). SK-N-SH cells, at a seeding density of $0.6X10^6$ cells per coverslip were cultured. The cultures were fixed with 4% paraformaldehyde and permeabilized with 0.05% triton X-100. These were washed thrice with PBS+Sucrose and blocked with 5% FBS in PBS+sucrose for 1hr at 37°C. The fixed cultures were incubated overnight with primary antibody at specified dilutions mentioned above at 4°C. The following day, cells were washed thrice with PBS+surcorse and secondary antibody at specified dilutions was added with a nuclear dye, DAPI (1μg/ml) (Sigma chemical co, MO, USA) and incubated for 1 hr at 37°C. These cover slips were washed thrice and mounted onto glass slides with 50% glycerol and were imaged with confocal microscope.

2.2.5 Western blot analysis

Cells were scraped at indicated time points and lysed with RIPA buffer. Cellular protein extract was separated on 10% SDS PAGE and transferred to PVDF membranes (Amersham). This membrane was blocked in TBST with 5% BSA and incubated overnight at 4°C with respective primary antibodies. This is followed by 1 hr incubation at room temperature with respective secondary antibodies conjugated with HRP. Proteins were detected using enhanced chemiluminescence substrate (Pierce). The visualized bands were quantified by densitometric analysis using image J software.

2.2.6 Alkaline Comet assay

The assay was done as described earlier (Singh, McCoy et al. 1988). 500 µl of ice-cold PBS with 0.1 million cells was added to 1.5 ml of 0.75% Low melting agarose (BRL inc, MD, USA). The agarose-cell suspension was gently layered on a 0.75% agarose precoated frosted-glass microscopic slide. After solidification of gel on ice, it was transferred to ice-cold lysis buffer (2.5M NaCl, 100mM EDTA, 10mMTris (pH 10.0) and 1% Triton X-100) and incubated for 2hrs at 4°C. Then they were equilibrated for 1hr in electrophoresis buffer (300mM NaOH and 1mM EDTA, pH 13) followed by electrophoresis (1hr, 1V/cm). After neutralization of these slides with 0.4M Tris, pH 7.5, they were placed in 100% ethanol for 5min and then air-dried. The DNA was then stained with 20µg/ml of ethidium bromide (Sigma Chemical Co., MO, USA) for 20 min and slides were washed twice for 5 min in TBE. To ensure random sampling,

50 images/slide were captured using confocal microscope (Lieca, IL, USA). Comet parameters like tail length and tail moment were scored using CometScoreTM Freeware v1.5 (TriTek Corporation, Sumerduck, VA, US).

2.2.7 Detection of intracellular ROS accumulation

Intracellular ROS accumulation was monitored by incubating cells with 7μM chloro methyl derivative of 2',7'-dichlorodihydrofluorescein diacetate (CMH2DCFDA) (Invitrogen, NY, USA) for 20 min. Cells were rinsed twice with HEPES buffer and fluorescence was measured using Tecan multilabel reader- INFINITE 200 PRO (Tecan, Mannedorf, Switzerland) at excitation and emission wavelengths of 485 nm and 535 nm, respectively. The final values were normalized for intracellular protein in each well and expressed in terms of fluorescence/μg protein. Protein concentration was measured using Bradford's reagent.

2.2.8 Caspase-3 activity assay

Caspase-3 activity was measured through cleavage of a colorless substrate specific for caspase-3 (AC-DEVD-AMC) releasing the chromophore, (AMC) 7- amino-methylcoumarin. Assaying was carried out in accordance with manufacturer's instructions (Caspase 3 assay kit, BD Pharmingen, San Jose, CA, USA). Caspase-3 activity was evaluated as follows. Cell lysates from VM neurons were diluted in assay buffer (1X HEPES buffer) containing caspase-3 substrate (Ac-DEVD-ANC) to a final concentration of 50 μM and 60 μg protein equivalent cells per ml and incubated at 37ºC for 1 h. Samples were measured for AMC chromophore fluorescence,

liberated from Ac-DEVD-AMC using a spectroflurometer with excitation at 380nm and emission at 459nm.

2.2.9 Nano particle preparation

Nano curcumin was prepared using sol-oil chemistry as reported earlier (Krishna, Mandraju et al. 2009). 10 mg of curcumin (Sigma USA) /100µl of DMSO (Sigma USA) was gently mixed with 40 mg of lactoferrin (Symbiotics USA)/1ml of ice cold PBS(pH 7.4). This mixture was slowly added to 25 ml of olive oil (Leonardo Italy) with continuous dispersion by gentle vortexing. This sample was sonicated using narrow stepped titanium probe of ultrasonic homogenizer (300V/T, Biologics Inc., Manassas, Virginia, USA) for 15 min at 4°C. The resulting mixture was immediately frozen for 10 min in liquid nitrogen and then thawed on ice for 4 hrs. The particles thus formed were pelleted by centrifugation at 6000 rpm for 10 min at 4°C. To completely remove the oil from the pellet, it is thoroughly washed twice with ice cold diethyl ether and then dispersed in 1 ml of PBS.

2.2.10 Nano particle characterization

Morphology of nano particles was analyzed through field emission scanning electron microscope (FE-SEM, Philips FEI-XL 30 ESEM; FEI, Hillsboro, OR, USA) operated at 20 KV, and Atomic force microscope (AFM; SPM400). For FE-SEM analysis gold coated nano particles were used and for AFM analysis, the samples were spin coated on glass slides. Characterization of these particles was done according to the earlier

reported protocol (Golla, Bhaskar et al. 2013) following the manufacturer's instructions. Dynamic light scattering (DLS) analysis was done using nanopartica nanoparticle analyzer system (Horiba Scientific) equipped with a diode-pumped solid-state laser of wavelength 532 nm and a temperature controller unit, for determining the size and polydisperity of nano particles.

2.2.11 Evaluation of loading efficiency

The nano particle pellet was lyophilized and dispersed in PBS (pH 5). The whole mixture was transferred to 14 kda molecular weight cut-off activated dialysis membrane tubing with both end fixed with clamps. The bag was kept in conical flask containing 50 ml of PBS pH 5. Whole setup was placed at room temperature in shaking condition at rate of 90 revolutions per minute. Aliquot at 30 min was taken out and filtered through 0.2 micron syringe filter. Then the drug was quantified using HPLC (Waters). A standard curve was plotted using various known concentration of drug and unknown concentration of the drug from the aliquot was measured from it. Then the percentage of encapsulation was calculated using following formula

$$\text{Encapsulation Efficiency (\%)} = \frac{W_t}{W_i} \times 100$$

Where W_t is the amount of drug in nanoparticles and W_i is the initial quantity of drug used for nanoparticles preparation.

2.2.12 Estimation of Curcumin delivered to cells:

2 X10^6 SK-N-SH cells were seeded in 30 mm culture dishes and supplemented with 3 ml DMEM with 10% serum. At specified time points, cells were harvested and lysed with 500 µl of 0.1% tritonX-100 in PBS with mild sonication. Samples were mixed with 100 µl of 30% silver nitrate, 1 ml of methanol and centrifuged at 12000 rpm for 15 min. Curcumin (Excitation 458 nm and Emission 530 nm) present in this supernatant was estimated using fluorescence spectrometer (Shimadzu FL 2000; Shimadzu, Kyoto, Japan). A standard curve was plotted using different known concentrations of drug and unknown concentration of the drug from the supernatant was measured from it.

2.2.13 siRNA transfection

SK-N-SH cells were transfected using lipofectamine 3000 (Invitrogen, NY, USA) with 0.5µM of mycoilin specific siRNA (sc-40753A, Santa Cruz Biotechnology, Texas, USA). Cells transfected with 0.5 µM of non-silencing siRNA (Scrambled) (sc-37007, Santa Cruz Biotechnology, Texas, USA) were taken as control.

2.2.14 Micro array analysis

VM neurons at 7th DIV were treated with 15nM rotenone and the cells were processed at 9th DIV for micro array analysis. VM neurons at 7th DIV treated with DMSO alone and processed at 9th DIV were taken as control. The samples were

collected in triplicate and processed for micro array analysis at Genotypic Technology Pvt Ltd, Bangalore, India, and using whole rat genome micro array kit provided by Agilent. Briefly, total RNA was isolated using Quiagen RNeasy mini-kit with DNAse treatment. Purity and concentration of RNA was estimated using Nanodrop spectrophotometer. Following labeling and hybridization samples were scanned for fluorescent signals. A fold change of 0.6 was used to detect the up-regulation and down-regulation in each of the treated replicates with a gemometrican mean fold of 0.8. Expression signals were normalized usig Genespring GX 12.6.1 software and were presented on a log scale, where lower levels of expression was represented in colder colours and higher levels of expression was represented in warmer colours.

2.2.15 Real Time PCR analysis

Microarray data was validated by quantitative real time PCR (q-RT PCR). Using gene specific primers (Table2.1 and Table 2.2), 10 μL of cDNA was synthesized from 1 μg total RNA in the presence of random hexamers and Super Script First strande synthesis system (Invitrogen, NY, USA) and power SYBR green PCR master mix (Applied Biosystem, CA, USA). DNAse I (Fermentas, GmbH, Germany) was used to eliminate any traces of DNA in total RNA. 18srRNA was considered as internal control. No template control (NTC) was set up to ensure no contamination of PCR reagents in amplified cDNA. PCR was done with ABI Prism H7500 fast thermal cycler Applied Biosystem, CA, USA) with 0.2 μL of 1st strand cDNA template, 20 p

mol of each primer and 5 µL of master mix making a total volume of 10µL. Fluorescence emitted by SYBR green which is in direct proportion to DNA amplification was analyzed. Using 2 $^{-\Delta\Delta C}$T method by Livak and Schmittgen 2001, relative fold change in gene expression was assayed.

Table 2.1: Primers used for q-RT PCR analysis of rat VM neuronal transcriptome.

No	Gene & primers	5'<-----Sequence----->3'	Amplicon size in bp
1	Vegfb_FP	TGCCCTCTTCTGGTGTGTC	
2	Vegfb_RP	TGGAAGAGTAGTCGGGTGC	183
3	Poli_FP	TCGGATGCCACCTGCTTTC	
4	Poli_RP	GAAAGACAATACTCCTCTCG	204
5	Ctnna3_FP	GGGCAGTTGTCAGAAGAGG	
6	Ctnna3_RP	AACACACATCTTACACACTGG	242
7	Myoc_FP	GTTACTACCAGACCTTGAGAG	
8	Myoc_RP	ATCTGTAGCCTTAGAAACTGG	131
9	Neurog1_FP	ATGAGCCCCTGAAGACGAG	
10	Neurog1_RP	AGCCCACTCCTTGTGTCTC	142
11	Neurod6_FP	TCAGGTTGCCCACCGACAG	

12	Neurod6_RP	TAGAGTGGGAGGTGAATGAC	141
13	Actb_FP	CTCTTCCAGCCTTCCTTCC	170
14	Actb_RP	ATCTCCTTCTGCATCCTGTC	

Table 2.2 Primers used for q-RT PCR analysis of SK-N-SH cell transcriptome.

No	**Gene & primers**	**5'<-----Sequence----->3'**	**Amplicon size in bp**
1	Vegfb_FP	AGCACCAAGTCCGGATG	195
2	Vegfb_RP	GTCTGGCTTCACAGCACTG	
3	Poli_FP	GGATGGAGAAGCTGGGGGTG	155
4	Poli_RP	TGAAGCATTTGGTGTGGGCA	
5	Ctnna3_FP	CAATACTCTGTCCTGCAGTAGGC	195
6	Ctnna3_RP	CACTGGCTCTTTTCGAACGTC	
7	Myoc_FP	GTGTACTCGGGGAGCCTCTA	162
8	Myoc_RP	AGCCAAGTCAATGTCCGTGT	

9	Neurog1_FP	AGCGCCTTTCTATCTGTCCG	118
10	Neurog1_RP	AGGAAGCCGGATAGGTCACT	
11	Neurod6_FP	GGCTGGTACCCACTTACAGG	111
12	Neurod6_RP	CCCATGCCATCTGCTAGTGA	
13	Actb_FP	CATGTACGTTGCTATCCAGGC	250
14	Actb_RP	CTCCTTAATGTCACGCACG AT	

2.2.16 Statistical analysis

Experiments were performed in triplicate and repeated independently thrice. Data was averaged and presented as mean ± SD. Statistical comparisons were made using paired't' test, two way ANOVA followed by a post hoc analysis (Scheffe's type). Statically significance level was set as acceptable when p value was less than 0.05.

Chapter-3

Enriched rat primary VM neurons as an *in-vitro* culture model.

Introduction

The hallmark feature of PD is the selective loss of neurons in the SNpc region of brain (Lang and Lozano 1998). Primary neuronal culture is an *in vitro* approach attempting to reduce the inherent complexity of brain and is being widely used as an *in-vitro* model (Aksenova, Aksenov et al. 2005; Bhanu, Mandraju et al. 2010). Various culture models of VM neurons reported earlier involve either use of feeder cells or mixed cultures (Ahmadi, Linseman et al. 2003; Tolosa, Zhou et al. 2013). But detail analysis of VM neuron enriched culture is not available. Hence, this paper demonstrates an *in-vitro* evaluation of maturation of VM neuron enriched culture. Such information will be very useful in understanding VM neuron specific molecular signaling processes that occur during differentiation, network formation and eventually development. In case of Cerebellar granule neurons, glial cell contamination was circumvented by supplementing growth media with a mitotic inhibitor that eliminates non-neuronal mitotic cells (Bhanu, Mandraju et al. 2010; Bilimoria and Bonni 2008; Gupta, Swain et al. 2012). In the current study, we have used mitotic inhibitor to obtain VM neuron enriched culture to gain insights into VM neuron specific cellular mechanisms.

Nestin is a neurofilament protein expressed in progenitor cells (Paek, Shin et al. 2010; Palm, Salin-Nordstrom et al. 2000; Varghese, Das et al. 2009) and lack of its immune reactivity *in vitro* was used to classify the culture as mature cells (Bertrand, Aksenova et

al. 2011), while MAP-2 is widely accepted as a mature neuronal marker (Cossette, Levesque et al. 2005; Cavallaro, Mariani et al. 2008; Wang, Wang et al. 2013). We used these markers to classify mature and precursor stages of *in-vitro* VM neuronal culture.

Markers of oxidative stress and DNA damage were reported in VMc brain region of PD patients (Jenner and Olanow 1996; Zhang, Perry et al. 1999). Additionally Reactive Oxygen Species (ROS) was also implicated in neuronal death (Leonardi and Mytilineou 1998). Considering this importance of ROS and DNA damage, we have studied their levels in *in vitro* VM neuronal culture. Since topoisomerase II β plays important role in DNA repair, neuronal development, differentiation and longevity (Gupta, Swain et al. 2012; Yang, Li et al. 2000; Tiwari, Burger et al. 2012; Mandraju, Chekuri et al. 2011), expression of Topoisomerase II β was monitored during the VM neuronal culture *in vitro*.

The objective of this study is to characterize and investigate utility of VM neuron enriched culture to study VM neuron specific cellular mechanisms implicated in neurodegeneration and eventually PD etiology.

Results

In order to obtain VM neuron enriched culture, growth medium of VM neurons was supplemented with mitotic inhibitor AraC on 2nd-DIV. Similar to the observations made by Takeshima, Shimoda et al. 1994, in the presence of 2μM AraC, VM neuronal culture was maintained with minimal presence of glial cells (<5%) until 9th-DIV, that followed a catastrophic phase where most of the neurons died with truncated neurites and rounded soma resulting in viability of < 5% of neurons.

3.1 Viability and morphological features of VM neurons in absence of glial cells in *in vitro* culture

Viability of these VM neurons over this period of 9 days in culture was measured through MTT assay. The cells on 3rd DIV was taken as a starting point and considered to be 100% viable. Fig 3.1a depicts the survival of VM neurons *in vitro* that showed a gradual decline in viability reaching to 45% by 9th DIV ($P<0.0005$). Figure 3.1b, illustrates the adherence of cells with small soma bearing no neuritic outgrowths on 2nd DIV and a visible neuritic outgrowth by 3rd DIV, which developed into an extensive network by 7th DIV, reaching its magnitude on 9th DIV and got truncated by 10th DIV, showing a beaded dendritic appearance.

3.2.1 Maturation of VM neurons in presence and absence of glial cells in culture

As shown in Fig 3.2a, after 6thDIV, MAP-2 expression was predominant in most of the neuronal population whereas the Nestin expression was detected along with MAP-2 only until 6thDIV. These observations suggest that VM neuron enriched culture *in vitro* consist of neuronal precursor cells until 6thDIV and attain maturity by 7thDIV. Surprisingly, the maturation pattern of these neurons was similar, both in presence (absence of AraC in culture medium) and absence of glial cells. These observations suggest that presence of glial cells in neuronal culture might be important in later stages of maturation rather than at initial stages. So, 7thDIV of VM neuronal culture can be considered as a stage of maturity both in presence and absence of glial cells.

3.2.2 DA neurons and topoisomerase II β in VM neuron enriched culture *in-vitro*

Tyrosine hydroxylase (TH) expression was observed to assess DA neurons in the culture. Results in Fig 3.2b illustrates that DA neurons were present from 3rdDIV to 10thDIV and maximum expression of TH was present from 7thDIV to 10th DIV ($P<0.0005$). An interesting feature noted here was that only DA neurons survived until 10thDIV. These observations were corroborated with western blot analysis of TH protein in VM neuron enriched culture (Fig 3.2b.1). Since number of neurons was

significantly low on 10thDIV, expression levels of TH could not be analyzed using Western blot analysis. These observations establish that 7thDIV is the suitable time period to study DA neurons in VM neuron enriched culture.

3.2.3 ROS and DNA damage in VM neuron enriched culture *in vitro*

The representative bar graphs in Fig 3.2c and Fig 3.2d.1 illustrates an increase in ROS levels (using CM-H_2DCFDA dye) and DNA damage (estimated by alkaline comet assay) respectively, during the period of culture of VM neurons *in vitro*. Results of the representative comet tail lengths analyzed by fluorescent microscopy showed a slight DNA damage at 7thDIV, which significantly increased by 9thDIV ($P<0.0005$) (Fig 3.2d.2). The plausible cause for this increase in DNA damage could be due to the presence of increased ROS levels. These results together shows the presence of low level of ROS and DNA damage at 7thDIV, which should be considered while evaluating any compounds regarding oxidative stress and DNA damage.

3.3 Topoisomerase II β in VM neuron enriched culture in vitro

There was an increase in expression of topoisomerase II β until 9thDIV as shown through confocal microscopy and Western blot analysis (Fig 3.3a, 3.3b) corroborating its key role in neuronal protection during development. Moreover, the sudden decline in expression of topoisomerase II β on 10thDIV (Fig 3.3a) raises curiosity over the role of this protein in the sudden death of neurons

Fig 3.1: Cell viability and morphological features of VM neurons in absence of glial cells *in vitro*

a) Cells on 3rdDIV were taken as a starting point for the MTT viability assay and were considered to be 100% viable. The line graph in the figure depicts a gradual decline in cell viability until 9thDIV.

b) Cells on 2nd DIV had small soma and short neurites and these cell bodies became larger and more defined, while neurites got elongated from 3rdDIV-9thDIV. Once they attained maturity i.e from 7thDIV-9thDIV, the network had become more complex with a bundled appearance. At 10thDIV, neuritic dendrites got truncated with rounded soma.

Figure 3.1

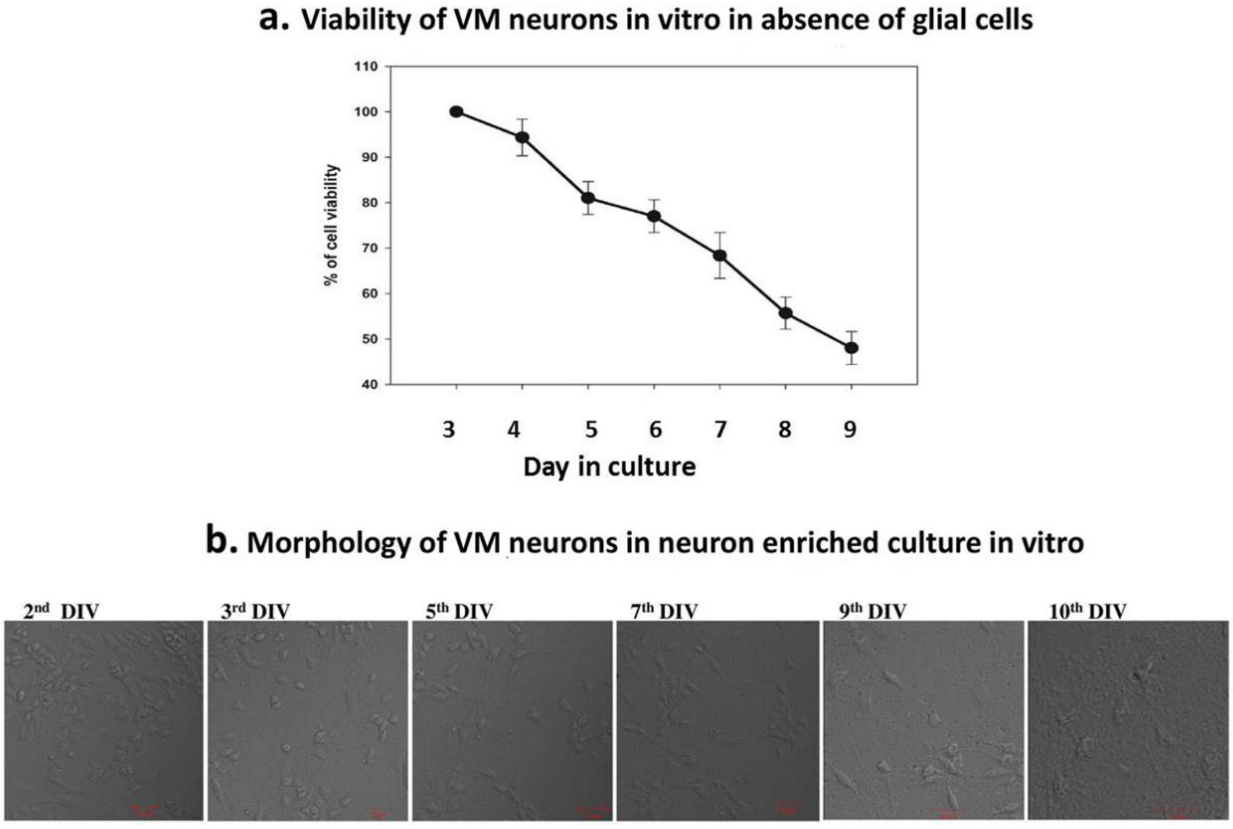
a. Viability of VM neurons in vitro in absence of glial cells
% of cell viability
110
100
90
80
70
60
50
40
3
4
5
6
7
8
9
Day in culture
b. Morphology of VM neurons in neuron enriched culture in vitro
2nd DIV
3rd DIV
5th DIV
7th DIV
9th DIV
10th DIV

Fig 3.2:

a) Maturation pattern of VM neurons in presence and absence of glial cells in vitro

VM neurons both in presence and absence of glial cells, exhibited expression of immature neuronal marker Nestin (stained red by alexafluor 594) on 3rdDIV which was slightly increased by 5thDIV and completely disappeared on 7thDIV. Expression of mature neuronal marker MAP-2 (stained green by alexafluor 488) was also observed on 3rdDIV which increased till 9thDIV. Here the nucleus was stained by DAPI (blue color).

b) DA neurons in VM neuron enriched culture in vitro

b) DA neurons (red) stained with TH (marker for DA neurons) antibody, were very few in numbers during initial days of culture and reached maximum in number by 7thDIV and continued to 10thDIV. Most of the neurons that survived on 10thDIV were DA neurons and had a beaded appearance of dendrites.

b.1) Expression of TH protein during the course of culture was estimated using western blot analysis. A significant increase in TH expression was observed from 7thDIV and continued to 10thDIV. Beta actin was taken as loading control.

b.1.1) Densitometric analysis of bands representing expression of TH, obtained through western blot analysis showed an increase from 7th DIV. Averages and standard deviations from three experiments were shown. Statistical significance was estimated by unpaired t test: *** $P<0.0005$.

c) ROS levels in VM neuron enriched culture in vitro

c) Levels of ROS in *in vitro* VM neurons showed a gradual increase during the culture period. There was a marked increase on 7thDIV and 9thDIV. Averages and standard deviations from three experiments were shown. Statistical significance was estimated by unpaired t test: ** $P<0.005$

d) DNA damage in VM neuron enriched culture in vitro

d.1) The degree of DNA damage is assessed through measurement of the extent of tail movement, which is the product of tail length and fraction of DNA in the comet tail as presented in the Bar graph. This depicts an increase in DNA damage levels on 9thDIV of VM neuronal culture. Averages and standard deviations from three experiments were shown. Statistical significance was estimated by unpaired t test: *** $P<0.0005$

d.2) Comet tail movement is a measure of DNA damage. There was no comet tail movement on 5thDIV, while 7thDIV showed a visible tail movement which got further elongated on 9thDIV suggesting a DNA damage on 9thDIV in VM neuron enriched culture in vitro.

Figure 3.2

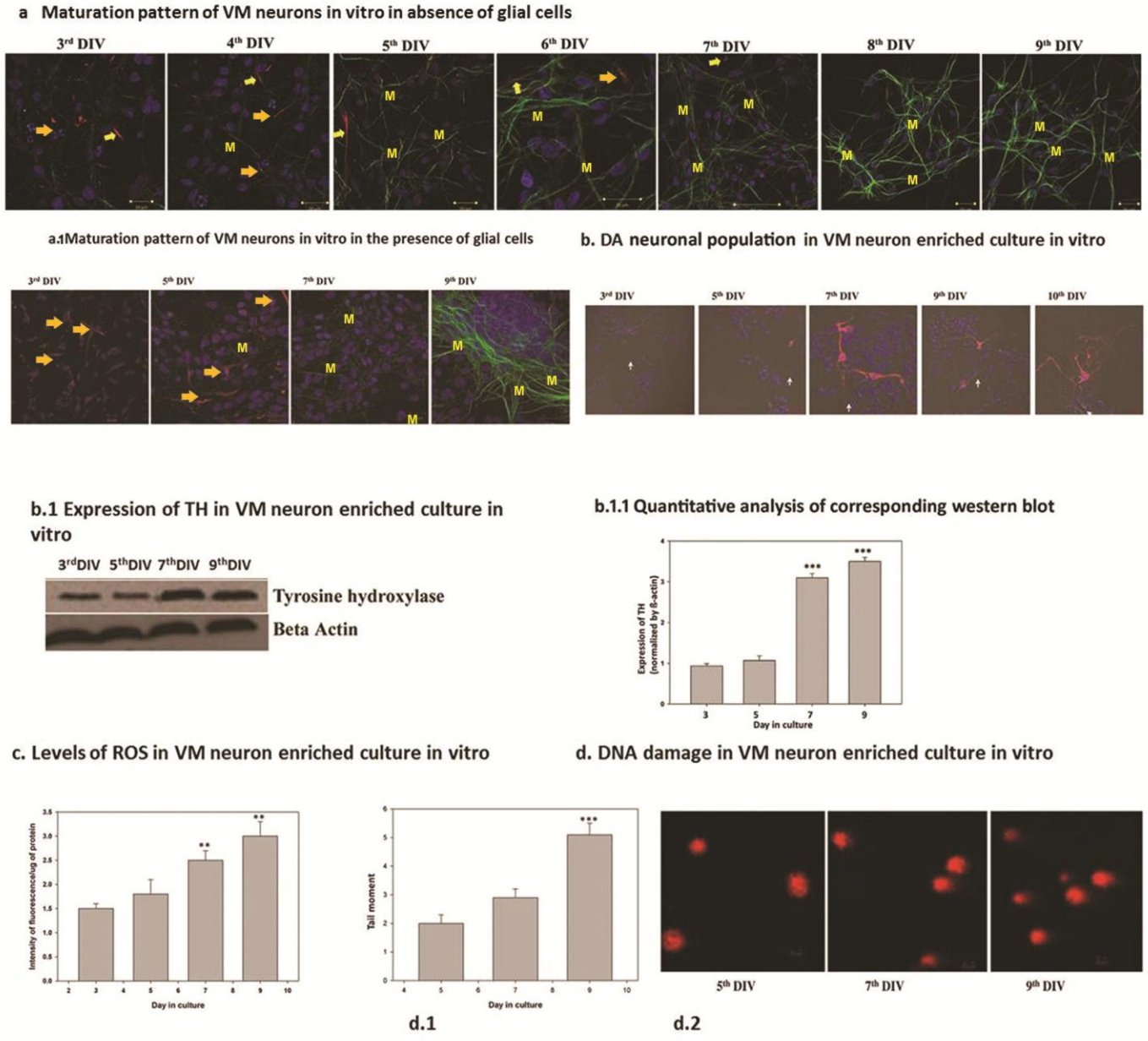
a Maturation pattern of VM neurons in vitro in absence of glial cells
3rd DIV
4th DIV
5th DIV
6th DIV
7th DIV
8th DIV
9th DIV
M
a.1Maturation pattern of VM neurons in vitro in the presence of glial cells
3rd DIV
5th DIV
7th DIV
9th DIV
b. DA neuronal population in VM neuron enriched culture in vitro
3rd DIV
5th DIV
7th DIV
9th DIV
10th DIV
b.1 Expression of TH in VM neuron enriched culture in vitro
3rdDIV 5thDIV 7thDIV 9thDIV
Tyrosine hydroxylase
Beta Actin
b.1.1 Quantitative analysis of corresponding western blot
Expression of TH (normalized by β-actin)
Day in culture
c. Levels of ROS in VM neuron enriched culture in vitro
Intensity of fluorescence/ug of protein
Day in culture
d. DNA damage in VM neuron enriched culture in vitro
Tail moment
Day in culture
d.1
5th DIV
7th DIV
9th DIV
d.2

Fig 3.3: Expression of topoisomerase II ß in VM neuron enriched culture in vitro

a). Topoisomerase II β had a sparse expression during initial days of culture and its expression gradually increased by 9^{th}DIV. 10^{th}DIV culture showed a decrease in its expression concomitant with cellular death.

b). Expression of topoisomerase II β was estimated using western blot analysis. Its expression gradually increased till 9^{th}DIV.

b.1). Densitometric analysis of bands representing expression of Topoisomerase II β, obtained through western blot analysis showed a significant increase from 5^{th} DIV. Averages and standard deviations from three experiments were shown. Statistical significance was estimated by unpaired t test: **P<0.005; *** P<0.0005.

Figure 3.3

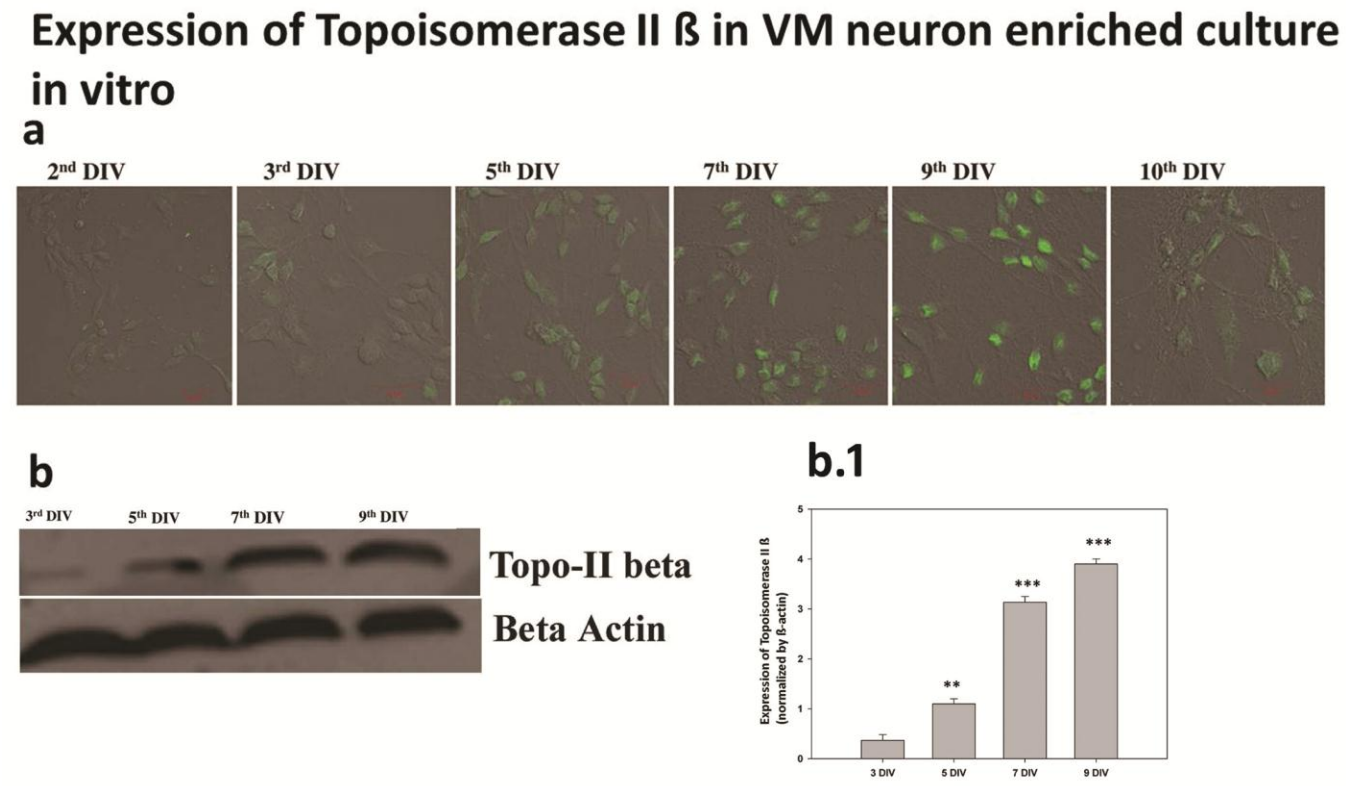
Expression of Topoisomerase II ß in VM neuron enriched culture in vitro
a
2nd DIV
3rd DIV
5th DIV
7th DIV
9th DIV
10th DIV
b
3rd DIV
5th DIV
7th DIV
9th DIV
Topo-II beta
Beta Actin
b.1
Expression of Topoisomerase II ß (normalized by ß-actin)
3 DIV
5 DIV
7 DIV
9 DIV

Discussion

We have characterized VM neuron enriched culture in terms of maturation, oxidative stress and DNA damage in order to establish them as an in vitro culture model. Neuronal progenitor cells differentiate to specific cellular lineages like neurons, glial cells etc. This differentiation process involves activation/expression of various intracellular and extra cellular factors. Each neuronal type possesses distinct characteristics and is associated with specific function in brain. Since maturation is a process of progenitor cell differentiating into post mitotic neuron, studying these events would throw light on neuron specific developmental mechanisms.

In the present study, we have observed a complete absence in expression of precursor cell marker nestin and the concomitant expression of mature neuronal marker MAP-2 by 7^{th}DIV of VM neuronal culture both in presence and absence of glial cells. This indicates, VM neurons attain maturity at 7^{th}DIV both in presence and absence of glial cells and thus suggest the role of glial cells at later stages of neuronal maturation. Although TH expression was evident from 3^{rd}DIV, there was a marked increase in its expression from 7^{th}DIV indicating the presence of higher number of DA neurons. Thus 7^{th}DIV is a suitable time period to get insights into cellular mechanisms, particularly of DA neurons in VM neuron enriched culture. These VM neurons in absence of glial cells were viable for 9 days followed by a sudden death of neurons corroborating earlier report of Takeshima, Shimoda et al. 1994.

The results of the present study showed a marginal increase in ROS and DNA damage during this time period, which peak at the 9thDIV. At physiological levels, ROS serve as signaling species and only an excessive amount of these molecules leads to oxidative stress (D'Autreaux and Toledano 2007). Present study indicates an increase in ROS levels which in turn might have lead to increased DNA damage assessed through alkaline comet assay on 9thDIV. ROS levels initially can be considered to be at near basal levels, as there was no significant amount of DNA damage until 9thDIV. It was observed through alkaline comet assay that there was no significant amount of DNA damage on 7thDIV and so this period of culture can be used to evaluate the effect of ROS and DNA damaging agents on VM neurons, which are gaining prominence in recent times.

Aging is associated with increased oxidative stress and its influence on neurodegeneration and unscheduled cell cycle re-entry was also reported (Klein and Ackerman 2003). Hence, the present study hypothesizes that ROS and DNA damage at 9thDIV of VM neuron enriched culture might be one of the factors leading to neuronal death.

Topoisomerase II β was reported to be highly expressed when neuronal cells become post mitotic from progenitor phase (Tiwari, Burger et al. 2012). Western blot analysis and immunofluorescence observations showed an increase in topoisomerase II β expression on 7th DIV to 9th DIV suggesting the entry of VM neurons into postmitotic phase from progenitor phase. A decreased expression of topoisomerase II β on

10^{th}DIV from much more concentrated pattern on 9^{th}DIV suggests a crucial role of topoisomerase II β in the catastrophe after 9^{th}DIV. This is strengthened by recent report, where topoisomerase II β deficiency leads to premature death of postmitotic neurons due to its impaired regulation in transcriptional process (Tiwari, Burger et al. 2012).

Conclusion

These 9 days of neuronal culture can offer a good platform to study molecular mechanisms associated with VM neurons. Near basal levels of ROS, DNA damage and abundance of DA neurons on 7^{th} DIV, make it an ideal time period to understand epigenetics and signaling modifications that take place in these neurons. Further they can serve as a development and aging model *in vitro*. Also, such model can be employed in evaluating pro- and anti-survival activities of various bioactive molecules on VM neurons.

This study documents the suitability and utility of VM neuron enriched culture system, as it can be used for proteomic and genomic analysis to get deeper insights into VM neuronal specific neurodegenerative mechanisms. This model can also be used for developmental studies of VM neurons as immature neuronal precursor stage and mature post mitotic phase was clearly established.

Chapter-4

Rotenone induced neurotoxicity in cellular models of VM neurons and SK-N-SH cell line.

Introduction

Programmed cell death is a necessary event that occurs in large number of neurons during nervous system development (Oppenheim 1991). Once, the neurons are developed, they have limited regenerative potential and hence can't afford to remain susceptible to cell death (Kole, Annis et al. 2013). We hypothesize that these intrinsic changes in neurons may lead to differential ability in sustaining toxicity, depending on the age of neurons. Our study aims at investigating the age dependent sensitivity of VM neurons to neurotoxic agent like rotenone, which is known to induce molecular changes during PD.

PD is a neurodegenerative disorder that occurs in both sporadic and familial forms, which is characterized by a selective loss of DA neurons in SNPc region of brain (Dauer and Przedborski 2003). Its specific etiology is not fully understood, but important insights on contribution of environmental factor in the development of sporadic form were provided through study of epidemiology and neuropathology of PD (Di Monte, Lavasani et al. 2002). Rotenone, a flavonoid, is one such environmental factor that induces certain features of PD like dopaminergic neuronal degeneration, α-synuclein aggregation etc both *in-vitro* and *in-vivo* (Betarbet, Sherer et al. 2000; Chaves, Melo et al. 2010). *In-vitro* rotenone treatment of neuronal cells was shown to promote oxidative damage, accumulation of α-synuclein finally leading to

cell death (Sherer, Betarbet et al. 2002; Betarbet, Canet-Aviles et al. 2006). Rotenone induction of cell death through caspase-3 dependent apoptosis via enhancing the levels of ROS was also reported (Li, Ragheb et al. 2003; Moon, Lee et al. 2005). Owing to multifactorial nature of PD, cellular models form the preliminary choice and are being widely used to understand the complexity involved in pathogenesis of the disease (Alberio, Lopiano et al. 2012).Co- culture of VM neurons with astrocytes are usually employed in study of PD, but such studies may face the problem of ambiguity mediated by neuroprotective and neurodegenerative role of astrocytes (Rappold and Tieu 2010). Further to simulate action of rotenone on the developing brain, one needs to understand, the action of rotenone on various neuronal linages that occur during development.

Gene-environment interaction was well established in etiology of PD (Horowitz and Greenamyre 2010; Litvan, Chesselet et al. 2007; Tanner, Kamel et al. 2011). The main obstacle in treating PD is due to the limited knowledge on various molecular mechanisms that lead to PD. Studies focusing on few genes/proteins involved, might not be a practical attempt to unravel unknown factors that lead to PD. Transcriptome analysis of rotenone treated VM neurons is an alternative approach to identify such unknown key factors operating in etiology of PD.

Curcumin, a polyphenolic compound, extracted from the roots of the herb *curcuma longa* exhibits neuroprotective activity especially in case of neurodegenerative

diseases like AD (Garcia-Alloza, Borrelli et al. 2007) and PD (Mythri and Bharath 2012). Most of the current approaches are aimed at replenishing the dopamine levels which provide only symptomatic relief but not neuroprotection. Consequently curcumin which has antioxidant, anti-inflammatory properties is being explored as a neuroprotective agent for PD (Mythri and Bharath 2012; Liu, Li et al., 2013).

The aims of the present objective are: (a) to estimate and evaluate rotenone-mediated neurotoxic activity against immature and mature VM neurons; (b) to examine the effect of curcumin on rotenone-mediated neurodegeneration; (c) Transcriptome analysis of rotenone treated VM neurons; (d) Validating the role of a key gene identified through above transcriptome analysis.

Results

As discussed in earlier chapter maturation pattern of VM neuron enriched culture was established using maturation marker proteins nestin and MAP-2. It was observed that by 7^{th} DIV, there was a complete absence of nestin and predominant presence of MAP-2. Thus VM neuron enriched culture before 7^{th} DIV was considered as immature and after 6^{th} DIV was considered as mature neurons.

4.1 Rotenone toxicity on VM neurons

To assess the rotenone toxicity at different developmental stages of VM neurons, 3^{rd}DIV neurons (immature phase) and 7^{th}DIV neurons i.e., mature neurons were

treated with rotenone for 2 days. Results of MTT assay suggest a concentration dependent toxicity of rotenone (Fig 4.1a) in both immature and mature VM neurons. However, mature neurons were relatively more susceptible to rotenone induced toxicity than immature neurons. To further examine and evaluate the above results independently, we have performed trypan blue dye exclusion assay and LDH release assay. Number of viable neurons was measured through trypan blue assay on treatment with 1-20nM concentrations of rotenone. Both immature and mature neurons had shown a concentration dependent decrease in number of viable neurons, but the effect is more significant in mature neurons (Fig 4.1b). To further confirm our observations, we have quantified LDH release into the medium on rotenone treatment in the concentration rage of 1 nM to 20 nM. While from 1 to 5 nM concentration of rotenone there was no significant increase in LDH release, a significant dose-dependent increase in LDH release was observed from 10nM to 20nM of rotenone in both immature and mature VM neurons. Further, in consistent with the results from MTT and Trypan blue exclusion assays (Fig. 4.1a and 4.1b), mature neurons were shown to release more LDH compared to immature neurons on treatment with rotenone (Fig 4.1c).

The results of MTT assay showed that the viability of immature VM neurons was reduced to 70% and mature VM neurons to 45%, when treated with 15nM of rotenone and so the same concentration was used for further assays.

4.2 Assessment of PD-like conditions in immature and mature neurons on rotenone treatment

To confirm critical signs of PD, formation of Lewy bodies and selective degeneration of DA neurons were analyzed in both immature and mature VM neurons after treatment with rotenone. Since α-synuclein aggregation is a critical component in Lewy body formation and TH is a marker for DA neurons, cells were immune-stained with α synuclein and TH antibodies. Results presented in Fig 4.2a depicts that, immature neurons did not show presence of α synuclein aggregates, whereas mature neurons exhibited formation of aggregates of α synuclein, when treated with rotenone. Fig 4.2b depicts a significant loss of TH expression in mature neurons than in immature neurons on rotenone treatment. Bar graph presented in Fig 4.2c depicts a decrease in both total number of neurons and number of DA neurons on rotenone treatment. However, there was a significant decrease in number of DA neurons in mature VM neuronal culture than in immature neuronal culture. These observations, taken together, demonstrate that although both immature and mature VM neurons are susceptible to rotenone, only mature VM neuronal culture develops α-synuclein aggregation and DA neuron sensitivity, a PD like feature.

4.3 Caspase -3 activity in immature and mature VM neurons on rotenone treatment

As rotenone induced, capase-3 mediated apoptosis in VM neurons is reported earlier (Ahmadi et al., 2003), caspase-3 activity in immature and mature VM neurons was evaluated using caspase-3 fluorogenic substrate. Cells treated with DMSO alone were taken as a control. Results showed (Fig.4.3a) a decrease in caspase-3 activity in mature control cells compared to that of immature control cells. This suggests that immature cells were more apoptotic in nature relative to mature cells. Rotenone treated immature neurons showed a 1.3 fold increase and mature neurons showed a 2 fold increase in caspase-3 activity, with reference to their respective controls. This significant differential fold of increase in caspase-3 activity suggests that apoptosis induction by rotenone is influenced by age or maturation of neurons.

4.3.1 Levels of ROS in immature and mature VM neurons on rotenone treatment

Enhancement of ROS production on rotenone treatment was reported earlier (Li, Ragheb et al. 2003). Effect of rotenone on levels of ROS in immature and mature neurons was evaluated using CM-H2DCFDA dye. Bar graph in Fig 4.3b depicts increased ROS levels in both immature and mature neurons when treated with rotenone. However, mature neurons showed a significant increase in ROS levels (2 fold) than immature ones (1.5 fold) with respect to their respective controls. This

again suggests a differential effect of rotenone on production of ROS in immature and mature VM neurons and also, ROS-mediated rotenone neurotoxicity.

4.4 Effect of Curcumin on rotenone-induced toxicity in VM neurons

Curcumin, a polyphenolic compound from *Curcuma longa*, is a potent anti-oxidant (Ak and Gulcin 2008) and is widely used in various pathological conditions (Menon and Sudheer 2007). In order to validate ROS mediated differential rotenone neurotoxicity on immature and mature VM neurons, they were treated with 1 μM curcumin, 5 h before the treatment with rotenone. Viability of immature and mature VM neurons was determined by MTT assay on 5^{th}DIV and 9^{th}DIV respectively. Cells treated with DMSO alone were taken as control and considered to be at 100% viable. Bar graph in Fig 4.4a depicts a reduction in cellular death of both immature and mature VM neurons on pretreatment with Curcumin. However a greater effect of curcumin was seen in mature VM neurons than in immature VM neurons. A 30% reduction in cellular death was observed in mature VM neurons, while it was only 10% in immature VM neurons. A concomitant reduction in ROS levels was associated with the reduction of cellular death (Fig 4.4b). The differential pattern continued even in the reduction of ROS levels, with mature VM neurons showing a significant reduction than immature neurons.

4.5 Differential gene expression in rotenone treated VM neurons

VM neurons at 7th DIV were treated with 15nM rotenone for 48 hrs and processed at 9th DIV for micro array analysis. A heat map of whole rat transcriptome in VM neurons was created for depicting those statistically significant ($P<0.05$) changes upon rotenone treatment. Fig 4.5 shows a comparison between control VM neuron transcriptome and rotenone treated VM neuron transcriptome. This data have yielded 705 upregulated genes and 2415 down regulated genes. Those genes were analyzed with biointerpreter software and few pathways were identified based on involvement of genes regulated on rotenone treatment (Tables 4.1 and 4.2).

4.6 Quantitative analysis of gene expression

We have validated the above micro array data by quantitative analysis of selected individual gene expression using q-RT PCR. Six up-regulated genes with high fold change and with relevant neuronal functions were selected for this analysis. They were Vascular endothelial growth factor-B, Neurogenin-1, Neuronal differentiation-6, polymerase I, Catenin-3 and Myocilin. All these genes showed an increase in their expression upon rotenone treatment (Fig 4.6a) and thus confirmed observations in micro array data.

Furtherly expression of above six genes in SK-N-SH (dopaminergic neuronal cell line) upon rotenone treatment was analyzed by q-RT PCR. Among those genes only

myocilin had shown a very significant increase (5 fold) upon rotenone treatment (Fig 4.6b).

4.7 Effect of Rotenone on SK-N-SH cells upon knock down of myocilin expression

Expression of myocilin was knock downed using siRNA (Sc 40753) and confirmed through western blot analysis in SK-N-SH cells after 48hrs of siRNA transfection (Fig 4.7a). Cells were treated with 100 nM rotenone for 24hrs after 36 hrs of siRNA transfection. Viability of these cells was assessed by MTT assay. Cells treated with DMSO alone were taken as control and their viability was considered to be 100%. When compared with these cells, viability of rotenone treated cells decreased to 45% and viability of myocilin siRNA pre-treated and rotenone treated cells decreased to 57%. Inhibition of myocilin expression significantly ($P < 0.05$) reduced the neurotoxic effect of rotenone. (Fig 4.7b) This was even corroborated by LDH release assay, where myocilin siRNA + rotenone treated cells had shown significantly ($P <s 0.05$) lower levels of LDH release when compared to rotenone alone treated cells (Fig 4.7c).

4.8 Parkinsonian conditions in SK-N-SH cells upon rotenone treatment

Rotenone induced parkinsonian conditions like reduced expression of TH, α-synuclein aggregation and increase in ROS levels were shown in VM neurons earlier. These parkinsonian features were analyzed in rotenone treated SK-N-SH cells and

myocilin siRNA + rotenone treated SK-N-SH cells. Expression of TH and α-synuclein was observed through confocal imaging with respective antibodies. Corroborating earlier observation in VM neurons, there was a reduction in TH expression of SK-N-SH cells on rotenone treatment. Inhibition of myocilin expression did not showed any significant effect on TH expression when compared to rotenone alone treated cells. α-synuclein aggregation was not observed in SK-N-SH cell on rotenone treatment. However there was an increase in its expression on rotenone treatment. Inhibition of myocilin expression did not showed any significant effect on α-synuclein expression when compared to rotenone alone treated cells (Fig 4.8b). This was the same with ROS levels, where there was an increase in ROS levels upon rotenone treatment and was not reduced significantly upon myocilin siRNA treatment (Fig 4.8a). These observations suggest that myocilin might not interfere in induction of parkinsonian features by rotenone in SK-N-SH cells.

Fig 4.1: Viability of VM neurons on treatment with rotenone.

a) MTT assay

Immature (3rdDIV), Mature (7thDIV) VM neurons were treated with varying concentrations of rotenone and their viability after 48 h was presented as % viability in a bar graph. Cells treated with DMSO alone at 3rdDIV and 7thDIV were considered as control for immature and mature neurons and their respective viability at 5thDIV and 9thDIV were taken as 100%. Cell viability was checked by MTT assay. Averages and standard deviations from three experiments were shown. Statistical significance was estimated by two way ANOVA followed by a post hoc analysis with **, $P < 0.01$. *** $P<0.001$.

b) Trypan blue dye exclusion assay

Immature (3rdDIV), Mature (7thDIV) VM neurons were treated with varying concentrations of rotenone and% viable VM neurons after 48 h was presented in a bar graph. Cells were treated with DMSO alone at 3rdDIV,7thDIV and number of cells at 5thDIV and 9thDIV were considered as respective controls for immature and mature neurons. Number of viable cells (cells not stained with the dye) were counted using hemocytometer. Averages and standard deviations from three experiments were shown. Statistical significance was estimated by two way ANOVA followed by a post hoc analysis with **, $P < 0.01$. *** $P<0.001$.

c) LDH release assay

Immature (3rdDIV), Mature (7thDIV) VM neurons were treated with varying concentrations of rotenone and release of LDH by cells after 48 h was quantified in a line graph. Cells were treated with DMSO alone at 3rdDIV,7thDIV and LDH release into media at 5thDIV and 9thDIV was considered as respective controls for immature and mature neurons. These control values were subtracted from treated samples and present as ΔLDH U/L. Averages and standard deviations from three experiments were shown. Statistical significance was estimated by two way ANOVA followed by a post hoc analysis with **, $P < 0.01$. *** $P<0.001$.

Figure 4.1

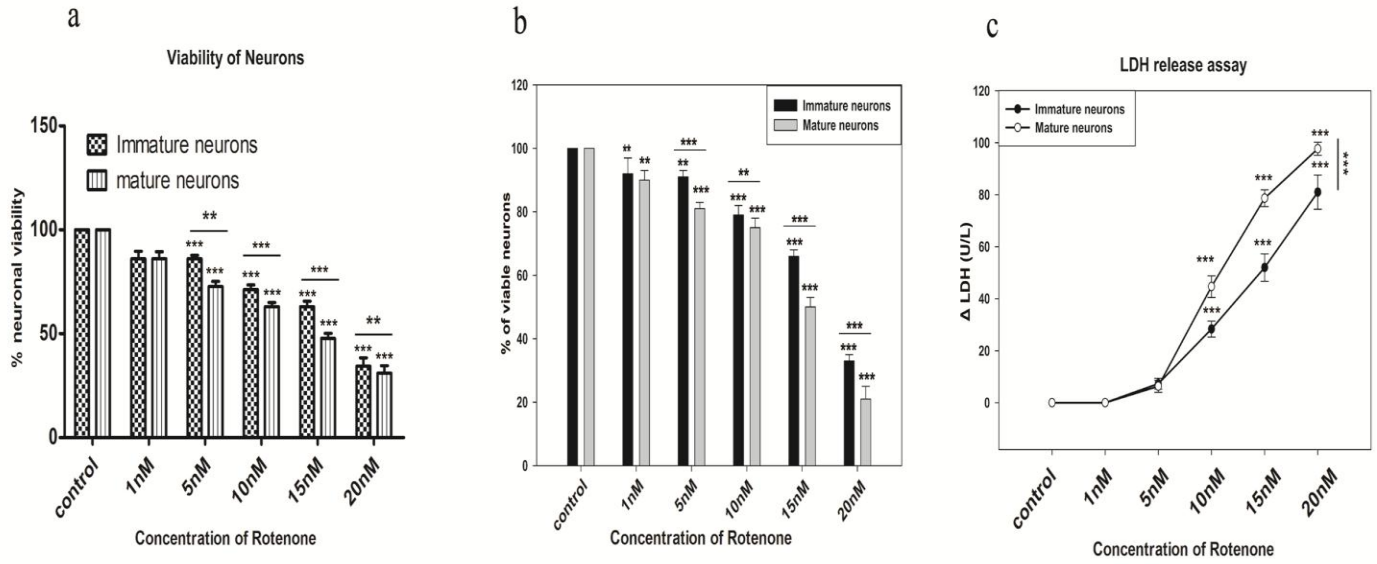
a
Viability of Neurons
% neuronal viability
Immature neurons
mature neurons
Concentration of Rotenone
control
1nM
5nM
10nM
15nM
20nM
b
% of viable neurons
Immature neurons
Mature neurons
Concentration of Rotenone
c
LDH release assay
Δ LDH (U/L)
Immature neurons
Mature neurons
Concentration of Rotenone

Fig 4.2: Parkinsonian conditions in VM neurons *in vitro* on rotenone treatment

Immature and mature VM neurons were treated with 15nM rotenone for 48 h and then assessed for Parkinsonian conditions in them.

a) Formation of α synuclein aggregates

VM neurons were immunostained with α synuclein in green (stained with alexafluor 488). α synuclein aggregates were shown with arrow marks. Control cells were treated with DMSO alone.

b) DA neurons on rotenone treatment in VM neuronal culture.

VM neurons were immunostained with TH in red (stained with alexafluor 594). TH is a marker for DA neurons. Control cells were treated with DMSO alone. Nucleus was stained with DAPI.

c) Number of total neurons on rotenone treatment in VM neuronal culture.

Number of total neurons per a field of confocal image with scale bar 20μm were counted and presented as number of cells/cm^2, where N=5 per group. Averages and standard deviations from three experiments were shown. Statistical significance was estimated by two way ANOVA followed by a post hoc analysis with *** $P<0.001$.

d) Number of TH+ neurons on rotenone treatment in VM neuronal culture.

Number of TH+ neurons per a field of confocal image with scale bar 20μm were counted and presented as number of cells/cm^2, where N=5 per group. Averages and standard deviations from three experiments were shown. Statistical significance was estimated by two way ANOVA followed by a post hoc analysis with *** $P<0.001$.

Figure 4.2

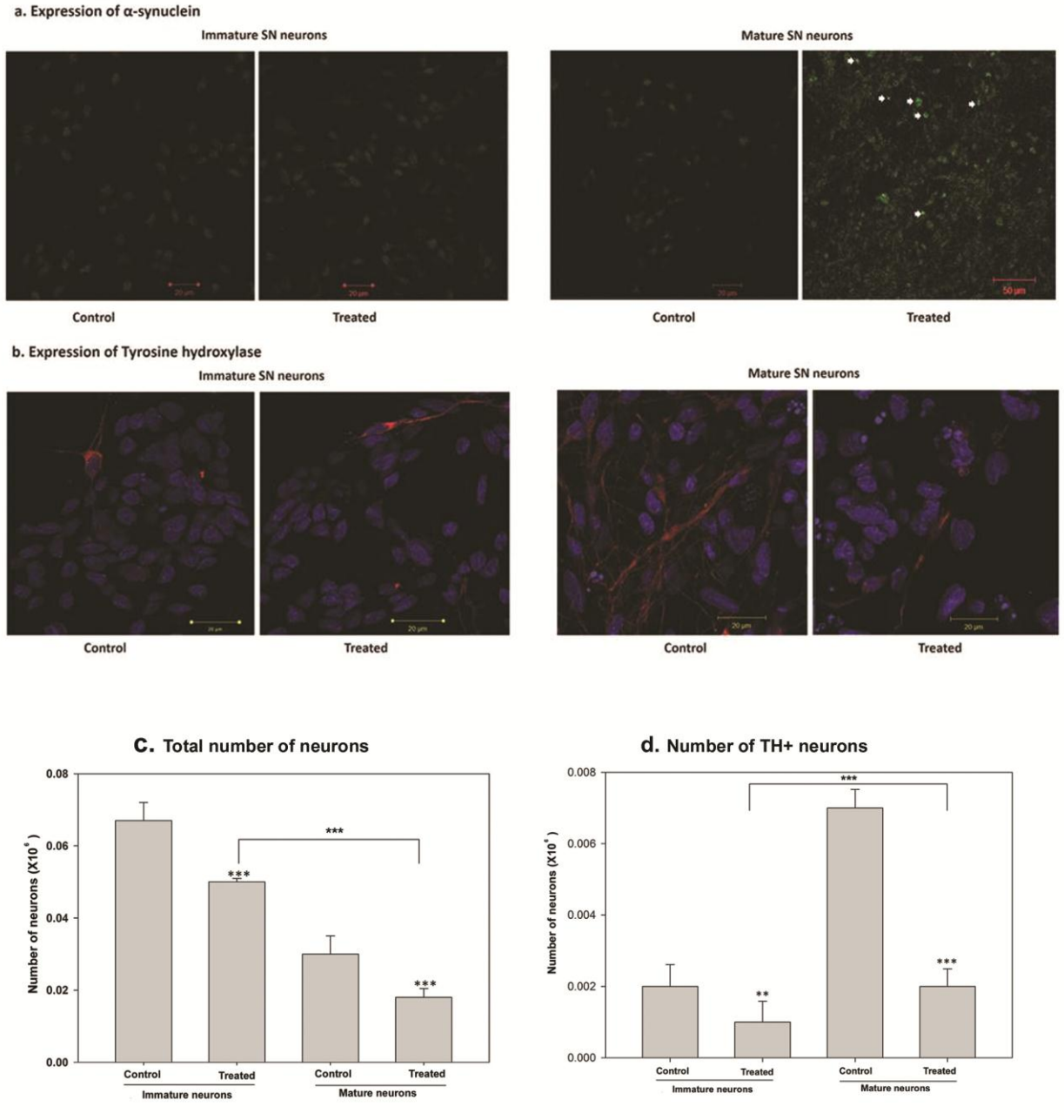
a. Expression of α-synuclein
Immature SN neurons
Mature SN neurons
Control
Treated
Control
Treated
b. Expression of Tyrosine hydroxylase
Immature SN neurons
Mature SN neurons
Control
Treated
Control
Treated
C. Total number of neurons
Number of neurons (X10⁶)
0.08
0.06
0.04
0.02
0.00
***
***
***
Control
Treated
Control
Treated
Immature neurons
Mature neurons
d. Number of TH+ neurons
Number of neurons (X10⁶)
0.008
0.006
0.004
0.002
0.000
***
**
***
Control
Treated
Control
Treated
Immature neurons
Mature neurons

Fig 4.3:

a) Caspase-3 activity in rotenone treated VM neurons *in vitro*

Immature and mature VM neurons were treated with 15nM rotenone for 48 h and caspase-3 activity was determined in respective cellular lysates by measuring cleavage of fluorogenic substrate AC-DEVD-AMC. Results were normalized to concentration of protein and expressed as relative fluorescence units per minute per mg of protein. Control cells were treated with DMSO alone. Averages and standard deviations from three experiments were shown. Statistical significance was estimated by two way ANOVA followed by a post hoc analysis with **, $P < 0.01$. *** $P<0.001$.

b) Levels of ROS on rotenone treatment in VM neurons *in vitro*

Immature and mature VM neurons were treated with 15nM rotenone for 48 h and levels of ROS were estimated using fluorescent dye CMH2DCFDA. Values were normalized for protein content and depicted as intensity of fluorescence per micro gram of protein. Control cells were treated with DMSO alone. Averages and standard deviations from three experiments were shown. Statistical significance was estimated by two way ANOVA followed by a post hoc analysis with **, $P < 0.01$. *** $P<0.001$.

Figure 4.3

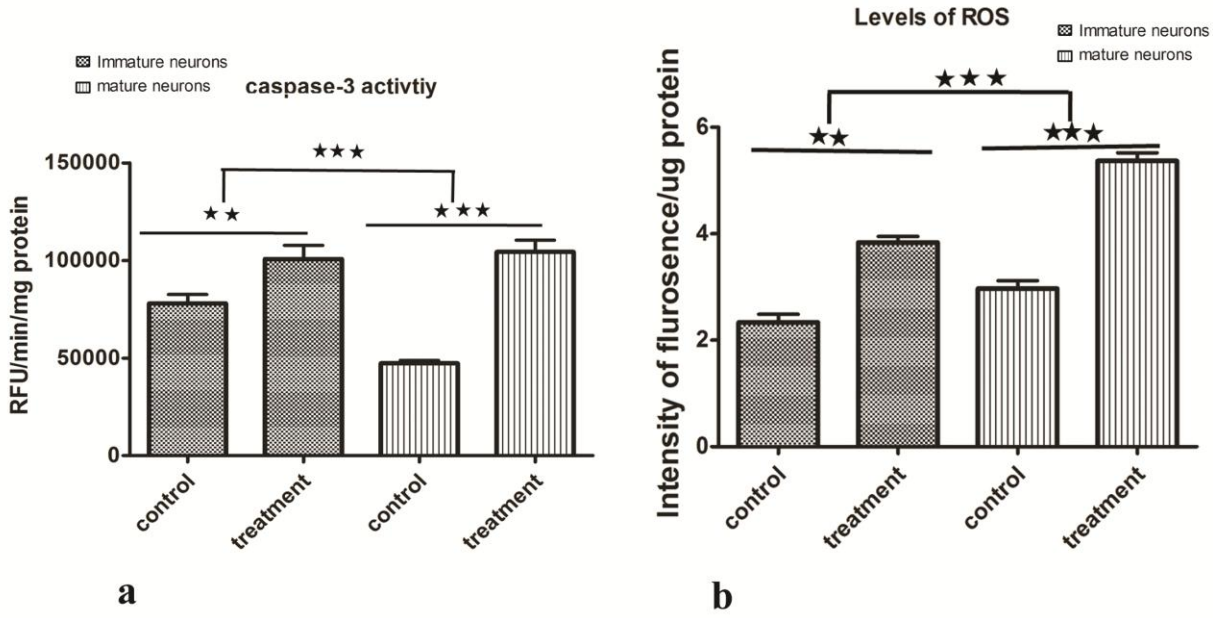
Immature neurons
mature neurons
caspase-3 activtiy
RFU/min/mg protein
150000
100000
50000
0
★★
★★★
★★★
control
treatment
control
treatment
a
Levels of ROS
Immature neurons
mature neurons
Intensity of flurosence/ug protein
6
4
2
0
★★
★★★
★★★
control
treatment
control
treatment
b

Fig 4.4: Curcumin mediated neuro protection against rotenone induced neurotoxicity in VM neurons *in-vitro*

a) Viability of Curcumin pretreated VM neurons, on rotenone treatment

VM neurons were pretreated with 1μM Curcumin, 5 h before treatment with 15nM rotenone. These immature and mature VM neurons, pretreated with Curcumin and VM neurons that were treated with rotenone alone were assessed for their viability after 48hrs. This was presented as % viability in a bar graph. Cells treated with DMSO alone were taken as controls and their viability was considered to be 100%. Cell viability was checked by MTT assay. Averages and standard deviations from three experiments were shown. Statistical significance was estimated by two way ANOVA followed by a post hoc analysis with **, $P < 0.01$. *** $P<0.001$.

b. Levels of ROS in Curcumin pretreated VM neurons, on rotenone treatment

VM neurons were pretreated with 1μM Curcumin, 5 h before treatment with 15nM rotenone. These immature and mature VM neurons, pretreated with Curcumin and VM neurons that were treated with rotenone alone were assessed for their ROS levels after 48 h using fluorescent dye CMH2DCFDA. Cells treated with DMSO alone were taken as control. Values were normalized for protein content and depicted as intensity of fluorescence per micro gram of protein. Averages and standard deviations from three experiments were shown. Statistical significance was estimated by two way ANOVA followed by a post hoc analysis with **, $P < 0.01$. *** $P<.001$.

Figure 4.4

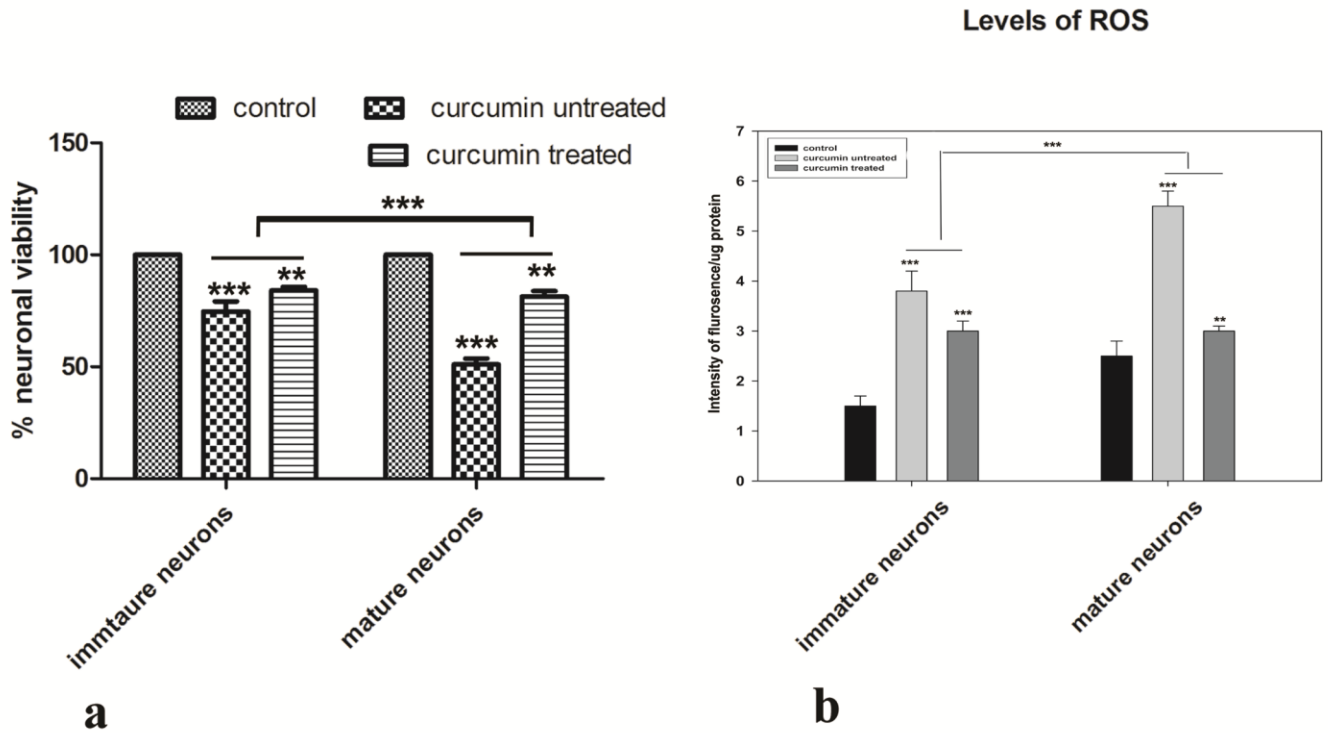
control
curcumin untreated
curcumin treated
% neuronal viability
150
100
50
0
***
**
***
**
***
immtaure neurons
mature neurons
a
Levels of ROS
control
curcumin untreated
curcumin treated
Intensity of flurosence/ug protein
7
6
5
4
3
2
1
0
***
***
***
***
**
immature neurons
mature neurons
b

Fig 4.5: Heat map of differentially regulated gene expression in rotenone treated VM neurons

Heat map represents the entire genome of rat VM neurons and display statistically significant ($P<0.05$ with multiple testing corrections applied). A fold change of 0.6 was used to detect the up-regulation and down-regulation in each of the treated replicates with a gemometrican mean fold of 0.8. Expression signals were nromalized usig Genespring GX 12.6.1 software and were presented on a log scale, where lower levels of expression was represented in colder colours and higher levels of expression was represented in warmer colours. Control cells were treated with DMSO alone. Maximum fold change observed in up-regulated genes and down-regulated genes was 7.75 and - 6.59 respectively.

Figure 4.5

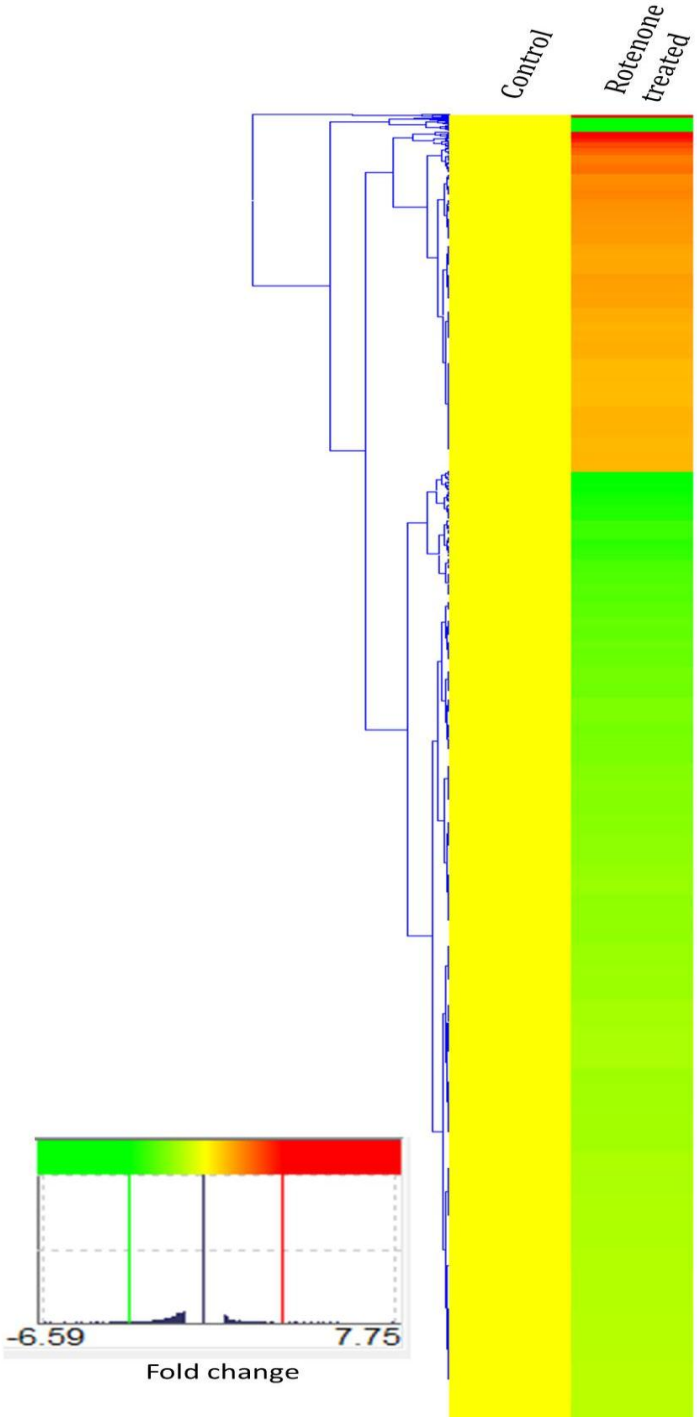

Fig 4.6: Validation of differential gene expression by q-RT PCR

a. 15 nM rotenone treated VM neuronal transcriptome was analyzed for the expression levels of above genes when compared to control VM neurons treated with DMSO alone. Values were represented as fold change in mean ± SD and n=3. Paired t test was performed to determine statistical significance. (***P<0.0005)

b. 100 nM rotenone treated SK-N-SH cellular transcriptome was analyzed for the expression levels of above genes when compared to control SK-N-SH cells treated with DMSO alone. Values were represented as fold change in mean ± SD and n=3. Paired t test was performed to determine statistical significance. (*P<0.05; **P<0.005; ****P <0.0005)

Figure 4.6

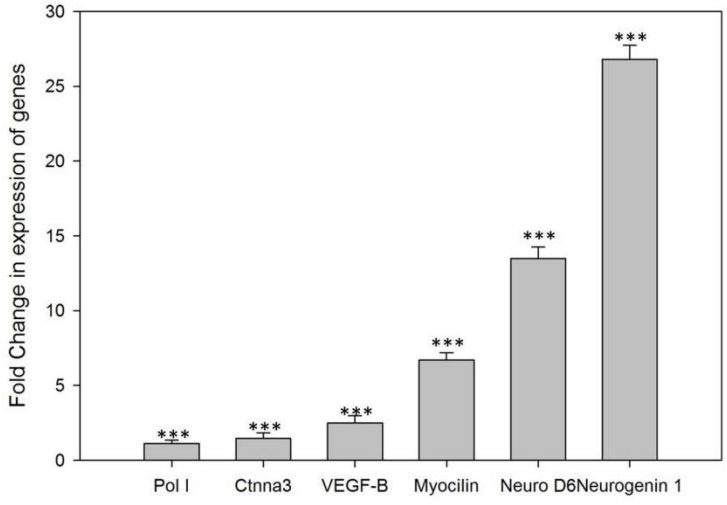
Fold Change in expression of genes
30
25
20
15
10
5
0
***
***
***
***
***
***
Pol I
Ctnna3
VEGF-B
Myocilin
Neuro D6
Neurogenin 1

a

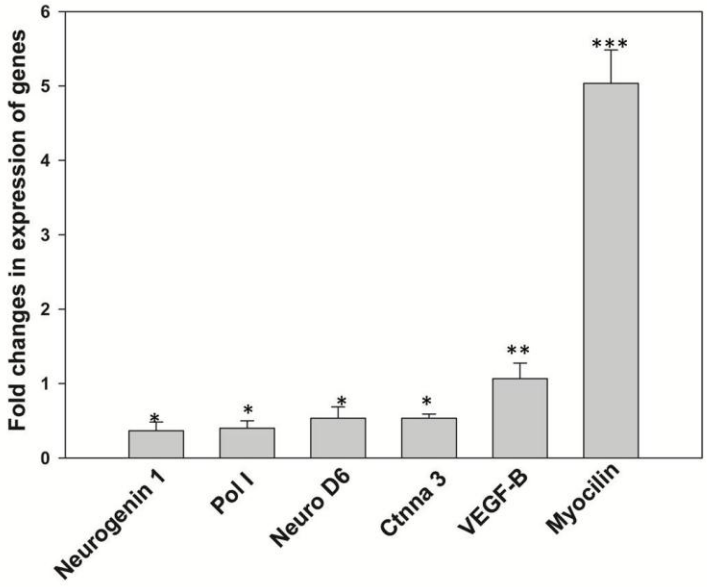
Fold changes in expression of genes
6
5
4
3
2
1
0
*
*
*
*
**
***
Neurogenin 1
Pol I
Neuro D6
Ctnna 3
VEGF-B
Myocilin

b

Fig 4.7: Myocilin knocked down SK-N-SH cells on rotenone treatment

a. Myocilin expression was knocked down in SK-N-SH cells by transfecting with siRNA. Reduction in myocilin expression was confirmed by corresponding western blot. B-actin was taken as a loading control.

b. Viability of myocilin knocked down SK-N-SH cells after rotenone treatment was estimated by MTT assay. Cells treated with DMSO alone were taken as control and considered to be 100% viable. Data was presented in mean ± SD (n=3). Satistical significance was tested with paired t test with *P<0.05; **P<0.005; ***P<0.0005.

c. LDH released into myocilin knocked down SK-N-SH cells after rotenone treatment was estimated by LDH release assay. Cells treated with DMSO alone were taken as control and considered to be 100% viable. These control values were subtracted from treated samples and present as ΔLDH U/L. Data was presented in mean ± SD (n=3). Satistical significance was tested with paired t test with *P<0.05; **P<0.005; ***P<0.0005.

Figure 4.7

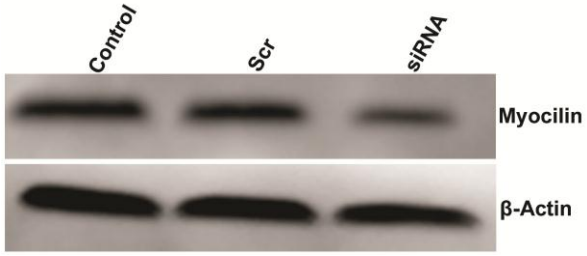

a

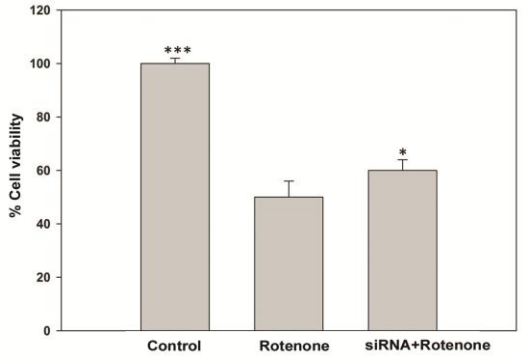

b

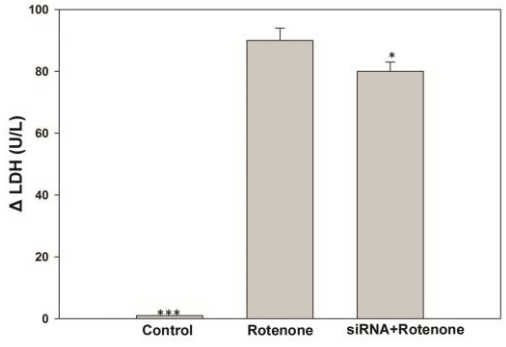

c

Fig 4.8: Parkinsonian features in rotenone treated SK-N-SH cells

a. Parkinosonian feature like elevated ROS levels wer estimated in rotenone treated SK-N-SH cells, rotenone + myocilin siRNA transfected SK-N-SH using fluorescent dye CMH2DCFDA. Values were normalized for protein content and depicted as intensity of fluorescence per micro gram of protein. Control cells were treated with DMSO alone. Averages and standard deviations from three experiments were shown. Statistical significance was estimated by paired t test with *** $P<0.0005$.

b. Parkinsonian features like reduced TH expression and increased α-synuclein expression was found in rotenone treated SK-N-SH cells. Myocilin expression knocked down cells had not shown any inhibition of rotenone induced parkinsonian features. Red fluorescence represents TH expression (marked with arrows) and green fluorescence represents α-synuclein expression. Nucleus was stained with DAPI (Blue).

Figure 4.8

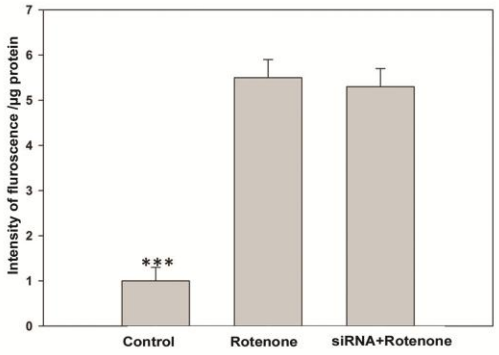
Intensity of fluroscence /µg protein
7
6
5
4
3
2
1
0
***
Control
Rotenone
siRNA+Rotenone

a

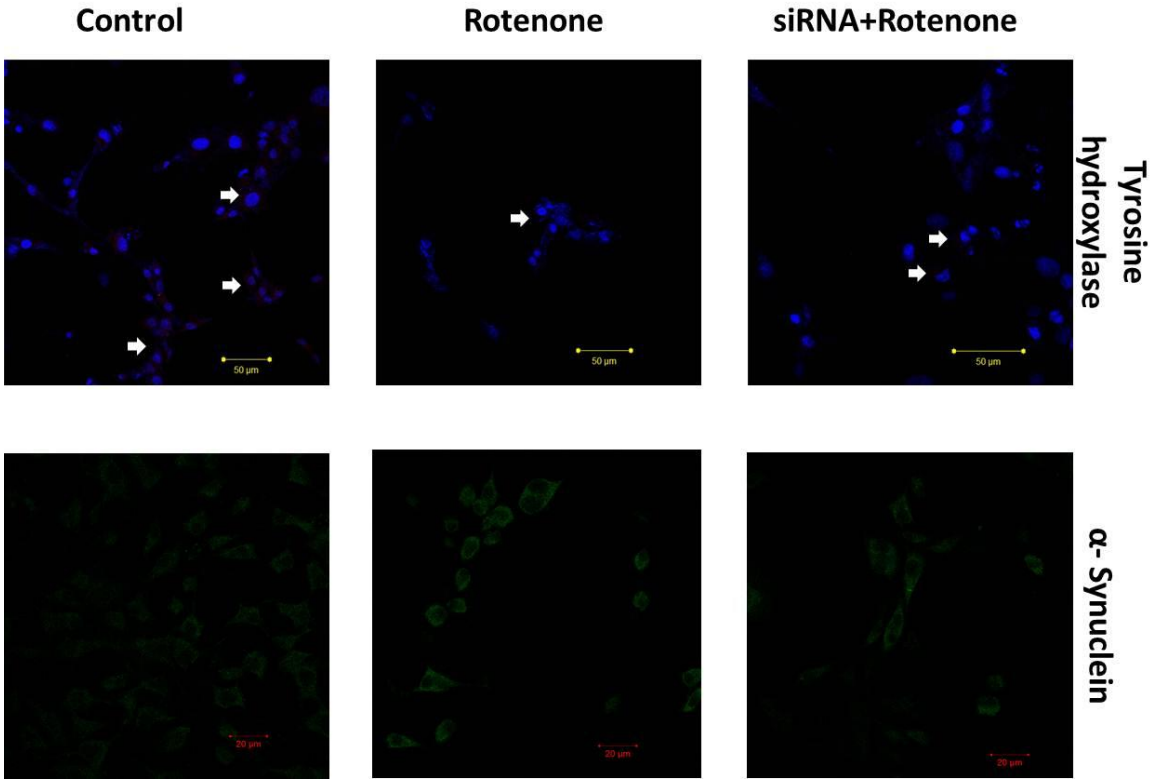
Control
Rotenone
siRNA+Rotenone
Tyrosine hydroxylase
α- Synuclein
50 µm
20 µm

b

Table 4.1: Pathways with involvement of up-regulated genes

Pathway name	Kegg ID	Genes	No. of genes
Metabolic pathways	mmu01100	BAAT,GAD2,P4HA3,PLA2G12A,ENO3,ACMSD,TGDS,HDC,PAH,CBS,HSD11B2,HSD11B1,PIPOX,NOS3,POLR3GL,SLC27A5,SLC33A1,DPYD,ASNS,GLS2,ALDOC,ACER2,ABAT,COX6A2,MAOB,ALG13	26
MAPK signaling pathway	mmu04010	PPP3R2,CACNB4,PRKX,GADD45G,PLA2G12A,MAP3K9,RPS6KA5,FGFR3,DUSP1,CACNA1E,FGF8,NTRK2	12
Pathways in cancer	mmu05200	LEF1,WNT3,FGFR3,CTNNA3,RXRG,RB1,WNT7A,WNT8B,FGF8,VEGFB,VEGFA	11
Neuroactive ligand-receptor interaction	mmu04080	GPR83,HTR4,ADCYAP1R1,GRIK2,CHRNE,HRH1,PYY,TRPV1,NTSR2,GRP,NPY	11
Focal adhesion	mmu04510	ITGA7,RELN,THBS4,MYLK2,TNC,COL11A2,ROCK1,CAV2,VEGFB,VEGFA	10
Calcium	mmu040	PPP3R2,PRKX,HTR4,NOS3,TRPC1,MYLK2,HRH1,	9

signaling pathway	20	PHKA2,CACNA1E	
Wnt signaling pathway	mmu04310	PPP3R2,PRKX,LEF1,WNT3,CXXC4,WNT7A,WNT8B,ROCK1,NKD2	9
Cytokine-cytokine receptor interaction	mmu04060	IL7,INHBB,CCL19,ACVR2B,IL22RA2,IFNG,VEGFB,VEGFA	8
TGF-beta signaling pathway	mmu04350	PITX2,THBS4,INHBB,ACVR2B,IFNG,ROCK1	6
Axon guidance	mmu04360	PPP3R2,ROBO3,EPHB3,ABLIM3,SEMA3E,ROCK1	6
Melanogenesis	mmu04916	PRKX,LEF1,WNT3,WNT7A,WNT8B	5
Arrhythmogenic right	mmu05412	ITGA7,CACNB4,LEF1,CTNNA3,DMD	5

ventricular cardiomyopathy (A			
Bladder cancer	mmu05219	RPS6KA5,FGFR3,RB1,VEGFB,VEGFA	5
Regulation of actin cytoskeleton	mmu04810	ITGA7,FGFR3,MYLK2,ROCK1,FGF8	5
ECM-receptor interaction	mmu04512	ITGA7,RELN,THBS4,TNC,COL11A2	5
"""Alanine, aspartate and glutamate metabolism"""	mmu00250	GAD2,ACY3,ASNS,GLS2,ABAT	5

Drug metabolism - cytochrome P450	mmu00982	GSTO2,GSTM7,GSTT2,FMO5,MAOB	5
Vascular smooth muscle contraction	mmu04270	PRKX,PLA2G12A,MYLK2,AGT,ROCK1	5
Systemic lupus erythematosus	mmu05322	SNRPD1,HIST3H2BA,H2AFY,IFNG	4
Aldosterone-regulated sodium reabsorption	mmu04960	NEDD4L,HSD11B2,HSD11B1,ATP1B2	4

VEGF signaling pathway	mmu04370	PPP3R2,PLA2G12A,NOS3,VEGFA	4
Dilated cardiomyopathy (DCM)	mmu05414	ITGA7,CACNB4,PRKX,DMD	4
Oocyte meiosis	mmu04114	PPP3R2,PRKX,CPEB1,MAD2L2	4
Arginine and proline metabolism	mmu00330	P4HA3,NOS3,GLS2,MAOB	4
Notch signaling pathway	mmu04330	DLL3,DLL1,HES5,MFNG	4
Leukocyte transendothelial	mmu04670	VCAM1,CTNNA3,ROCK1,CLDN23	4

migration			
Endocytosis	mmu04144	NEDD4L,FGFR3,ACAP1,CAV2	4
Malaria	mmu05144	VCAM1,THBS4,IFNG,SELE	4
Basal cell carcinoma	mmu05217	LEF1,WNT3,WNT7A,WNT8B	4
Jak-STAT signaling pathway	mmu04630	IL7,IL22RA2,IFNG,SPRY2	4
Hedgehog signaling pathway	mmu04340	PRKX,WNT3,WNT7A,WNT8B	4
Hypertrophic cardiomyopathy (HCM)	mmu05410	ITGA7,CACNB4,DMD,AGT	4
"""Glycine, serine	mmu00260	CBS,PIPOX,MAOB	3

and threonine metabolism"""			
Pancreatic cancer	mmu05212	RB1,VEGFB,VEGFA	3
Histidine metabolism	mmu00340	HDC,ACY3,MAOB	3
Gastric acid secretion	mmu04971	PRKX,MYLK2,ATP1B2	3
Cell cycle	mmu04110	GADD45G,RB1,MAD2L2	3
Cell adhesion molecules (CAMs)	mmu04514	VCAM1,SELE,CLDN23	3
Peroxisome	mmu04146	BAAT,PIPOX,ABCD2	3

p53 signaling pathway	mmu04115	GADD45G,BBC3,CCNG1	3
Progesterone-mediated oocyte maturation	mmu04914	PRKX,CPEB1,MAD2L2	3
Cardiac muscle contraction	mmu04260	CACNB4,ATP1B2,COX6A2	3
beta-Alanine metabolism	mmu00410	GAD2,DPYD,ABAT	3
Bacterial invasion of	mmu05100	CTNNA3,MAD2L2,CAV2	3

epithelial cells			
Ubiquitin mediated proteolysis	mmu04120	NEDD4L,UBE3A,BIRC6	3
Metabolism of xenobiotics by cytochrome P450	mmu00980	GSTO2,GSTM7,GSTT2	3
Amoebiasis	mmu05146	PRKX,COL11A2,IFNG	3
Chemokine signaling pathway	mmu04062	PRKX,CCL19,ROCK1	3
Pyrimidine metabolis	mmu00240	POLR3GL,DPYD,ENTPD1	3

m			
mTOR signaling pathway	mmu04150	DDIT4,VEGFB,VEGFA	3
Glutathione metabolism	mmu00480	GSTO2,GSTM7,GSTT2	3
Alzheimer's disease	mmu05010	PPP3R2,COX6A2	2
Tight junction	mmu04530	CTNNA3,CLDN23	2
Taurine and hypotaurine metabolism	mmu00430	BAAT,GAD2	2
Primary bile acid	mmu00120	BAAT,SLC27A5	2

biosynthesis			
Natural killer cell mediated cytotoxicity	mmu04650	PPP3R2,IFNG	2
Salivary secretion	mmu04970	PRKX,ATP1B2	2
Renal cell carcinoma	mmu05211	VEGFB,VEGFA	2
Purine metabolism	mmu00230	POLR3GL,ENTPD1	2
Non-small cell lung cancer	mmu05223	RXRG,RB1	2
Adipocytokine signaling	mmu04920	RXRG,NPY	2

pathway			
Hematopoietic cell lineage	mmu04640	IL7,CD9	2
Apoptosis	mmu04210	PPP3R2,PRKX	2
Ether lipid metabolism	mmu00565	PLA2G12A,ENPP2	2
Small cell lung cancer	mmu05222	RXRG,RB1	2
Glycolysis / Gluconeogenesis	mmu00010	ENO3,ALDOC	2
GnRH signaling pathway	mmu04912	PRKX,PLA2G12A	2

Spliceosome	mmu03040	SNRPD1,SF3B1	2
Insulin signaling pathway	mmu04910	PRKX,PHKA2	2
Prostate cancer	mmu05215	LEF1,RB1	2
Retinol metabolism	mmu00830	CYP26B1,LRAT	2
Phenylalanine metabolism	mmu00360	PAH,MAOB	2
Type I diabetes mellitus	mmu04940	GAD2,IFNG	2
Butanoate metabolism	mmu00650	GAD2,ABAT	2

T cell receptor signaling pathway	mmu04660	PPP3R2,IFNG	2
Huntington's disease	mmu05016	BBC3,COX6A2	2
PPAR signaling pathway	mmu03320	RXRG,SLC27A5	2
Nitrogen metabolism	mmu00910	ASNS,GLS2	2
Thyroid cancer	mmu05216	LEF1,RXRG	2
Neurotrophin signaling pathway	mmu04722	RPS6KA5,NTRK2	2
Steroid hormone	mmu00140	HSD11B2,HSD11B1	2

biosynthesis			
Melanoma	mmu05218	RB1,FGF8	2
Tryptophan metabolism	mmu00380	ACMSD,MAOB	2
Long-term potentiation	mmu04720	PPP3R2,PRKX	2
Endometrial cancer	mmu05213	LEF1,CTNNA3	2
Antigen processing and presentation	mmu04612	NFYB,IFNG	2
Proximal	mmu049	GLS2,ATP1B2	2

tubule bicarbonate reclamation	64		
Regulation of autophagy	mmu04140	GABARAPL1,IFNG	2
Adherens junction	mmu04520	LEF1,CTNNA3	2
Arachidonic acid metabolism	mmu00590	PLA2G12A	1
Biosynthesis of unsaturated fatty acids	mmu01040	BAAT	1
alpha-	mmu005	PLA2G12A	1

Linolenic acid metabolism	92		
D-Glutamine and D-glutamate metabolism	mmu00471	GLS2	1
B cell receptor signaling pathway	mmu04662	PPP3R2	1
Dorso-ventral axis formation	mmu04320	CPEB1	1
Long-term	mmu04730	PLA2G12A	1

depression			
Leishmaniasis	mmu05140	IFNG	1
Linoleic acid metabolism	mmu00591	PLA2G12A	1
Maturity onset diabetes of the young	mmu04950	NEUROD1	1
Proteasome	mmu03050	IFNG	1
Fc epsilon RI signaling pathway	mmu04664	PLA2G12A	1
Circadian	mmu047	RORB	1

rhythm - mammal	10		
Glycosaminoglycan degradation	mmu00531	HS3ST3A1	1
Cysteine and methionine metabolism	mmu00270	CBS	1
Selenoamino acid metabolism	mmu00450	CBS	1
Olfactory transduction	mmu04740	PRKX	1
Chagas	mmu051	IFNG	1

disease	42		
Amyotrophic lateral sclerosis (ALS)	mmu05014	PPP3R2	1
Oxidative phosphorylation	mmu00190	COX6A2	1
Graft-versus-host disease	mmu05332	IFNG	1
Primary immunodeficiency	mmu05340	RAG1	1
Drug metabolism - other enzymes	mmu00983	DPYD	1
Cytosolic	mmu046	POLR3GL	1

DNA-sensing pathway	23		
Tyrosine metabolism	mmu00350	MAOB	1
Taste transduction	mmu04742	PRKX	1
Viral myocilinarditis	mmu05416	DMD	1
Gap junction	mmu04540	PRKX	1
Acute myeloid leukemia	mmu05221	LEF1	1
Parkinson's disease	mmu05012	COX6A2	1
Colorectal	mmu052	LEF1	1

cancer	10		
Glycosphingolipid biosynthesis - ganglio series	mmu00604	SLC33A1	1
"""Valine, leucine and isoleucine degradation"""	mmu00280	ABAT	1
Complement and coagulation cascades	mmu04610	PROC	1
"""Phenylalanine, tyrosine	mmu00400	PAH	1

and tryptophan biosynthesi"""			
Glycosaminoglycan biosynthesis - heparan sulfate	mmu00534	HS3ST3A1	1
Glycerophospholipid metabolism	mmu00564	PLA2G12A	1
Glioma	mmu05214	RB1	1
Phagosome	mmu04145	THBS4	1
Lysine	mmu003	PIPOX	1

degradation	10		
N-Glycan biosynthesis	mmu00510	ALG13	1
Vasopressin-regulated water reabsorption	mmu04962	PRKX	1
Type II diabetes mellitus	mmu04930	CACNA1E	1
RNA polymerase	mmu03020	POLR3GL	1
ABC transporters	mmu02010	ABCD2	1

Chronic myeloid leukemia	mmu05220	RB1	1
Fructose and mannose metabolism	mmu00051	ALDOC	1
Pantothenate and CoA biosynthesis	mmu00770	DPYD	1
Renin-angiotensin system	mmu04614	AGT	1
RNA degradation	mmu03018	ENO3	1
Prion	mmu050	PRKX	1

diseases	20		
Sphingolipid metabolism	mmu00600	ACER2	1
Allograft rejection	mmu05330	IFNG	1
Propanoate metabolism	mmu00640	ABAT	1
Pentose phosphate pathway	mmu00030	ALDOC	1
SNARE interactions in vesicular transport	mmu04130	VAMP4	1

Table 4.2: Pathways with involvement of down regulated genes

Pathway name	Kegg ID	Genes	No. of genes
Metabolic pathways	mmu01100	NDUFA10,AGPAT2,XDH,PLCG2,BDH2,DHODH,PIGN,ALDH1A1,B3GALT5,PLA2G7,ADA,UPP1,TBXAS1,GMDS,NME4,CD38,ANPEP,QPRT,CBR3,TPH2,ACSM5,HPGDS,GDA,A4GALT,PRODH2,GK2,HSD3B6,DEGS2,PON3,POLE,HPSE2,HMGCS2,MBOAT1,GBA,SGMS2,ALOX5,NNMT,HAAO,GALNT10,KMO,DNMT3L,BCKDHB,AOX1,MTAP,B3GNT3,IDO1,GLB1,GCNT1,PTGS1,CYP2U1,DBH,SHMT1,CYP27A1,NAT1,GALNT4,CEL,ALDH3B1,BST1,MAN1C1,GGT5,PNP,PLA2G4E,DGKH,EPHX2,HSD17B1,ENPP3,CNDP1,PAPSS2,HPSE,SPHK1,DHRS4,UAP1,NDST1,PTGDS,TK1,PTGIS	76
Cytokine-	mmu04060	TNFRSF14,IL7R,TNFRSF1B,TNFRSF1A,IL15,IL10,IL18,IL1B,IL22,IL1R2,BMP7,BMP2,TNFSF13B,CCL3,CCL	60

cytokine receptor interaction		2,CCL9,CCL7,CCL6,GHR,IL10RA,IL10RB,CTF1,KDR,IL2RA,IFNGR1,CCR8,CCR5,CCR4,XCL1,C3,PGF,PF4,IL17RB,IL17RA,CXCL1,CXCL9,CXCR1,TGFBR2,LIFR,CSF1R,TGFB3,TGFB2,TGFB1,CSF3R,CXCL13,CXCL16,CXCL11,CXCL10,NGFR,IL4,CCL12,CCL11,CCL20,CCL28,TNFSF15,TNFRSF8,IL4RA,TNFSF9,TNF,IL21R	
Pathways in cancer	mmu05200	ITGA6,TCF7L1,PLCG2,RAD51,WNT9A,FZD6,BMP2,BIRC3,NFKB2,WNT6,CDKN2B,E2F3,STAT5A,CASP8,MMP9,FN1,CEBPA,GLI2,FGF3,GLI1,FGF7,CDH1,PGF,CDK6,FGF10,FGF18,RAC2,TGFBR2,CSF1R,TGFB3,TGFB2,TGFB1,CSF3R,NTRK1,WNT2B,WNT16,CCNE1,CCNE2,FADD,STAT1,RUNX1	41
Neuroactive ligand-receptor interaction	mmu04080	GLP2R,CHRNA2,CHRNA5,NTS,PTAFR,PTGER3,PTGER2,PTGER1,SCT,AGTR1A,GHR,HTR2B,POMC,HTR1A,F2RL2,GRIN2A,MAS1,EDNRA,OPRK1,GHRHR,CHRM1,GCGR,NPBWR1,SSTR4,CNR2,GRIA1,P2RX4,P2RX3,NPFFR1,GPR50,P2RY6,P2RY2,C3AR1,NPY1R,NPY5R,C5AR1,TSPO,P2RY13,P2RY14,LPAR6	40
Chemo	mmu04	PRKCD,FGR,GNG5,NCF1,RAP1B,GNG11,CCL3,CCL	37

kine signalin g pathwa y	062	2,CCL9,CCL7,CCL6,SHC3,CCR8,CCR5,CCR4,VAV1,XC L1,PF4,HCK,JAK3,CXCL1,CXCL9,RAC2,PXN,CXCR1, ADCY4,CXCL13,CXCL16,ADCY7,CXCL11,CXCL10,C CL12,CCL11,CCL20,LYN,CCL28,STAT1	
Cell adhesio n molecul es (CAMs)	mmu04 514	ITGA6,ITGA8,ITGAM,ITGB2,SDC1,CD86,CD99,CD8 A,SIGLEC1,CLDN22,CLDN17,CLDN11,OCLN,MADC AM1,ALCAM,CD4,PECAM1,CLDN4,CDH1,CDH3,CD 274,F11R,CNTNAP1,ICAM2,ICAM1,MPZ,PTPRC	27
Chagas disease	mmu05 142	MYD88,TNFRSF1A,IL10,IL1B,TLR2,TLR4,TLR6,TLR9 ,CD3G,IRAK4,CCL3,CCL2,CASP8,IFNGR1,C1QC,C1Q A,C1QB,C3,GNA14,GNA15,TGFBR2,TGFB3,TGFB2,T GFB1,CCL12,FADD,TNF	27
Toll-like recepto r	mmu04 620	MYD88,IL1B,CD86,TLR2,TLR3,TLR4,TLR6,TLR7,TLR 8,TLR9,CD14,IKBKE,IRAK4,CCL3,CASP8,SPP1,LY96, MAP3K8,CXCL9,CXCL11,CXCL10,IRF5,IRF7,FADD,S TAT1,TNF	26

signaling pathway			
Phagosome	mmu04145	ITGA5,ITGAM,ITGB5,ITGB2,CYBA,CYBB,NCF2,NCF1,NCF4,TUBB6,FCGR2B,TLR2,TLR4,TLR6,CD14,COLEC12,PLA2R1,THBS1,CTSS,MRC1,C3,CD209F,TFRC,SCARB1,MARCO,MSR1	26
Leukocyte transendothelial migration	mmu04670	ITGAM,ITGB2,PLCG2,CYBA,CYBB,NCF2,NCF1,NCF4,CD99,MYL9,RAP1B,CLDN22,CLDN17,CLDN11,OCLN,SIPA1,MMP9,PECAM1,CLDN4,VAV1,VCL,F11R,RAC2,PXN,ICAM1	25
Regulation of actin cytoskeleton	mmu04810	ITGA5,ITGA6,ITGA8,ITGAX,ITGAM,ITGB5,ITGB2,MYL9,CD14,MYH9,IQGAP1,FN1,ARPC5L,FGF3,FGF7,ARPC1B,VAV1,FGF10,FGF18,VCL,RAC2,PXN,CHRM1,NCKAP1L	24

Hematopoietic cell lineage	mmu04640	ITGA5,ITGA6,IL7R,ITGAM,IL1B,CD8A,IL1R2,CD14,CD37,CD38,CD33,ANPEP,CD3G,CD4,IL2RA,TFRC,CR2,CSF1R,CSF3R,IL4,GP1BA,GP1BB,IL4RA,TNF	24
Complement and coagulation cascade	mmu04610	THBD,FGA,C1S,A2M,VWF,SERPING1,C1QC,C1QA,C1QB,F7,C3,C6,C2,PLAU,CFB,CFH,CFI,CFD,CR2,PLAUR,C3AR1,F10,MASP1,C5AR1	24
MAPK signaling pathway	mmu04010	TNFRSF1A,IL1B,IL1R2,FLNA,CD14,RAP1B,NFKB2,MAP3K13,RASGRF1,FGF3,FGF7,FGF10,MAP3K8,FGF18,RAC2,TGFBR2,TGFB3,TGFB2,TGFB1,NTRK1,PLA2G4E,PTPN7,TNF,NTF3	24
Focal adhesion	mmu04510	ITGA5,ITGA6,ITGA8,ITGB5,FLNA,MYL9,RAP1B,BIRC3,THBS1,SHC3,RASGRF1,VWF,KDR,SPP1,FN1,VAV1,PGF,VCL,RAC2,PXN,PARVA,PARVG	22
Jak-STAT	mmu04630	IL7R,IL15,IL10,IL22,IL13RA2,SPRY4,GHR,IL10RA,IL10RB,CTF1,STAT5A,IL2RA,IFNGR1,JAK3,LIFR,CSF3R,	22

signaling pathway		IL4,IL4RA,STAT1,STAT6,PTPN6,IL21R	
Leishmaniasis	mmu05140	MYD88,ITGAM,ITGB2,CYBA,IL10,IL1B,NCF2,NCF1,NCF4,TLR2,TLR4,IRAK4,IFNGR1,C3,TGFB3,TGFB2,TGFB1,IL4,STAT1,PTPN6,TNF	21
Amoebiasis	mmu05146	ITGAM,ITGB2,IL10,IL1B,TLR2,TLR4,IL1R2,CD14,SERPINB6B,SERPINB9,SERPINB2,FN1,SERPINB1A,SERPINB1B,VCL,GNA14,GNA15,TGFB3,TGFB2,TGFB1,TNF	21
Malaria	mmu05144	MYD88,ITGB2,SDC1,IL10,IL18,IL1B,TLR2,TLR4,TLR9,CCL2,THBS1,PECAM1,KLRB1B,TGFB3,TGFB2,TGFB1,CCL12,GYPC,ICAM1,TNF,KLRA1	21
Cell cycle	mmu04110	ATM,BUB1,SFN,MCM2,MCM3,MCM5,MCM6,ANAPC11,CDKN1C,CDKN2B,E2F3,CDK6,CDC6,TGFB3,TGFB2,TGFB1,CCNE1,CCNE2,CDC25C,CCNA2	20
Systemic lupus erythe	mmu05322	IL10,CD86,FCGR2B,C1S,HIST2H4,HIST1H4B,HIST1H4M,GRIN2A,C1QC,C1QA,C1QB,C3,C6,C2,HIST1H2BF,HIST1H2BH,HIST1H2AC,HIST3H2A,TNF	19

matosus			
Calcium signaling pathway	mmu04020	PLCG2,PTAFR,PTGER3,PTGER1,ITPR3,CD38,AGTR1A,HTR2B,GRIN2A,EDNRA,GNA14,GNA15,BST1,CHRM1,ADCY4,ADCY7,P2RX4,P2RX3,SPHK1	19
Endocytosis	mmu04144	CHMP4C,FOLR2,DAB2,KDR,IL2RA,PSD4,CCR5,ARAP1,TFRC,CXCR1,TGFBR2,CSF1R,TGFB3,TGFB2,TGFB1,NTRK1,EHD4,RAB11FIP1,EPN3	19
Natural killer cell mediated cytotoxicity	mmu04650	TYROBP,ITGB2,PLCG2,CD48,SHC3,IFNGR1,LCP2,VAV1,HCST,CD244,RAC2,KLRB1B,ICAM2,ICAM1,PTPN6,TNF,KLRA1,FCER1G	18
NOD-like	mmu04621	IL18,IL1B,BIRC3,CCL2,CCL7,NAIP5,CASP8,CASP1,PSTPIP1,PYCARD,CXCL1,MEFV,NLRP3,CCL12,CCL11,	18

receptor signaling pathway		CARD9,NLRC4,TNF	
Apoptosis	mmu04210	ATM,MYD88,TNFRSF1A,CASP12,IL1B,TRADD,BIRC3,IRAK3,IRAK4,IRAK2,CASP8,CASP6,CAPN1,NTRK1,ENDOD1,FADD,TNF	17
B cell receptor signaling pathway	mmu04662	PLCG2,CD72,FCGR2B,CD79B,BTK,BLNK,VAV1,RAC2,IFITM1,CR2,INPP5D,LYN,DAPP1,PTPN6,LILRB3,PIK3AP1	16
Purine metabolism	mmu00230	XDH,ADA,GUCY2C,NME4,GDA,ADCY10,POLE,ENTPD4,PDE5A,PDE6A,PNP,ADCY4,ADCY7,ENPP3,NPR1,PAPSS2	16
Dilated	mmu05	ITGA5,ITGA6,ITGA8,ITGB5,TPM2,TPM1,DES,TNNT	15

cardio myopathy (DCM)	414	2,TGFB3,TGFB2,TGFB1,ADCY4,ADCY7,TNF,TTN	
Lysosome	mmu04142	CD68,CLN5,LAPTM5,SLC11A1,GBA,ENTPD4,CTSE, CTSH,CTSS,CTSZ,CTSA,LGMN,GLB1,NAPSA,SUMF1	15
Vascular smooth muscle contraction	mmu04270	PRKCD,PRKG1,ITPR3,MYL9,KCNMB1,AGTR1A,MRVI1,EDNRA,ACTG2,ADCY4,ADCY7,PLA2G4E,NPPC,NPR1,RAMP1	15
Fc gamma R-mediated phagocytosis	mmu04666	PRKCD,PLCG2,NCF1,FCGR2B,ARPC5L,ARPC1B,VAV1,HCK,RAC2,INPP5D,PLA2G4E,LYN,SPHK1,PTPRC	14
Arachid	mmu00	TBXAS1,CBR3,HPGDS,ALOX5,GPX2,GPX7,PTGS1,C	13

onic acid metabolism	590	YP2U1,GGT5,PLA2G4E,EPHX2,PTGDS,PTGIS	
T cell receptor signaling pathway	mmu04660	DLG1,TEC,IL10,CD8A,CD3G,CD4,LCP2,VAV1,MAP3K8,IL4,PTPN6,TNF,PTPRC	13
Hypertrophic cardiomyopathy (HCM)	mmu05410	ITGA5,ITGA6,ITGA8,ITGB5,TPM2,TPM1,DES,TNNT2,TGFB3,TGFB2,TGFB1,TNF,TTN	13
Tight junction	mmu04530	PRKCD,MYL9,CLDN22,CLDN17,CLDN11,OCLN,MYH4,MYH9,CLDN4,HCLS1,F11R,MYH15	12

Fc epsilon RI signaling pathway	mmu04664	PRKCD,PLCG2,BTK,LCP2,VAV1,RAC2,INPP5D,PLA2G4E,IL4,LYN,TNF,FCER1G	12
Neurotrophin signaling pathway	mmu04722	PRKCD,IRS3,ARHGDIB,PLCG2,RAP1B,IRAK3,IRAK4,IRAK2,SHC3,NTRK1,NGFR,NTF3	12
Alzheimer's disease	mmu05010	NDUFA10,TNFRSF1A,CASP12,IL1B,ITPR3,CASP8,GRIN2A,CAPN1,LPL,FADD,TNF	11
ECM-receptor interact	mmu04512	ITGA5,ITGA6,ITGA8,ITGB5,SDC1,THBS1,VWF,SPP1,FN1,GP1BA,GP1BB	11

ion			
Bacterial invasion of epithelial cells	mmu05100	ITGA5,SHC3,FN1,ARPC5L,ARPC1B,CDH1,HCLS1,RHOG,VCL,PXN,ARHGAP10	11
Pancreatic cancer	mmu05212	RAD51,E2F3,PGF,CDK6,RAC2,TGFBR2,TGFB3,TGFB2,TGFB1,STAT1	10
RIG-I-like receptor signaling pathway	mmu04622	TRADD,IKBKE,CASP8,TRIM25,ISG15,TMEM173,CXCL10,IRF7,FADD,TNF	10
PPAR signalin	mmu03320	NR1H3,CPT1A,GK2,HMGCS2,FABP4,FABP1,CYP27A1,APOA2,LPL,ANGPTL4	10

g pathway			
Adherens junction	mmu04520	TCF7L1,IQGAP1,CDH1,FARP2,VCL,RAC2,TGFBR2,SNAI2,PVRL4,PTPN6	10
Melanogenesis	mmu04916	TCF7L1,WNT9A,FZD6,WNT6,POMC,ADCY4,ADCY7,WNT2B,WNT16	9
Salivary secretion	mmu04970	PRKG1,FXYD2,ITPR3,CD38,KCNN4,BST1,ADCY4,ADCY7,SLC4A2	9
TGF-beta signaling pathway	mmu04350	BMP7,BMP2,THBS1,CDKN2B,TGFBR2,TGFB3,TGFB2,TGFB1,TNF	9
Gastric acid	mmu04971	CFTR,ITPR3,KCNJ15,KCNJ16,KCNJ10,KCNJ1,ADCY4,ADCY7,SLC4A2	9

secretion			
Oocyte meiosis	mmu04114	BUB1,ITPR3,ANAPC11,PGR,ADCY4,ADCY7,CCNE1,CCNE2,CDC25C	9
Cytosolic DNA-sensing pathway	mmu04623	IL18,IL1B,IKBKE,CASP1,PYCARD,RIPK3,TMEM173,CXCL10,IRF7	9
Viral myocilinarditis	mmu05416	ITGB2,CD86,CXADR,MYH4,MYH9,CASP8,RAC2,ICAM1,MYH15	9
Chronic myeloid leukemia	mmu05220	SHC3,E2F3,STAT5A,CDK6,TGFBR2,TGFB3,TGFB2,TGFB1,RUNX1	9
Basal cell	mmu05217	TCF7L1,WNT9A,FZD6,BMP2,WNT6,GLI2,GLI1,WNT2B,WNT16	9

carcinoma			
Hedgehog signaling pathway	mmu04340	WNT9A,NHEJ1,BMP7,BMP2,WNT6,GLI2,GLI1,WNT2B,WNT16	9
Wnt signaling pathway	mmu04310	TCF7L1,WNT9A,FZD6,WNT6,SFRP4,SFRP5,RAC2,WNT2B,WNT16	9
Glutathione metabolism	mmu00480	OPLAH,MGST2,ANPEP,GPX2,GPX7,GSTA2,GSTA3,GGT5,GSTM2	9
Arrhythmogenic right	mmu05412	ITGA5,ITGA6,ITGA8,TCF7L1,ITGB5,DES,PKP2,GJA1	8

ventricular cardiomyopathy (A			
Small cell lung cancer	mmu05222	ITGA6,BIRC3,CDKN2B,E2F3,FN1,CDK6,CCNE1,CCNE2	8
Intestinal immune network for IgA production	mmu04672	IL15,IL10,CD86,TNFSF13B,MADCAM1,TGFB1,IL4,CCL28	8
Amyotrophic	mmu05014	TNFRSF1B,TNFRSF1A,CASP12,CASP1,GRIN2A,NEFH,GRIA1,TNF	8

lateral sclerosis (ALS)			
Axon guidance	mmu04360	FES,UNC5C,RHOD,RAC2,NTNG1,EFNB1,SEMA3D,SEMA3A	8
Primary immunodeficiency	mmu05340	IL7R,CD8A,ADA,BTK,CD4,BLNK,JAK3,PTPRC	8
Adipocytokine signaling pathway	mmu04920	IRS3,TNFRSF1B,TNFRSF1A,TRADD,CPT1A,POMC,TNF	7
p53 signaling pathwa	mmu04115	ATM,SFN,THBS1,CASP8,CDK6,CCNE1,CCNE2	7

y			
Nicotinate and nicotinamide metabolism	mmu00760	CD38,QPRT,NNMT,AOX1,BST1,PNP,ENPP3	7
Taste transduction	mmu04742	ITPR3,TAS2R144,TAS2R138,TAS2R137,TAS2R119,TAS2R125,ADCY4	7
Gap junction	mmu04540	PRKG1,TUBB6,ITPR3,HTR2B,ADCY4,ADCY7,GJA1	7
Progesterone-mediated oocyte maturation	mmu04914	BUB1,ANAPC11,PGR,ADCY4,ADCY7,CDC25C,CCNA2	7

Melanoma	mmu05218	E2F3,FGF3,FGF7,CDH1,CDK6,FGF10,FGF18	7
Prion diseases	mmu05020	CASP12,IL1B,EGR1,C1QC,C1QA,C1QB,C6	7
Antigen processing and presentation	mmu04612	B2M,CD74,CD8A,CD4,CTSS,LGMN,TNF	7
Pyrimidine metabolism	mmu00240	DHODH,UPP1,NME4,POLE,ENTPD4,PNP,TK1	7
Aldosterone-regulated sodium reabsorption	mmu04960	IRS3,FXYD2,SFN,SLC9A3R2,NR3C2,KCNJ1	6

Glycerolipid metabolism	mmu00561	AGPAT2,GK2,MBOAT1,CEL,LPL,DGKH	6
Renal cell carcinoma	mmu05211	RAP1B,PGF,TGFB3,TGFB2,TGFB1,ETS1	6
VEGF signaling pathway	mmu04370	PLCG2,KDR,RAC2,PXN,PLA2G4E,SPHK1	6
DNA replication	mmu03030	MCM2,MCM3,MCM5,MCM6,POLE,DNA2	6
Colorectal cancer	mmu05210	TCF7L1,RAC2,TGFBR2,TGFB3,TGFB2,TGFB1	6
Metabo	mmu00	MGST2,GSTA2,GSTA3,ALDH3B1,CYP1B1,GSTM2	6

lism of xenobiotics by cytochrome P450	980		
Renin-angiotensin system	mmu04614	ACE2,ANPEP,AGTR1A,CPA3,CTSA,MAS1	6
Tryptophan metabolism	mmu00380	TPH2,HAAO,KMO,AOX1,IDO1,CYP1B1	6
Drug metabolism - cytochrome P450	mmu00982	MGST2,AOX1,GSTA2,GSTA3,ALDH3B1,GSTM2	6

Long-term depression	mmu04730	PRKG1,ITPR3,PLA2G4E,LYN,GRIA1	5
Bladder cancer	mmu05219	THBS1,E2F3,MMP9,CDH1,PGF	5
GnRH signaling pathway	mmu04912	PRKCD,ITPR3,ADCY4,ADCY7,PLA2G4E	5
Parkinson's disease	mmu05012	NDUFA10,SLC6A3,UBE2L6,SLC18A2,UBE1Y1	5
Glycerophospholipid metabolism	mmu00564	AGPAT2,MBOAT1,LCAT,PLA2G4E,DGKH	5
Nitroge	mmu00	CAR13,CAR12,CAR8,CAR4,CAR7	5

n metabolism	910		
Asthma	mmu05310	IL10,IL4,CCL11,TNF,FCER1G	5
Sphingolipid metabolism	mmu00600	DEGS2,GBA,SGMS2,GLB1,SPHK1	5
Autoimmune thyroid disease	mmu05320	IL10,CD86,TG,IL4	4
Histidine metabolism	mmu00340	ASPA,FTCD,ALDH3B1,CNDP1	4
Peroxisome	mmu04146	XDH,EPHX2,SOD2,DHRS4	4
Graft-	mmu05	IL1B,CD86,TNF,KLRA1	4

versus-host disease	332		
Drug metabolism - other enzyme	mmu00983	XDH,UPP1,NAT1,TK1	4
Insulin signaling pathway	mmu04910	IRS3,SHC3,INPP5D,PYGL	4
Prostate cancer	mmu05215	TCF7L1,E2F3,CCNE1,CCNE2	4
Acute myeloid leukemia	mmu05221	TCF7L1,STAT5A,CEBPA,RUNX1	4

Cardiac muscle contraction	mmu04260	FXYD2,TPM2,TPM1,TNNT2	4
Huntington's disease	mmu05016	NDUFA10,CASP8,TGM2,SOD2	4
Glioma	mmu05214	PLCG2,SHC3,E2F3,CDK6	4
Ubiquitin mediated proteolysis	mmu04120	BIRC3,ANAPC11,UBE2L6,UBE1Y1	4
ABC transporters	mmu02010	CFTR,ABCG3,ABCG2,ABCG5	4
Steroid hormo	mmu00140	HSD3B6,CYP7B1,HSD17B1,CYP1B1	4

ne biosynthesis			
Amino sugar and nucleotide sugar metabolism	mmu00520	GMDS,AMDHD2,CMAH,UAP1	4
Long-term potentiation	mmu04720	ITPR3,RAP1B,GRIN2A,GRIA1	4
Phosphatidylinositol signaling	mmu04070	PLCG2,ITPR3,INPP5D,DGKH	4

system			
ErbB signaling pathway	mmu04012	PLCG2,SHC3,STAT5A,NRG2	4
Allograft rejection	mmu05330	IL10,CD86,IL4,TNF	4
Non-small cell lung cancer	mmu05223	PLCG2,E2F3,CDK6	3
Glycosaminoglycan biosynthesis -	mmu00532	CHST11,CHST14,DSE	3

chondroitin sulfa			
Proteasome	mmu03050	PSMB9,PSMB8,PSMA8	3
Glycosaminoglycan degradation	mmu00531	HPSE2,GLB1,HPSE	3
O-Glycan biosynthesis	mmu00512	GALNT10,GCNT1,GALNT4	3
Retinol metabolism	mmu00830	ALDH1A1,RETSAT,DHRS4	3
Tyrosine metabo	mmu00350	AOX1,DBH,ALDH3B1	3

lism			
Type I diabetes mellitus	mmu04940	IL1B,CD86,TNF	3
Sulfur metabolism	mmu00920	CHST11,PAPSS2,SULT1A1	3
Butanoate metabolism	mmu00650	BDH2,ACSM5,HMGCS2	3
"""Valine, leucine and isoleucine degradation"""	mmu00280	HMGCS2,BCKDHB,AOX1	3

Thyroid cancer	mmu05216	TCF7L1,CDH1,NTRK1	3
Type II diabetes mellitus	mmu04930	PRKCD,IRS3,TNF	3
Porphyrin and chlorophyll metabolism	mmu00860	HMOX1,CP,BLVRA	3
Glycosphingolipid biosynthesis - lacto and	mmu00601	B3GALT5,B3GNT3,FUT7	3

neolact			
Glycosphingolipid biosynthesis - globo series	mmu00603	B3GALT5,A4GALT	2
"""Glycine, serine and threonine metabolism"""	mmu00260	CHDH,SHMT1	2
Primary bile acid biosynt	mmu00120	CYP7B1,CYP27A1	2

hesis			
Synthesis and degradation of ketone bodies	mmu00072	BDH2,HMGCS2	2
Dorso-ventral axis formation	mmu04320	ETV6,ETS1	2
Maturity onset diabetes of the young	mmu04950	IAPP,HHEX	2
One carbon pool by	mmu00670	SHMT1,FTCD	2

folate			
Cysteine and methionine metabolism	mmu00270	DNMT3L,MTAP	2
Ether lipid metabolism	mmu00565	PLA2G7,PLA2G4E	2
Selenoamino acid metabolism	mmu00450	GGT5,PAPSS2	2
Notch signaling pathwa	mmu04330	MAML2,DTX3L	2

y			
Glycosphingolipid biosynthesis - ganglio series	mmu00604	GLB1,ST6GALNAC2	2
Lysine degradation	mmu00310	BBOX1,PLOD1	2
Steroid biosynthesis	mmu00100	SOAT1,CEL	2
Cyanoamino acid metabolism	mmu00460	SHMT1,GGT5	2
Caffein	mmu00	XDH,NAT1	2

e metabolism	232		
Pantothenate and CoA biosynthesis	mmu00770	ENPP3,VNN1	2
Other glycan degradation	mmu00511	GBA,GLB1	2
Endometrial cancer	mmu05213	TCF7L1,CDH1	2
Proximal tubule bicarbo	mmu04964	SLC38A3,FXYD2	2

nate reclamation			
SNARE interactions in vesicular transport	mmu04130	VAMP8,STX17	2
Starch and sucrose metabolism	mmu00500	ENPP3,PYGL	2
Pyruvate metabolism	mmu00620	ACOT12,ACYP2	2

Base excision repair	mmu03410	POLE,PARP3	2
alpha-Linolenic acid metabolism	mmu00592	PLA2G4E	1
Taurine and hypotaurine metabolism	mmu00430	GGT5	1
Inositol phosphate metabolism	mmu00562	PLCG2	1
Nucleo	mmu03	POLE	1

tide excision repair	420		
Non-homologous end-joining	mmu03450	NHEJ1	1
Linoleic acid metabolism	mmu00591	PLA2G4E	1
Phototransduction	mmu04744	PDE6A	1
Glycosylphosphatidylinositol(GPI)-	mmu00563	PIGN	1

anchor biosynthe			
Riboflavin metabolism	mmu00740	ENPP3	1
Vitamin B6 metabolism	mmu00750	AOX1	1
Glycolysis / Gluconeogenesis	mmu00010	ALDH3B1	1
Olfactory transduction	mmu04740	PRKG1	1

Fatty acid metabolism	mmu00071	CPT1A	1
Arginine and proline metabolism	mmu00330	PRODH2	1
Homologous recombination	mmu03440	RAD51	1
Oxidative phosphorylation	mmu00190	NDUFA10	1
Spliceosome	mmu03040	SNRPF	1

Protein export	mmu03060	SPCS3	1
Phenylalanine metabolism	mmu00360	ALDH3B1	1
Galactose metabolism	mmu00052	GLB1	1
Glycosaminoglycan biosynthesis - heparan sulfate	mmu00534	NDST1	1
beta-Alanine	mmu00410	CNDP1	1

metabolism			
N-Glycan biosynthesis	mmu00510	MAN1C1	1
Vasopressin-regulated water reabsorption	mmu04962	ARHGDIB	1
Fructose and mannose metabolism	mmu00051	GMDS	1
RNA degrada	mmu03018	DCP1A	1

tion			
"""Alanine, aspartate and glutamate metabolism"""	mmu00250	ASPA	1
Pentose phosphate pathway	mmu00030	RBKS	1
Terpenoid backbone biosynthesis	mmu00900	HMGCS2	1

mTOR signaling pathway	mmu04150	PGF	1

Discussion:

The major symptoms of PD are a result of the profound and selective loss of neurons in the SNc region of the brain (Lang et al., 1998). Adult neurogenesis was reported earlier in ageing population (Tatsunori, Kazunobu et al., 2011) suggesting the presence of both immature and mature neurons in ageing brain. As neurodegenerative diseases occur at high frequency during ageing, it would be interesting to know if PD like features is exhibited by mature and/or immature neurons when treated with rotenone. As reported earlier, VM neurons in the absence of astrocytes, were viable for 9-10 days in culture *in vitro* (Takeshima, Shimoda et al. 1994). As glial cells influence the viability of VM neurons in both ways i.e neuroprotective and neurodegenerative (Rappold and Tieu 2010; Gao, Hong et al. 2002), we assessed the rotenone (1-20nM) induced toxicity on VM neurons in neurons enriched culture. The results revealed that both immature and mature VM neurons were sensitive to rotenone in a concentration-dependent manner. Mature VM neurons were relatively more sensitive viz., 15nM rotenone concentration was found to be causing around 30% and 55% loss in viability of immature and mature VM neurons respectively. These observations were further confirmed through trypan blue dye exclusion assay and LDH release assay. These observations support earlier observation that cell death varies from immature to mature neurons (Kole, Annis et al. 2013; Lesuisse and Martin 2002). It should be noted that these observations were

from lower number of glial cells. This neurotoxicity might be further enhanced by presence of microglia as per earlier report (Gao, Hong et al. 2002).

Even though immature neurons were observed to be susceptible to rotenone neurotoxicity, it is quite interesting to note that aggregation of α synuclein, a critical component of lewy bodies and diagnostic feature of PD (Iwatsubo 2003) was observed only in mature VM neurons. This might be a cause or consequence of an increased cellular stress (Basaiawmoit and Rattan 2010). Corroborating our view of increased cellular stress, there was a greater increase in ROS levels in mature VM neurons than in immature VM neurons on rotenone treatment. This reinforces earlier study depicting a greater vulnerability of mature neurons than immature neurons to chromium (VI) toxicity, even though ROS levels increased in both immature and mature neurons (Dashti, Soodi et al. 2014). This could be due to differential regulation of few cellular pathways in immature and mature neurons.

Furthermore, analysis of TH staining revealed an interesting observation, where control immature VM neurons have relatively lower level of DA neurons than the control mature VM neurons. This might be because of the ongoing maturation in immature culture. This relative change in number of DA neurons could be one of the reasons for differential effects of rotenone on immature versus mature VM neurons. DA neurons in both immature and mature VM cultures were decreased in number on rotenone treatment. Assessment of caspase-3 activity, which corroborated earlier

report (Li, Ragheb et al. 2003), suggests that the death of neurons upon rotenone treatment could be through apoptotic pathway. An increase in caspase-3 activity on treatment with rotenone was observed in both immature and mature VM neurons, when compared to their respective controls. Nevertheless, control immature VM neurons showed greater caspase -3 activities, than control mature VM neurons, suggesting greater pro-apoptotic response in immature VM neurons. This might be due to the active apoptosis in developing neurons, in order to have a regulated formation of neural networks. A higher enhancement in caspase-3 activity was observed in mature VM neurons than in immature ones, when compared to their respective controls during rotenone treatment. This observation might suggest that different pathways get triggered in mature neurons compared to immature neurons on rotenone treatment.

All the above observations like enhanced ROS levels decrease in number of DA neurons and α-synuclien aggregation were reported earlier in the brains of PD patients (Lang and Lozano 1998; Dias, Junn et al. 2013; Stefanis 2012). This in vitro study thus mimicked the PD features in in vivo system.

To confirm this differential ROS mediated rotenone neurotoxicity on immature and mature VM neurons, they were pretreated with a potent antioxidant, Curcumin, which was reported to be a potent therapeutic agent in treatment of PD via reducing the intracellular ROS levels (Liu, Li et al., 2013). Results showed a

reduction in ROS levels in the VM neurons treated with curcumin and rotenone, when compared to the cells that were treated with rotenone alone. This reduction followed a differential pattern, with mature VM neurons showing a greater reduction in ROS levels and so, a greater increase in their viability, when compared to immature neurons. These observations suggest a greater neuro protective role of curcumin in mature VM neurons, which are known to be more prone to rotenone induced neurotoxicity. This is in accordance with earlier study showing greater neuroprotectivity of Rosmarinic acid on mature neurons than immature neurons (Dashti, Soodi et al. 2014). The results clearly establish a differential manifestation of rotenone toxicity in immature and mature VM neurons. This study can also be used to test the neurotoxicity of other chemicals on VM neurons that may lead to PD.

The cellular mechanisms in mature VM neurons that make them more resistive to normal cell death might also have a role in making them more sensitive to rotenone induced cell death. Investigating these pathways will give us deeper insights on age-dependent vulnerability of VM neurons to toxic compounds like rotenone.

Furthermore whole transcriptome analysis of VM neurons upon rotenone treatment was performed to identify key genes involved in rotenone induced neurotoxicity. Micro array analysis had revealed 705 upregulated genes and 2415 down regulated genes. This data was validated selecting few up-regulated genes with high fold change and relevant neurological functions. All these genes had shown an increase in their

expression upon q-RT PCR analysis and thus micro array data was validated. As tranfection efficiency was too low for primary VM neurons, we have selected dopaminergic neuronal cell line SK-N-SH for this purpose. A transfection efficiency of 40% was achieved in SK-N-SH cell using lipofectamine 3000. Quantitative analysis of expression of those 6 genes in SK-N-SH upon rotenone treatment was done through q-RT PCR. Out of those 6 genes, only myocilin had shown a significant 5 fold change increase in its expression. Myocilin is a protein associated with few types of glaucoma (Tamm 2002). A compromised ubiquitin-proteasome system and myocilin aggregation upon its up-regulation was reported earlier (Qiu, Shen et al. 2014). One of the many factors associated with PD is altered function of ubiquitin-proteasome system (Olanow and McNaught 2006). This similarity suggests a probable association of myocilin with PD. Involvement of myocilin in PD was investigated by reducing its expression in SK-N-SH cells using siRNA technology. SK-N-SH cells viability was shown to be reduced to 50% with 100nM rotenone treatment (Tamilselvam, Braidy et al. 2013) and so the same concentration of rotenone was used for further rotenone treatments to SK-N-SH cells. Corroborating earlier reports of Tamilselvam, Braidy et al. 2013, 100nM rotenone treatment reduced the viability of MTT to 45%. This effect of rotenone was further confirmed through LDH release assay. Interestingly in myocilin knocked down SK-N-SH cells, rotenone reduced the viability to 57%, which is significant ($P<0.05$) when compared to rotenone alone treated cells. Unlike rotenone treated VM neruons, SK-N-SH cells had not shown any

α-synuclein aggregation on rotenone treatment. However an increase in its expression was observed. This difference might be attributed to difference in concentration and/or cell type where certain regulatory elements needed for successful induction of PD might be absent. Reduction in TH expression and elevation in ROS levels were observed in SK-N-SH cells on rotenone treatment. Reduction in myocilin expression has not shown any reduction in rotenone's effect in SK-N-SH cells. Taken together, the data suggests that myocilin might have a role in rotenone induced neurotoxicity but in studies using cell line there is no evidence of parkinsonian features.

Conclusion:

The results of this study establish that rotenone exerts differential effects on immature and mature VM neurons. PD-like features viz. Lewy body formation, enhanced ROS levels and neurodegeneration potentially occur in mature VM neurons. Further, Curcumin could serve as a neuroprotective agent for reducing ROS environment in VM neurons. Whole transcriptome analsyis of rotenone treated VM neurons yielded 705 upregulated genes and 2415 down regulated genes and the pathways they were involved. Among them myocilin was shown to have a role in rotenone induced neurotoxicity.

Chapter-5

Neuroprotective effect of curcumin-loaded lactoferrin nano particles against rotenone induced neurotoxicity.

Introduction

Curcumin is a polyphenolic compound, extracted from the roots of the herb *curcuma longa* (turmeric). It is known to be associated with anti-microbial (Mahady, Pendland et al. 2002), anti-carcinogenic (Kuttan, Bhanumathy et al. 1985), anti-inflammatory (Srimal and Dhawan 1973) and anti-oxidant (Sharma 1976) properties. It also exhibits neuroprotective activity especially in case of neurodegenerative diseases like AD (Garcia-Alloza, Borrelli et al. 2007) and PD (Mythri and Bharath 2012). PD is an age associated movement disorder with a hallmark feature of selective degeneration of dopaminergic neurons in SNPc of ventral mid brain (Lang and Lozano 1998). The specific etiology of PD is not yet completely understood. However, study of PD patients implicates oxidative damage and mitochondrial impairment (Dawson and Dawson 2003). Rotenone, a compound present in pesticides has been shown to accumulate ROS, cause oxidative damage and eventually cellular death (Li, Ragheb et al. 2003). It has been shown to induce certain features of PD both *in vitro* and *in vivo* (Betarbet, Sherer et al. 2000; Chaves, Melo et al. 2010). Most of the current approaches are aimed at restoring the dopamine levels which provide only symptomatic relief but not neuroprotection. Therefore curcumin which has antioxidant, anti-inflammatory properties is being explored as a neuroprotective agent for PD (Mythri and Bharath 2012; Liu, Li et al., 2013). It has also been hypothesized that extensive use of curcumin might be the reason behind significantly lower

prevalence of neurological disorders in Asian Indian population (Ganguli, Chandra et al. 2000). In spite of these beneficiary effects, curcumin is not recommended as therapeutic agent due to its poor bioavailability, limited absorption, and rapid elimination from the body (Mythri and Bharath 2012; Anand, Kunnumakkara et al. 2007). Various approaches were used earlier to enhance the bioavailability of curcumin. They include, usage of adjuvants to limit the metabolism of curcumin (Shoba, Joy et al. 1998), usage of various compositions of nano particles (Li, Braiteh et al. 2005; Padhye, Chavan et al. 2010; Doggui, Sahni et al. 2012). Though these approaches are biocompatible, they lack in target specificity. The receptors of lactoferrin play a role in iron uptake by cells and earlier it was reported that expression of lactoferrin receptors increased in mesencephalon of patients with PD (Faucheux, Nillesse et al. 1995). Encapsulation of curcumin with this lactoferrin protein provides the target specificity alongside with general advantages of nanoparticles like optimum size for cellular uptake and improved intracellular localization. In the present study we have used sol-oil technique and had formulated curcumin loaded lactoferrin nano particles (nano curcumin). Physiochemical characterization, cellular uptake and neuroprotective effect of nano curcumin was assessed in dopaminergic neuronal cell line SK-N-SH.

Results

5.1 Size, Poly dispersity index (PDI), zeta potential and encapsulation efficiency of nano curcumin

Nano curcumin was prepared as described in methods using sol-oil chemistry. FE-SEM analysis of the lactoferrin nano particles displayed a spherical nature with a size range of 22-35 nm diameter (without curcumin) and 43-60 nm diameter (with curcumin) (Fig5.1a). Surface morphological analysis of the particle using AFM also confirmed the size range at approximately 52 nm diameters. It also has shown significant projections, which might help in molecular recognition of these particles (Fig 5.1b). DLS analysis has revealed a size of 100$\pm$5 nm (Fig 5.1c) with PDI value of 0.3 and zeta potential of -19 mev. Encapsulation efficiency of nano curcumin was calculated according to the formula mentioned in method section and found to be at 61.3% $\pm$ 2.4%.

5.2 Cellular uptake and retention of nano curcumin in SK-N-SH cells

Drug internalization and sustained retention inside the cells are key aspects in developing efficient drug delivery system. Curcumin being a self-fluorescent compound, its cellular uptake and retention through nano formulation was compared with its soluble form by confocal microscopic analysis. Cells were treated with 2μM sol curcumin and equivalent nano curcumin. Internalization of sol curcumin was

observed at 2 hrs, whereas nano curcumin was observed at 4 hrs. Curcumin was retained in cells until 4 hrs through soluble form and this retention was enhanced to 8 hrs through lactoferrin nano formulation (Fig 5.2a, 5.2b). To investigate the cellular uptake of curcumin at higher concentration, cells were treated with 0.1mM sol curcumin and equivalent nano curcumin individually. Quantitative analysis of cellular uptake of curcumin was done through spectrofluorimetric estimation. The data indicates the efficient uptake of curcumin through lactoferrin nano particles which showed an increase in drug uptake from 30 min to 4 hrs in a linear manner followed by a drop at 8 hrs and thereafter remained constant up to 20 hrs. This is followed by a steep reduction in concentration of drug by 36 hrs. Whereas in case of sol curcumin, the concentration of delivered drug was initially high at 2 hrs and followed a gradual decline from 2 hrs to 36 hrs (Fig 5.2c).

5.3 Neuro-protective activity of nano curcumin in SK-N-SH cells

Neuroprotective activity of nano curcumin was investigated against rotenone induced neurotoxicity in SK-N-SH cells by MTT assay and LDH release assay. Cells were pretreated with 2μM sol curcumin and equivalent nano curcumin individually for 2 hrs and were treated with 100 nM rotenone for 12 hrs. Cells treated with DMSO alone were considered as control. Viability of cells was measured using MTT assay and the results had shown a decrease in viability of neurons upon rotenone treatment. On pretreatment with sol curcumin or nano curcumin, these cells were rescued from

rotenone induced neurotoxicity but to a greater extent through nano formulation (Fig 5.3a). This was further confirmed by LDH release assay where there was a significant decrease of LDH release in rotenone treated cells upon pretreatment with nano curcumin than sol curcumin (Fig 5.3b). These results clearly establish the neuroprotective ability of lactoferrin encapsulated curcumin in SK-N-SH cells.

5.4 Reduction of ROS levels in SK-N-SH cells on pretreatment with nano curcumin

Rotenone induces neurotoxicity via enhancing ROS levels. Antioxidant activity of nano curcumin was demonstrated through pretreatment of rotenone treated cells with 2μM sol curcumin and equivalent nano curcumin individually followed by a 12 hrs treatment with 100nM rotenone. Cells treated with DMSO alone were considered as control. Levels of ROS were estimated using CMH2DCFDA dye. Fig5.4 had demonstrated that rotenone induced ROS levels were efficiently reduced on pre treatement with sol curcumin and nano curcumin. These results demonstrate the antioxidant activity of lactoferrin encapsulated curcumin in SK-N-SH cells.

5.5 Neuroprotective effect of nano curcumin on dopaminergic neurons

SK-N-SH cells are dopaminergic cells and TH is an enzymatic marker for dopaminergic cells. Neuroprotective effect of nano curcumin on these cells was demonstrated by estimating the expression of TH in these cells with anti TH

antibody. SK-N-SH cells on treatment with 100nM rotenone for 12 hrs significantly lost their TH expression but efficiently retained on pretreatment with 2μM sol curcumin and equivalent nano curcumin individually. Nano curcumin had shown a greater extent of neuroprotectivity than sol curcumin (Fig 5.5a). Since α-synuclein expression is a critical component in lewy body formation, a hall mark feature of PD, its expression was estimated using anti α-synuclein antibody on treatment with rotenone. Expression of α-synuclein significantly increased on treatment with rotenone in SK-N-SH cells. This expression of α-synuclein was efficiently suppressed on pretreatment with sol curcumin and nano curcumin individually, but to a greater extent in nano curcumin pretreated cells (Fig 5.5b).

Fig 5.1: Estimation of size of nano particles

a) SEM analysis: Size of lactoferrin nano particles without curcumin and lactoferrin nano particles loaded with curcumin
b) AFM analysis: Surface morphology and size analysis of lactoferrin nano particles without curcumin and lactoferrin nano particles loaded with curcumin.
c) DLS analysis: Hydrodynamic size of lactoferrin nano particles loaded with curcumin.

Figure 5.1

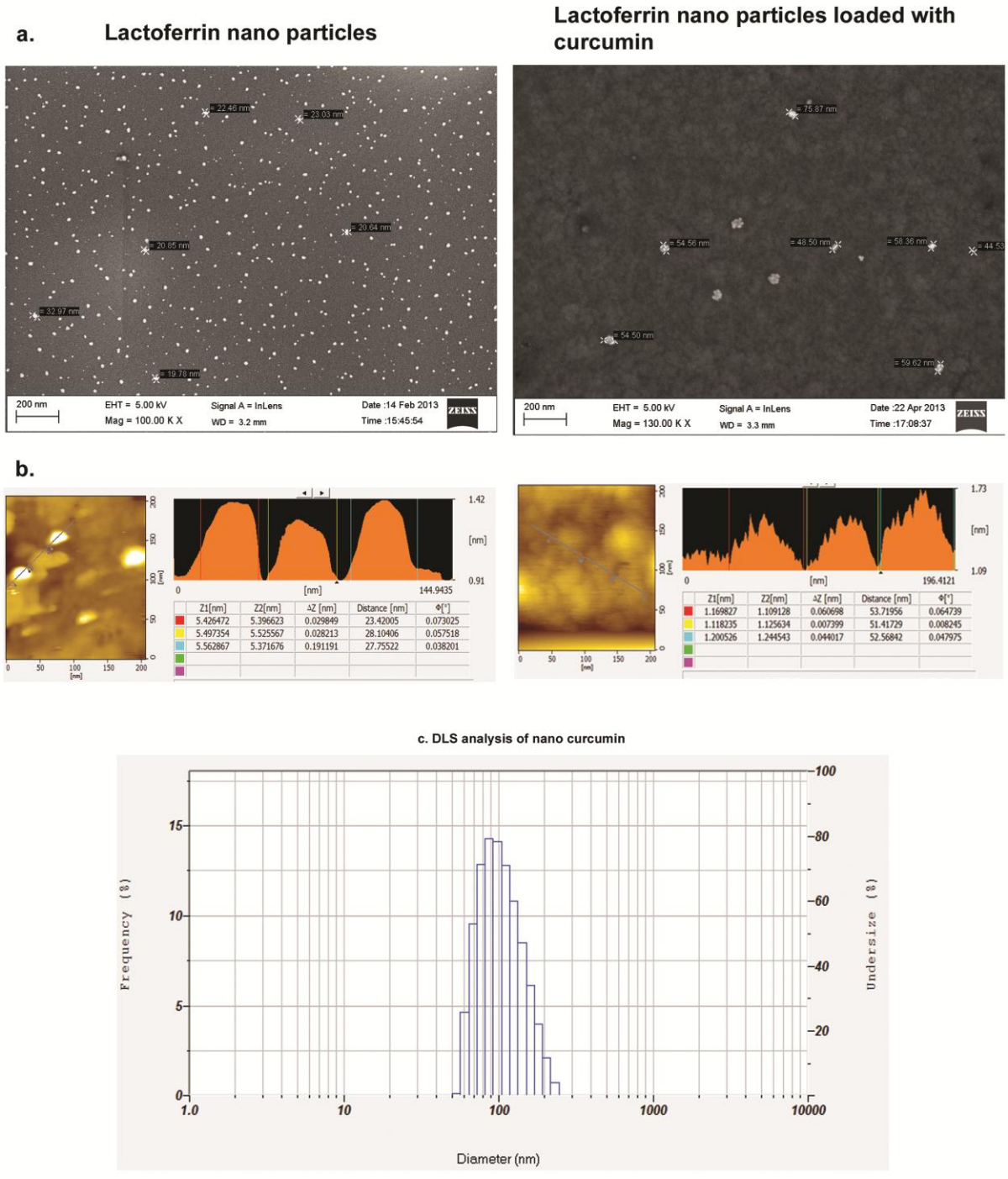
a.
Lactoferrin nano particles
Lactoferrin nano particles loaded with curcumin
200 nm
EHT = 5.00 kV
Mag = 100.00 K X
Signal A = InLens
WD = 3.2 mm
Date :14 Feb 2013
Time :15:45:54
ZEISS
200 nm
EHT = 5.00 kV
Mag = 130.00 K X
Signal A = InLens
WD = 3.3 mm
Date :22 Apr 2013
Time :17:08:37
ZEISS
b.
c. DLS analysis of nano curcumin
Frequency (%)
Undersize (%)
Diameter (nm)
1.0
10
100
1000
10000

Fig 5.2: Cellular uptake of sol curcumin and nano curcumin

a) Presence of curcumin in SK-N-SH cells at different time points following a 2μM sol curcumin treatment was measured through confocal microscopy at curcumin excitation wavelength 458nm and emission wavelength 530nm.
b) Presence of curcumin in SK-N-SH cells at different time points following a nano curcumin treatment equivalent to 2μM sol curcumin was measured through confocal microscopy at curcumin excitation wavelength 458nm and emission wavelength 530nm.
c) Concentration of curcumin in SK-N-SH cells was quantitatively measured through spectrofluorometry at different time points following a 0.1mM sol curcumin and equivalent nano curcumin treatment individually. Curcumin excitation wavelength was 458nm and emission wavelength was 530nm. Concentration of the drug was estimated through a standard graph of known concentrations. Data from each point was taken from triplicates (n=3) and presented in mean ± SD.

Figure 5.2

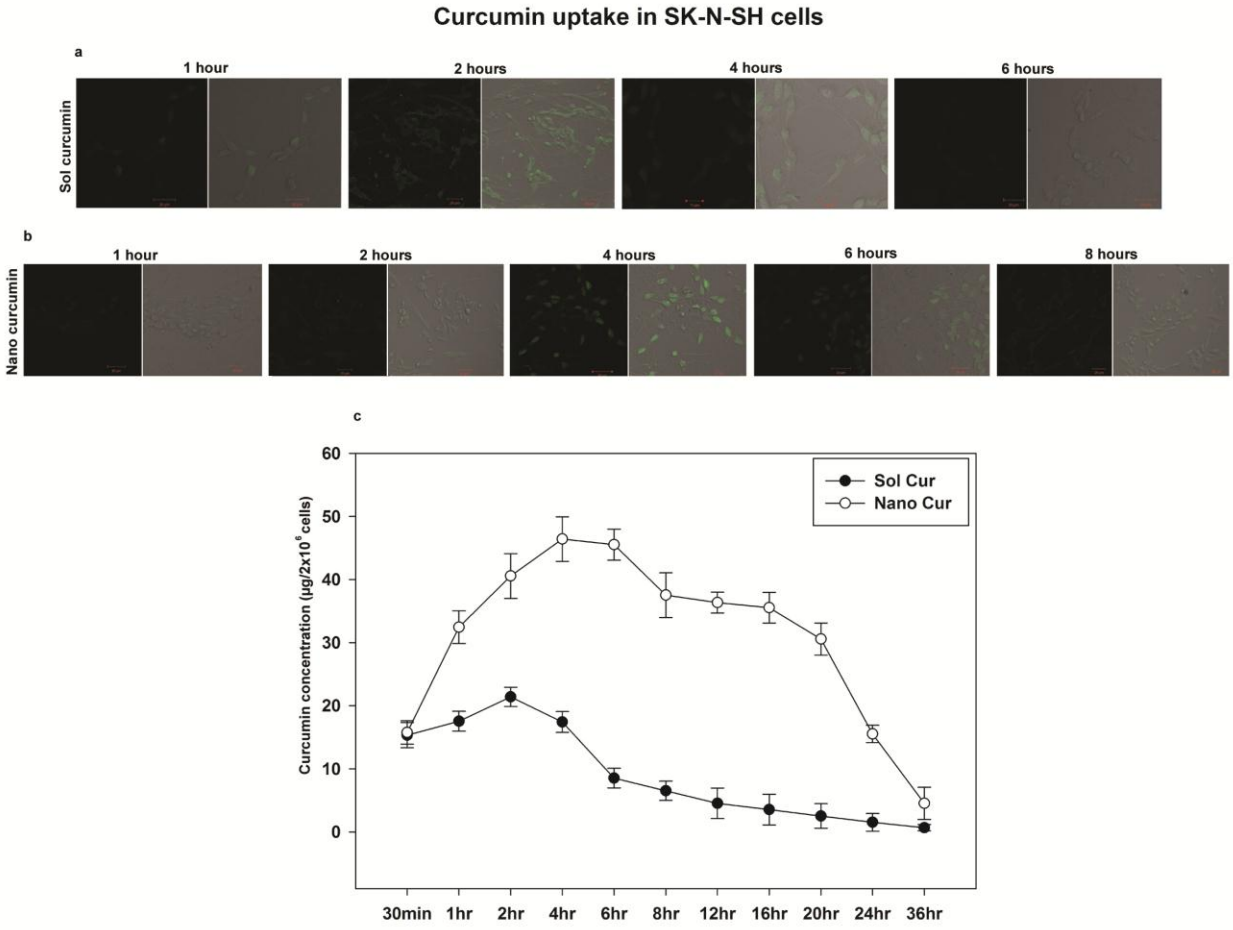
Curcumin uptake in SK-N-SH cells
a
1 hour
2 hours
4 hours
6 hours
Sol curcumin
b
1 hour
2 hours
4 hours
6 hours
8 hours
Nano curcumin
c
Curcumin concentration (µg/2x10^6 cells)
60
50
40
30
20
10
0
Sol Cur
Nano Cur
30min
1hr
2hr
4hr
6hr
8hr
12hr
16hr
20hr
24hr
36hr

Fig 5.3:

a) Viability of SK-N-SH cells was measured through MTT assay on pretreatment with 2μM sol curcumin and equivalent nano curcumin individually for 2 hrs followed by a rotenone treatment for 12 hrs. Data was represented as % viability in a bar graph. Viability of control cells was considered to be 100%. Averages and standard deviations from three experiments were shown in mean ± SD. Statistical significance was estimated by paired t test with **, $P < 0.005$. *** $P<0.0005$.

b) LDH release into media from SK-N-SH cells was measured on pretreatment with 2μM sol curcumin and equivalent nano curcumin individually for 2 hrs followed by a rotenone treatment for 12 hrs. LDH released from cells treated with DMSO alone is considered as control and subtracted from treated samples and present as ΔLDH U/L. Averages and standard deviations from three experiments were shown. Statistical significance was estimated by paired t test with *** $P<0.0005$.

Figure 5.3

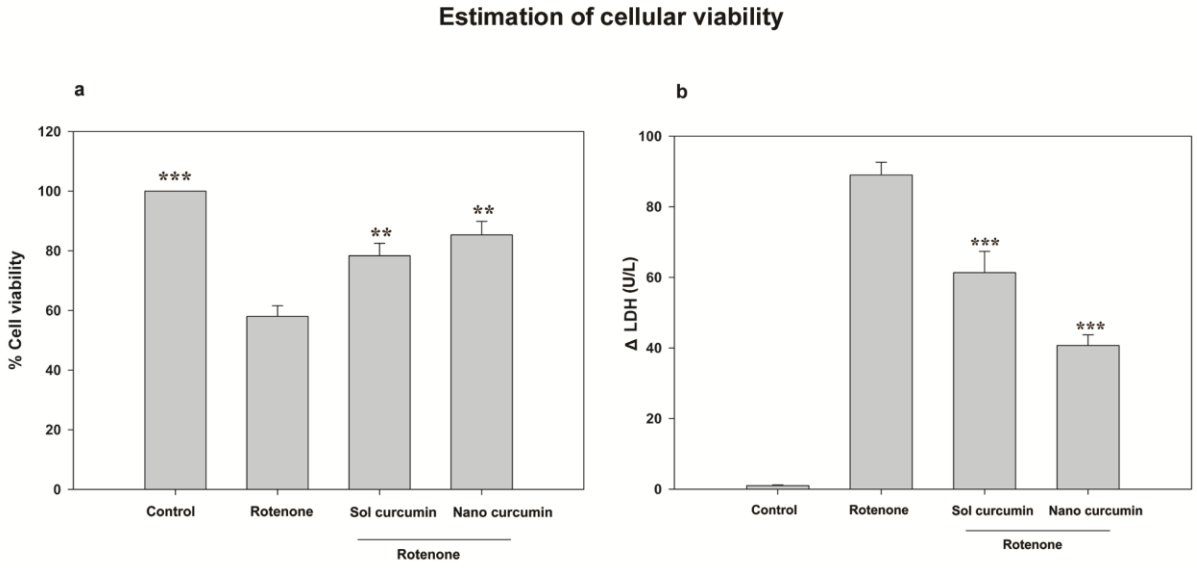
Estimation of cellular viability
a
% Cell viability
120
100
80
60
40
20
0
***
**
**
Control
Rotenone
Sol curcumin
Nano curcumin
Rotenone
b
Δ LDH (U/L)
100
80
60
40
20
0
***
***
Control
Rotenone
Sol curcumin
Nano curcumin
Rotenone

Fig 5.4:

Levels of ROS in sol curcumin/ nano curcumin pretreated SK-N-SH cells on rotenone treatment were measured using fluorescent dye CMH2DCFDA. Cells treated with DMSO alone were taken as control. Values were normalized for protein content and depicted as intensity of fluorescence per micro gram of protein. Averages and standard deviations from three experiments were shown. Statistical significance was estimated by paired t test with **, $P < 0.005$. *** $P<.0005$.

Figure 5.4

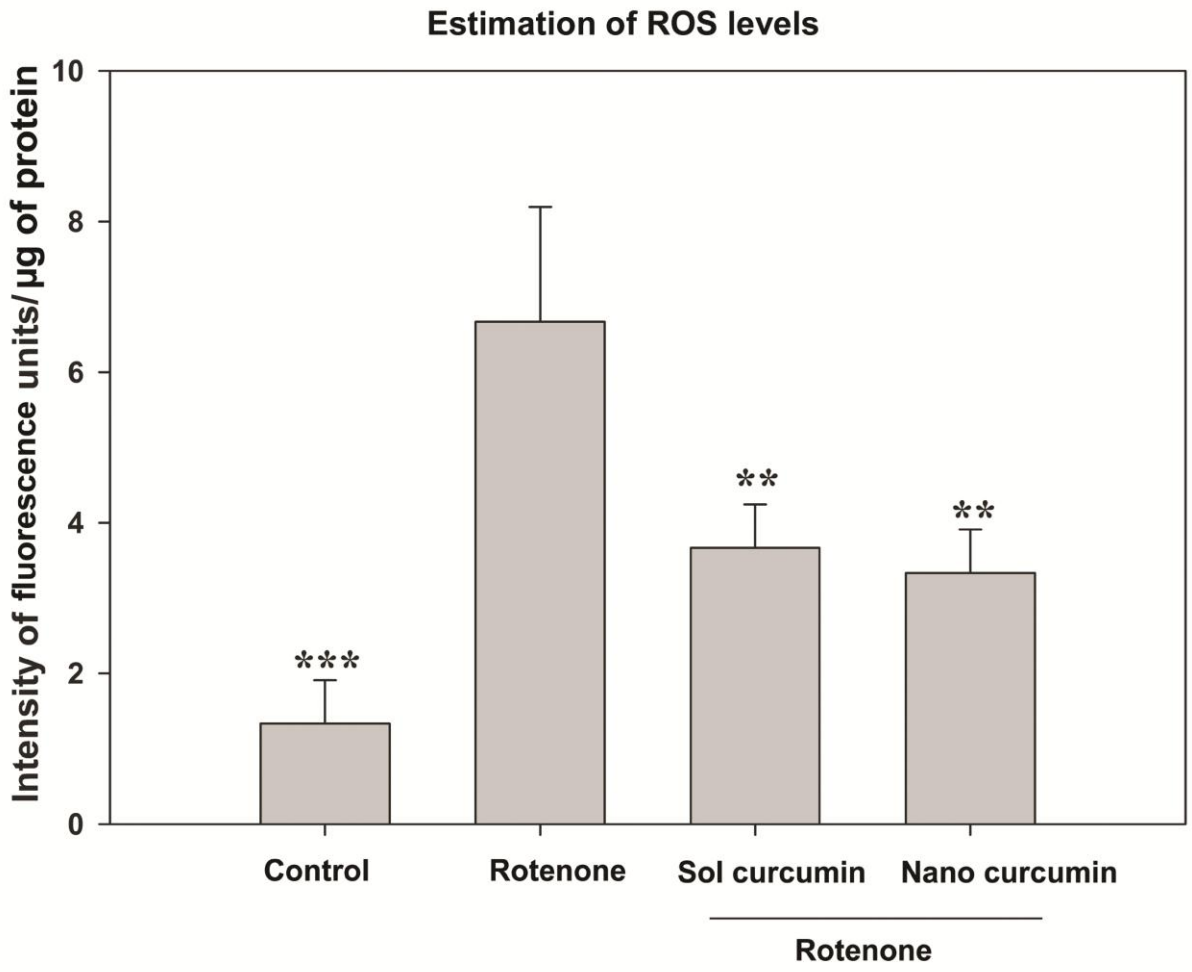
Estimation of ROS levels
Intensity of fluorescence units/µg of protein
10
8
6
4
2
0
***
**
**
Control
Rotenone
Sol curcumin
Nano curcumin
Rotenone

Fig 5.5:

a.1) Expression of TH in sol curcumin/ nano curcumin pretreated SK-N-SH cells on rotenone treatment was measured using anti TH antibody through western blot analysis. Beta-actin was taken as loading control.

a.2) Densitometric analysis of the above bands representing expression of TH was performed using image j software. Averages and standard deviations from three experiments were shown in mean ± SD. Statistical significance was estimated by paired t test with **, $P < 0.005$. *** $P<0.0005$.

b.1) Expression of α-synuclein in sol curcumin/ nano curcumin pretreated SK-N-SH cells on rotenone treatment was measured using anti α-synuclein antibody through western blot analysis. Beta-actin was taken as loading control.

b.2) Densitometric analysis of the above bands representing expression of α-synuclein was performed using image j software. Averages and standard deviations from three experiments were shown in mean ± SD. Statistical significance was estimated by paired t test with **, $P < 0.005$. *** $P<0.0005$.

Figure 5.5

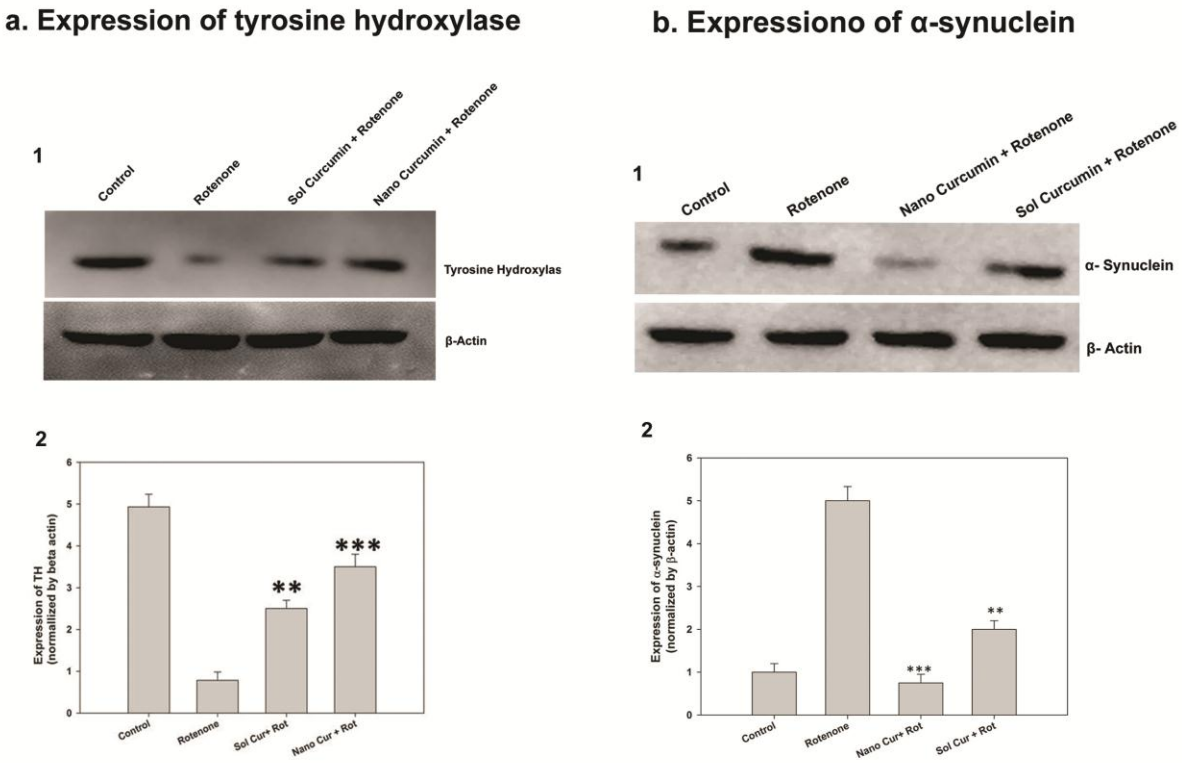
a. Expression of tyrosine hydroxylase
1
Control
Rotenone
Sol Curcumin + Rotenone
Nano Curcumin + Rotenone
Tyrosine Hydroxylas
β-Actin
2
Expression of TH (normalized by beta actin)
**
***
Control
Rotenone
Sol Cur+ Rot
Nano Cur + Rot
b. Expressiono of α-synuclein
1
Control
Rotenone
Nano Curcumin + Rotenone
Sol Curcumin + Rotenone
α- Synuclein
β- Actin
2
Expression of α-synuclein (normalized by β-actin)
***
**
Control
Rotenone
Nano Cur+ Rot
Sol Cur + Rot

Discussion:

PD is an age-associated movement disorder characterized by a selective degeneration of dopaminergic neuronal cells in substantia nigra pars compacta region of ventral mid brain, eventually leading to depletion in dopamine levels in striatum (Lang and Lozano 1998). Most of the drugs such as L-dihydroxy phenyl alanine (Levodopa) are used to replenish decreased dopamine levels in the striatum at early PD (Miyasaki, Martin et al. 2002). Other approaches including usage of MAO-B inhibitors, anti-cholinergic drugs and dopamine receptor agonists provide only symptomatic relief before levodopa is required (Olanow, Watts et al. 2001). These drugs do not prevent degeneration of dopaminergic neurons and in long term usage; they may further develop distinct motor complications. In this scenario several new therapeutic strategies with limited side effects and focusing primarily on protecting neurons from degeneration are being evaluated. Consequently natural biomolecules with high beneficial medicinal properties are being explored that can be used either independently or as adjuvants with existing drugs.

One such natural product is *curcuma longa,* a common indian spice. Curcumin, a polyphenol and an active ingredient of *curcuma longa* was known to be associated with several beneficial properties against human disorders. The most beneficial effect of curcumin neuroprotection is through its antioxidant activity. Neuroprotective activity of curcumin was successfully reported in various PD models (Mythri, Harish et al.

2011; Rajeswari 2006; Liu, Yu et al. 2011; Wang, Boddapati et al. 2010). Adding to this, curcumin aided neurogenesis was also reported (Kim, Son et al. 2008; Xu, Ku et al. 2007). Difficulty of curcumin in crossing blood brain barrier and its quick elimination from the body limits its bioavailability and thereby its neuro therapeutic potential. Various approaches have been attempted to increase the bioavailability of curcumin (Prasad, Tyagi et al. 2014) but they lack target specificity.

Lactoferrin as a carrier molecule to transport curcumin may circumvent the above limitations. Lactoferrin belongs to transferrin group of proteins with a function of iron storage and transport protein having a molecular weight of ~80 kd. Higher expression of lactoferrin receptors was reported in mesencephalon of PD patients (Faucheux, Nillesse et al. 1995). Adding to this, transcytosis of lactoferrin through blood brain barrier by receptor mediated endocytosis was also reported (Fillebeen, Descamps et al. 1999). We hypothesize that these properties of lactoferrin can enhance the specificity and efficacy of curcumin in brains of PD patients.

In the present study, we focused on the neuroprotective activity of curcumin loaded lactoferrin nano particles in dopaminergic neuronal cell line SK-N-SH. Nano particles were prepared as described earlier. The size of nano particles affects their therapeutic efficacy (Davis 1997). Nanoparicles of size >400 nm are captured by immune cells and thereby restricts their biodisturbution (Wisse and Leuw et al., 1984). Their access to brain will also be limited with greater size (Sonavane, Tomoda et al. 2008).

Nanocurcumin prepared was of appropriate size range 43-60 nm as shown through SEM and AFM analysis. DLS analysis determined the size of these particles at ~ 100 nm. This variation in size might be due to particles surface charge and their interactions with water shell. Zeta potential of these particles was found to be -19± 2 mV. The low zeta potential might be due to high molecular weight of lactoferrin molecules that lead to a shift in the plane of shear from the surface of the particle to farer distance (Honary and Zahir et al., 2013). The PDI value of these nanoparticles was 0.3, indicating a homogeneous nano formulation. The drug encapsulation efficiency of these particles was determined to be at ~61.3%, which is better than other curcumin loaded nano formulations like PLG ~31% (Doggui, Sahni et al. 2012). Curcumin is a natural fluorescent compound visible in green spectrum and so can be quantified within the cells through confocal microscopy. Dopaminergic cell line treated with sol curcumin and nanocurcumin individually exhibited the fluorescence indicating the delivery of curcumin to cells. However, nanocurcumin showed greater cellular uptake and retention than its soluble counterpart. This was even confirmed at prolonged time periods when cells were delivered with higher concentrations of sol curcumin and equivalent nano curcumin individually. The mode of nano particle entry into the cells might be through receptor mediated endocytosis. This mode of entry has been reported in our earlier work, where doxorubicin was encapsulated in

lactoferrin nanoparticles (Golla, Bhaskar et al. 2013). Other modes of entry also can't be ruled out due to the nano size of these particles.

Rotenone, a compound usually present in pesticides is one of the environmental causative agents of PD. Dopaminergic cell line SK-N-SH was treated with rotenone and its neurotoxicity was assessed on pretreatment with solcurcumin and nanocurcumin. Viability of dopaminergic cells on pretreatment with solcurcumin, nanocurcumin individually and on treatment with rotenone, was assessed by MTT assay and LDH release assay. Curcumin as both sol form and nano formulation increased the viability of rotenone treated cells. However nanocurcumin showed a better neuroprotection than sol form. This was even confirmed through LDH release assay. Rotenone induced neurotoxicity in dopaminergic cells via enhanced levels of ROS was reported earlier (Li, Ragheb et al. 2003). Adding to this, oxidative damage in brains of PD patients was also reported (Hwang 2013). Effective delivery of antioxidants to specific cells to reduce the oxidative stress will be an ideal strategy to treat PD. Enhancement of ROS levels on rotenone treatment was reduced on pretreatment with both sol curcumin and nanocurcumin individually, but to a greater extent when nanocurcumin was used. The decrease in ROS levels on pretreatment with curcumin is in corroboration with earlier reports (Liu, Yu et al. 2011). Decrease in expression of TH and increase of α-synuclein levels in dopaminergic neurons are the hallmark features of PD. These features were observed in dopaminergic cells on

treatment with rotenone through western blot analysis. In consistency with earlier reports (Vajragupta, Boonchoong et al. 2003; Wang, Boddapati et al. 2010) pretreatment of cells with curcumin showed an increase in TH expression and decrease in α-synuclein levels. Nano curcumin ameliorated these PD features in dopaminergic cells relatively good when compared to its counterpart sol curcumin. Further studies are required to confirm efficacy of nanoformulation in an in vivo.model.

Conclusion:

In summary, curcumin loaded lactoferrrin nano particles were characterized and their neuroprotective ability against rotenone induced neurotoxicity in vitro was demonstrated.

Conclusions

Primary VM neuronal cultures are gaining importance in the study of molecular mechanisms leading to PD and development of treatment strategies. In practice, these neurons are co- cultured with glial cells, making it difficult for assessment of neuronal specific proteomic and genomic analyses. Hence, development of VM neuron enriched culture is indispensable for such analyses. In current study,

- Enriched rat primary VM neurons were established as an *in vitro* culture model and were found to survive for 9 days *in vitro*, followed by a sudden death phase resulting in < 5% of neuronal viability.
- They had attained maturity at 7^{th} DIV both in presence and absence of glial cells.
- This VM neuron enriched culture was shown to be rich in DA neurons from 7^{th}DIV and survived up to 10^{th}DIV.
- ROS and DNA damage showed an increase in their respective levels at 9^{th}DIV.
- Furthermore, expression of Topoisomerase II β, a key player in neuronal development, was found to increase until 9^{th}DIV followed by a sudden decrease on 10^{th}DIV.

Rotenone induced neuronal toxicity in VM neurons in culture is widely accepted as an important model for investigation of PD. However, little is known about developmental stage dependent toxic effects of rotenone on VM neurons *in vitro*. In current study,

- Rotenone induced cell death in both immature and mature neurons was found to be concentration-dependent, but to a greater extent in mature neurons.
- While rotenone-treated mature VM neurons showed α-synuclein aggregation and sensitivity to DA neurons, immature VM neurons exhibited only DA neuronal sensitivity but not α-synuclein aggregation.
- On rotenone treatment, enhancement of caspase-3 activity and ROS production were higher in mature VM neurons than in immature neurons.
- Whole transcriptome analysis of rotenone treated mature VM neurons was done.
- This data had yielded 705 up-regulated genes and 2415 down-regulated genes.
- Those genes were analyzed and few pathways were identified based on involvement of genes regulated on rotenone treatment.
- Inhibition of myocilin expression in SK-N-SH cells, significantly ($P < 0.05$) reduced the neurotoxic effect of rotenone.
- However, inhibition of myocilin did not show any influence on rotenone induced parkinsonian features like elevated ROS levels, decreased TH expression and increased α-synuclein expression.

Curcumin is known to have neuroprotective role and possess antioxidant, anti-inflammatory activities. In current study**,**

- Curcumin loaded lactoferrin nano particles prepared by sol-oil chemistry were used to protect dopaminergic cell line SK-N-SH against rotenone induced neurotoxicity.
- These curcumin loaded nano particles were of 43-60 nm diameter size and around 100 nm hydrodynamic size.
- The encapsulation efficiency was 61.3% ± 2.4%.
- Cellular uptake of curcumin through these nano particles was investigated.
- These curcumin loaded lactoferrin nanoparticles showed greater intracellular drug uptake, sustained retention and greater neuroprotection than soluble counterpart.

References

Ahmadi, F. A., D. A. Linseman, T. N. Grammatopoulos, S. M. Jones, R. J. Bouchard, C. R. Freed, K. A. Heidenreich and W. M. Zawada (2003). "The pesticide rotenone induces caspase-3-mediated apoptosis in ventral mesencephalic dopaminergic neurons." J Neurochem **87**(4): 914-921.

Ak, T. and I. Gulcin (2008). "Antioxidant and radical scavenging properties of curcumin." Chem Biol Interact **174**(1): 27-37.

Aksenova, M. V., M. Y. Aksenov, C. F. Mactutus and R. M. Booze (2005). "Cell culture models of oxidative stress and injury in the central nervous system." Curr Neurovasc Res **2**(1): 73-89.

Alberio, T., L. Lopiano and M. Fasano (2012). "Cellular models to investigate biochemical pathways in Parkinson's disease." FEBS J **279**(7): 1146-1155.

Ali, R. E. and S. I. Rattan (2006). "Curcumin's biphasic hormetic response on proteasome activity and heat-shock protein synthesis in human keratinocytes." Ann N Y Acad Sci **1067**: 394-399.

Anand, P., A. B. Kunnumakkara, R. A. Newman and B. B. Aggarwal (2007). "Bioavailability of curcumin: problems and promises." Mol Pharm **4**(6): 807-818.

Basaiawmoit, R. V. and S. I. Rattan (2010). "Cellular stress and protein misfolding during aging." Methods Mol Biol **648**: 107-117.

Bertrand, S. J., M. V. Aksenova, M. Y. Aksenov, C. F. Mactutus and R. M. Booze (2011). "Endogenous amyloidogenesis in long-term rat hippocampal cell cultures." BMC Neurosci **12**: 38.

Betarbet, R., R. M. Canet-Aviles, T. B. Sherer, P. G. Mastroberardino, C. McLendon, J. H. Kim, S. Lund, H. M. Na, G. Taylor, N. F. Bence, R. Kopito, B. B. Seo, T. Yagi, A. Yagi, G. Klinefelter, M. R. Cookson and J. T. Greenamyre (2006). "Intersecting pathways to neurodegeneration in Parkinson's disease: effects of the pesticide rotenone on DJ-1, alpha-synuclein, and the ubiquitin-proteasome system." Neurobiol Dis **22**(2): 404-420.

Betarbet, R., T. B. Sherer, G. MacKenzie, M. Garcia-Osuna, A. V. Panov and J. T. Greenamyre (2000). "Chronic systemic pesticide exposure reproduces features of Parkinson's disease." Nat Neurosci **3**(12): 1301-1306.

Bhanu, M. U., R. K. Mandraju, C. Bhaskar and A. K. Kondapi (2010). "Cultured cerebellar granule neurons as an in vitro aging model: topoisomerase IIbeta as an additional biomarker in DNA repair and aging." Toxicol In Vitro **24**(7): 1935-1945.

Bilimoria, P. M. and A. Bonni (2008). "Cultures of cerebellar granule neurons." CSH Protoc **2008**: pdb prot5107.

Cai, X., H. Jia, Z. Liu, B. Hou, C. Luo, Z. Feng, W. Li and J. Liu (2008). "Polyhydroxylated fullerene derivative C(60)(OH)(24) prevents mitochondrial dysfunction and oxidative damage in an MPP(+) -induced cellular model of Parkinson's disease." J Neurosci Res **86**(16): 3622-3634.

Cavallaro, M., J. Mariani, C. Lancini, E. Latorre, R. Caccia, F. Gullo, M. Valotta, S. DeBiasi, L. Spinardi, A. Ronchi, E. Wanke, S. Brunelli, R. Favaro, S. Ottolenghi and S. K. Nicolis (2008). "Impaired generation of mature neurons by neural stem cells from hypomorphic Sox2 mutants." Development **135**(3): 541-557.

Chaves, R. S., T. Q. Melo, S. A. Martins and M. F. Ferrari (2010). "Protein aggregation containing beta-amyloid, alpha-synuclein and hyperphosphorylated tau in cultured cells of hippocampus, substantia nigra and locus coeruleus after rotenone exposure." BMC Neurosci **11**: 144.

Cossette, M., D. Levesque and A. Parent (2005). "Neurochemical characterization of dopaminergic neurons in human striatum." Parkinsonism Relat Disord **11**(5): 277-286.

Craik, F., Salthouse, T (2000). "The Handbook of Aging and Cognition (2nd ed.)." Mahwah, NJ: Lawrence Erlbaum.

D'Autreaux, B. and M. B. Toledano (2007). "ROS as signalling molecules: mechanisms that generate specificity in ROS homeostasis." Nat Rev Mol Cell Biol **8**(10): 813-824.

Dale, W. M. and C. Russell (1956). "A study of the irradiation of catalase by ionizing radiations in the presence of cysteine, cystine and glutathione." Biochem J **62**(1): 50-57.

Dashti, A., M. Soodi and N. Amani (2014). "Cr (VI) induced oxidative stress and toxicity in cultured cerebellar granule neurons at different stages of development and protective effect of Rosmarinic acid." Environ Toxicol. Dauer, W. and S. Przedborski (2003). "Parkinson's disease: mechanisms and models." Neuron **39**(6): 889-909.

Davis, S. S. (1997). "Biomedical applications of nanotechnology--implications for drug targeting and gene therapy." Trends Biotechnol **15**(6): 217-224.

Dawson, T. M. and V. L. Dawson (2003). "Molecular pathways of neurodegeneration in Parkinson's disease." Science **302**(5646): 819-822.

Dawson, T. M., H. S. Ko and V. L. Dawson (2010). "Genetic animal models of Parkinson's disease." Neuron **66**(5): 646-661.

De-Paula, V. J., M. Radanovic, B. S. Diniz and O. V. Forlenza (2012). "Alzheimer's disease." Subcell Biochem **65**: 329-352.

Di Monte, D. A., M. Lavasani and A. B. Manning-Bog (2002). "Environmental factors in Parkinson's disease." Neurotoxicology **23**(4-5): 487-502.

Dias, V., E. Junn and M. M. Mouradian (2013). "The role of oxidative stress in Parkinson's disease." J Parkinsons Dis **3**(4): 461-491.

Doggui, S., J. K. Sahni, M. Arseneault, L. Dao and C. Ramassamy (2012). "Neuronal uptake and neuroprotective effect of curcumin-loaded PLGA nanoparticles on the human SK-N-SH cell line." J Alzheimers Dis **30**(2): 377-392.

Faucheux, B. A., N. Nillesse, P. Damier, G. Spik, A. Mouatt-Prigent, A. Pierce, B. Leveugle, N. Kubis, J. J. Hauw, Y. Agid and et al. (1995). "Expression of lactoferrin receptors is increased in the mesencephalon of patients with Parkinson disease." Proc Natl Acad Sci U S A **92**(21): 9603-9607.

Fillebeen, C., L. Descamps, M. P. Dehouck, L. Fenart, M. Benaissa, G. Spik, R. Cecchelli and A. Pierce (1999). "Receptor-mediated transcytosis of lactoferrin through the blood-brain barrier." J Biol Chem **274**(11): 7011-7017.

Finkel, T., M. Serrano and M. A. Blasco (2007). "The common biology of cancer and ageing." Nature **448**(7155): 767-774.

Forno, L. S. (1996). "Neuropathology of Parkinson's disease." J Neuropathol Exp Neurol **55**(3): 259-272.

Ganguli, M., V. Chandra, M. I. Kamboh, J. M. Johnston, H. H. Dodge, B. K. Thelma, R. C. Juyal, R. Pandav, S. H. Belle and S. T. DeKosky (2000). "Apolipoprotein E polymorphism and Alzheimer disease: The Indo-US Cross-National Dementia Study." Arch Neurol **57**(6): 824-830.

Gao, H. M., J. S. Hong, W. Zhang and B. Liu (2002). "Distinct role for microglia in rotenone-induced degeneration of dopaminergic neurons." J Neurosci **22**(3): 782-790.

Garcia-Alloza, M., L. A. Borrelli, A. Rozkalne, B. T. Hyman and B. J. Bacskai (2007). "Curcumin labels amyloid pathology in vivo, disrupts existing plaques, and partially restores distorted neurites in an Alzheimer mouse model." J Neurochem **102**(4): 1095-1104.

Gazewood, J. D., D. R. Richards and K. Clebak (2013). "Parkinson disease: an update." Am Fam Physician **87**(4): 267-273.

Golla, K., C. Bhaskar, F. Ahmed and A. K. Kondapi (2013). "A target-specific oral formulation of Doxorubicin-protein nanoparticles: efficacy and safety in hepatocellular cancer." J Cancer **4**(8): 644-652.

Gonzalez-Barrios, J. A., M. Lindahl, M. J. Bannon, V. Anaya-Martinez, G. Flores, I. Navarro-Quiroga, L. E. Trudeau, J. Aceves, D. B. Martinez-Arguelles, R. Garcia-Villegas, I. Jimenez, J. Segovia and D. Martinez-Fong (2006). "Neurotensin polyplex as an efficient carrier for delivering the human GDNF gene into nigral dopamine neurons of hemiparkinsonian rats." Mol Ther **14**(6): 857-865.

Gupta, K. P., U. Swain, K. S. Rao and A. K. Kondapi (2012). "Topoisomerase IIbeta regulates base excision repair capacity of neurons." Mech Ageing Dev **133**(4): 203-213.

Hardy, J., M. R. Cookson and A. Singleton (2003). "Genes and parkinsonism." Lancet Neurol **2**(4): 221-228. Hegde, M. L., P. M. Hegde, L. M. Holthauzen, T. K. Hazra, K. S. Rao and S. Mitra (2010). "Specific Inhibition of NEIL-initiated repair of oxidized base damage in human genome by copper and iron: potential etiological linkage to neurodegenerative diseases." J Biol Chem **285**(37): 28812-28825.

Hof, P. R. and J. H. Morrison (2004). "The aging brain: morphomolecular senescence of cortical circuits." Trends Neurosci **27**(10): 607-613.

Holliday, R. (2004). "The multiple and irreversible causes of aging." J Gerontol A Biol Sci Med Sci **59**(6): B568-572.

Honary. S., F. Zahir. (2013). "Effect of Zeta Potential on the properties of nano-drug delivery systems- A review (Part 1)." Tropical Journal of Pharmaceutical Research, **12** 255-264.

Horowitz, M. P. and J. T. Greenamyre (2010). "Gene-environment interactions in

Parkinson's disease: the importance of animal modeling." Clin Pharmacol Ther **88**(4): 467-474.

Hwang, O. (2013). "Role of oxidative stress in Parkinson's disease." Exp Neurobiol **22**(1): 11-17.

Iwatsubo, T. (2003). "Aggregation of alpha-synuclein in the pathogenesis of Parkinson's disease." J Neurol **250 Suppl 3**: III11-14.

Jagatha, B., R. B. Mythri, S. Vali and M. M. Bharath (2008). "Curcumin treatment alleviates the effects of glutathione depletion in vitro and in vivo: therapeutic implications for Parkinson's disease explained via in silico studies." Free Radic Biol Med **44**(5): 907-917.

Jenner, P. (2003). "Oxidative stress in Parkinson's disease." Ann Neurol **53 Suppl 3**: S26-36; discussion S36-28.

Jenner, P. and C. W. Olanow (1996). "Oxidative stress and the pathogenesis of Parkinson's disease." Neurology **47**(6 Suppl 3): S161-170.

Jiao, Y., J. t. Wilkinson, X. Di, W. Wang, H. Hatcher, N. D. Kock, R. D'Agostino, Jr., M. A. Knovich, F. M. Torti and S. V. Torti (2009). "Curcumin, a cancer chemopreventive and chemotherapeutic agent, is a biologically active iron chelator." Blood **113**(2): 462-469.

Joe, B., M. Vijaykumar and B. R. Lokesh (2004). "Biological properties of curcumin-cellular and molecular mechanisms of action." Crit Rev Food Sci Nutr **44**(2): 97-111.

Kaiser, L. G., N. Schuff, N. Cashdollar and M. W. Weiner (2005). "Age-related glutamate and glutamine concentration changes in normal human brain: 1H MR spectroscopy study at 4 T." Neurobiol Aging **26**(5): 665-672.

Kiernan, M. C., S. Vucic, B. C. Cheah, M. R. Turner, A. Eisen, O. Hardiman, J. R. Burrell and M. C. Zoing (2011). "Amyotrophic lateral sclerosis." Lancet **377**(9769): 942-955.

Kim, S. J., T. G. Son, H. R. Park, M. Park, M. S. Kim, H. S. Kim, H. Y. Chung, M. P. Mattson and J. Lee (2008). "Curcumin stimulates proliferation of embryonic neural progenitor cells and neurogenesis in the adult hippocampus." J Biol Chem **283**(21): 14497-14505.

Klein, J. A. and S. L. Ackerman (2003). "Oxidative stress, cell cycle, and neurodegeneration." J Clin Invest **111**(6): 785-793.

Kole, A. J., R. P. Annis and M. Deshmukh (2013). "Mature neurons: equipped for survival." Cell Death Dis **4**: e689.

Krishna, A. D., R. K. Mandraju, G. Kishore and A. K. Kondapi (2009). "An efficient targeted drug delivery through apotransferrin loaded nanoparticles." PLoS One **4**(10): e7240.

Kuttan, R., P. Bhanumathy, K. Nirmala and M. C. George (1985). "Potential anticancer activity of turmeric (Curcuma longa)." Cancer Lett **29**(2): 197-202.

Lang, A. E. and A. M. Lozano (1998). "Parkinson's disease. First of two parts." N Engl J Med **339**(15): 1044-1053.

Leonardi, E. T. and C. Mytilineou (1998). "Cell culture models of neuronal degeneration and neuroprotection. Implications for Parkinson's disease." Adv Exp Med Biol **446**: 203-222.

Lesuisse, C. and L. J. Martin (2002). "Immature and mature cortical neurons engage different apoptotic mechanisms involving caspase-3 and the mitogen-activated protein kinase pathway." J Cereb Blood Flow Metab **22**(8): 935-950.

Li, L., F. S. Braiteh and R. Kurzrock (2005). "Liposome-encapsulated curcumin: in vitro and in vivo effects on proliferation, apoptosis, signaling, and angiogenesis." Cancer **104**(6): 1322-1331.

Li, N., K. Ragheb, G. Lawler, J. Sturgis, B. Rajwa, J. A. Melendez and J. P. Robinson (2003). "Mitochondrial complex I inhibitor rotenone induces apoptosis through enhancing mitochondrial reactive oxygen species production." J Biol Chem **278**(10): 8516-8525.

Litvan, I., M. F. Chesselet, T. Gasser, D. A. Di Monte, D. Parker, Jr., T. Hagg, J. Hardy, P. Jenner, R. H. Myers, D. Price, M. Hallett, W. J. Langston, A. E. Lang, G. Halliday, W. Rocca, C. Duyckaerts, D. W. Dickson, Y. Ben-Shlomo, C. G. Goetz and E. Melamed (2007). "The etiopathogenesis of Parkinson disease and suggestions for future research. Part II." J Neuropathol Exp Neurol **66**(5): 329-336.

Liu, Z., Y. Yu, X. Li, C. A. Ross and W. W. Smith (2011). "Curcumin protects against A53T alpha-synuclein-induced toxicity in a PC12 inducible cell model for

Parkinsonism." Pharmacol Res **63**(5): 439-444.

Liu,Z., T. Li, D. Yang, W.W. Smith (2013). "Curcumin protects against rotenone-induced neurotoxicity in cell and drosophila models of Parkinson's disease." Advances in Parkinson's Disease, **2**:18-27.

Livak, K. J. and T. D. Schmittgen (2001). "Analysis of relative gene expression data using real-time quantitative PCR and the 2(-Delta Delta C(T)) Method." Methods **25**(4): 402-408.

Lunn, J. S., S. A. Sakowski and E. L. Feldman (2014). "Concise review: Stem cell therapies for amyotrophic lateral sclerosis: recent advances and prospects for the future." Stem Cells **32**(5): 1099-1109.

Mahady, G. B., S. L. Pendland, G. Yun and Z. Z. Lu (2002). "Turmeric (Curcuma longa) and curcumin inhibit the growth of Helicobacter pylori, a group 1 carcinogen." Anticancer Res **22**(6C): 4179-4181.

Mandraju, R., A. Chekuri, C. Bhaskar, K. Duning, J. Kremerskothen and A. K. Kondapi (2011).
"Topoisomerase IIbeta associates with Ku70 and PARP-1 during double strand break repair of DNA in neurons." Arch Biochem Biophys **516**(2): 128-137.

Mattson, M. P. and T. Magnus (2006). "Ageing and neuronal vulnerability." Nat Rev Neurosci **7**(4): 278-294.

Menon, V. P. and A. R. Sudheer (2007). "Antioxidant and anti-inflammatory properties of curcumin." Adv Exp Med Biol **595**: 105-125.

Miller, R. G., J. D. Mitchell and D. H. Moore (2012). "Riluzole for amyotrophic lateral sclerosis (ALS)/motor neuron disease (MND)." Cochrane Database Syst Rev **3**: CD001447.

Miyasaki, J. M., W. Martin, O. Suchowersky, W. J. Weiner and A. E. Lang (2002). "Practice parameter: initiation of treatment for Parkinson's disease: an evidence-based review: report of the Quality Standards Subcommittee of the American Academy of Neurology." Neurology **58**(1): 11-17.

Mobbs, C. V., Hof, P. R (2009). "Handbook of the neuroscience of aging." Amsterdam: Elsevier/Academic Press.

Moon, Y., K. H. Lee, J. H. Park, D. Geum and K. Kim (2005). "Mitochondrial membrane depolarization and the selective death of dopaminergic neurons by rotenone: protective effect of coenzyme Q10." J Neurochem **93**(5): 1199-1208.

Moore, D. J., A. B. West, V. L. Dawson and T. M. Dawson (2005). "Molecular pathophysiology of Parkinson's disease." Annu Rev Neurosci **28**: 57-87.

Mosmann, T. (1983). "Rapid colorimetric assay for cellular growth and survival: application to proliferation and cytotoxicity assays." J Immunol Methods **65**(1-2): 55-63.

Mythri, R. B. and M. M. Bharath (2012). "Curcumin: a potential neuroprotective agent in Parkinson's disease." Curr Pharm Des **18**(1): 91-99.

Mythri, R. B., G. Harish, S. K. Dubey, K. Misra and M. M. Bharath (2011). "Glutamoyl diester of the dietary polyphenol curcumin offers improved protection against peroxynitrite-mediated nitrosative stress and damage of brain mitochondria in vitro: implications for Parkinson's disease." Mol Cell Biochem **347**(1-2): 135-143.

Nistico, R., B. Mehdawy, S. Piccirilli and N. Mercuri (2011). "Paraquat- and rotenone-induced models of Parkinson's disease." Int J Immunopathol Pharmacol **24**(2): 313-322.

Olanow, C. W. and K. S. McNaught (2006). "Ubiquitin-proteasome system and Parkinson's disease." Mov Disord **21**(11): 1806-1823.

Olanow, C. W., R. L. Watts and W. C. Koller (2001). "An algorithm (decision tree) for the management of Parkinson's disease (2001): treatment guidelines." Neurology **56**(11 Suppl 5): S1-S88.

Oppenheim, R. W. (1991). "Cell death during development of the nervous system." Annu Rev Neurosci **14**: 453-501.

Padhye, S., D. Chavan, S. Pandey, J. Deshpande, K. V. Swamy and F. H. Sarkar (2010). "Perspectives on chemopreventive and therapeutic potential of curcumin analogs in medicinal chemistry." Mini Rev Med Chem **10**(5): 372-387.

Paek, S. H., H. Y. Shin, J. W. Kim, S. H. Park, J. H. Son and D. G. Kim (2010). "Primary culture of central neurocytoma: a case report." J Korean Med Sci **25**(5): 798-803.

Palm, K., T. Salin-Nordstrom, M. F. Levesque and T. Neuman (2000). "Fetal and adult human CNS stem cells have similar molecular characteristics and developmental potential." Brain Res Mol Brain Res **78**(1-2): 192-195.

Pandey, N., J. Strider, W. C. Nolan, S. X. Yan and J. E. Galvin (2008). "Curcumin inhibits aggregation of alpha-synuclein." Acta Neuropathol **115**(4): 479-489.

Prasad, S., A. K. Tyagi and B. B. Aggarwal (2014). "Recent developments in delivery, bioavailability, absorption and metabolism of curcumin: the golden pigment from golden spice." Cancer Res Treat **46**(1): 2-18.

Qiu, Y., X. Shen, R. Shyam, B. Y. Yue and H. Ying (2014). "Cellular processing of myocilin." PLoS One **9**(4): e92845.

Rajeswari, A. (2006). "Curcumin protects mouse brain from oxidative stress caused by 1-methyl-4-phenyl-1,2,3,6-tetrahydropyridine." Eur Rev Med Pharmacol Sci **10**(4): 157-161.

Rappold, P. M. and K. Tieu (2010). "Astrocytes and therapeutics for Parkinson's disease." Neurotherapeutics **7**(4): 413-423.

Raz, N., U. Lindenberger, K. M. Rodrigue, K. M. Kennedy, D. Head, A. Williamson, C. Dahle, D. Gerstorf and J. D. Acker (2005). "Regional brain changes in aging healthy adults: general trends, individual differences and modifiers." Cereb Cortex **15**(11): 1676-1689.

Roos, R. A. (2010). "Huntington's disease: a clinical review." Orphanet J Rare Dis **5**: 40.

Rowland, L. P. and N. A. Shneider (2001). "Amyotrophic lateral sclerosis." N Engl J Med **344**(22): 1688-1700.

Roger Barker and Alan Johnson (2000) Neural cell culture: a practical approach, Nigral and striatal neuronsOxford; New York : IRL Press at Oxford University Press.

Sahin, E. and R. A. Depinho (2010). "Linking functional decline of telomeres, mitochondria and stem cells during ageing." Nature **464**(7288): 520-528.

Schapira, A. H., J. M. Cooper, D. Dexter, J. B. Clark, P. Jenner and C. D. Marsden (1990). "Mitochondrial complex I deficiency in Parkinson's disease." J Neurochem

54(3): 823-827.

Sharma, O. P. (1976). "Antioxidant activity of curcumin and related compounds." Biochem Pharmacol **25**(15): 1811-1812.

Sherer, T. B., R. Betarbet, A. K. Stout, S. Lund, M. Baptista, A. V. Panov, M. R. Cookson and J. T. Greenamyre (2002). "An in vitro model of Parkinson's disease: linking mitochondrial impairment to altered alpha-synuclein metabolism and oxidative damage." J Neurosci **22**(16): 7006-7015.

Shoba, G., D. Joy, T. Joseph, M. Majeed, R. Rajendran and P. S. Srinivas (1998). "Influence of piperine on the pharmacokinetics of curcumin in animals and human volunteers." Planta Med **64**(4): 353-356.

Singh, N. P., M. T. McCoy, R. R. Tice and E. L. Schneider (1988). "A simple technique for quantitation of low levels of DNA damage in individual cells." Exp Cell Res **175**(1): 184-191.

Sonavane, G., K. Tomoda and K. Makino (2008). "Biodistribution of colloidal gold nanoparticles after intravenous administration: effect of particle size." Colloids Surf B Biointerfaces **66**(2): 274-280.

Srimal, R. C. and B. N. Dhawan (1973). "Pharmacology of diferuloyl methane (curcumin), a non-steroidal anti-inflammatory agent." J Pharm Pharmacol **25**(6): 447-452.

Stefanis, L. (2012). "alpha-Synuclein in Parkinson's disease." Cold Spring Harb Perspect Med **2**(2): a009399.

Takeshima, T., K. Shimoda, Y. Sauve and J. W. Commissiong (1994). "Astrocyte-dependent and -independent phases of the development and survival of rat embryonic day 14 mesencephalic, dopaminergic neurons in culture." Neuroscience **60**(3): 809-823.

Tamilselvam, K., N. Braidy, T. Manivasagam, M. M. Essa, N. R. Prasad, S. Karthikeyan, A. J. Thenmozhi, S. Selvaraju and G. J. Guillemin (2013). "Neuroprotective effects of hesperidin, a plant flavanone, on rotenone-induced oxidative stress and apoptosis in a cellular model for Parkinson's disease." Oxid Med Cell Longev **2013**: 102741.

Tamm, E. R. (2002). "Myocilin and glaucoma: facts and ideas." Prog Retin Eye Res **21**(4): 395-428.

Tanner, C. M., F. Kamel, G. W. Ross, J. A. Hoppin, S. M. Goldman, M. Korell, C. Marras, G. S. Bhudhikanok, M. Kasten, A. R. Chade, K. Comyns, M. B. Richards, C. Meng, B. Priestley, H. H. Fernandez, F. Cambi, D. M. Umbach, A. Blair, D. P. Sandler and J. W. Langston (2011). "Rotenone, paraquat, and Parkinson's disease." Environ Health Perspect **119**(6): 866-872.

Tatsunori S., Kazunobu S., Jack M. Parent., Arturo Alvarez-Buylla (2011) Neurogenesis in the Adult Brain II: Clinical Implications. Spinger Tokyo Dordrecht Heidelberg London New York.

Thaloor, D., K. J. Miller, J. Gephart, P. O. Mitchell and G. K. Pavlath (1999). "Systemic administration of the NF-kappaB inhibitor curcumin stimulates muscle regeneration after traumatic injury." Am J Physiol **277**(2 Pt 1): C320-329.

Tiwari, V. K., L. Burger, V. Nikoletopoulou, R. Deogracias, S. Thakurela, C. Wirbelauer, J. Kaut, R. Terranova, L. Hoerner, C. Mielke, F. Boege, R. Murr, A. H. Peters, Y. A. Barde and D. Schubeler (2012). "Target genes of Topoisomerase IIbeta regulate neuronal survival and are defined by their chromatin state." Proc Natl Acad Sci U S A **109**(16): E934-943.

Tolosa, A., X. Zhou, B. Spittau and K. Krieglstein (2013). "Establishment of a survival and toxic cellular model for Parkinson's disease from chicken mesencephalon." Neurotox Res **24**(2): 119-129.
Troen, B. R. (2003). "The biology of aging." Mt Sinai J Med **70**(1): 3-22.

Vajragupta, O., P. Boonchoong, H. Watanabe, M. Tohda, N. Kummasud and Y. Sumanont (2003). "Manganese complexes of curcumin and its derivatives: evaluation for the radical scavenging ability and neuroprotective activity." Free Radic Biol Med **35**(12): 1632-1644.

Varghese, K., M. Das, N. Bhargava, M. Stancescu, P. Molnar, M. S. Kindy and J. J. Hickman (2009). "Regeneration and characterization of adult mouse hippocampal neurons in a defined in vitro system." J Neurosci Methods **177**(1): 51-59.

Wang, J., X. X. Du, H. Jiang and J. X. Xie (2009). "Curcumin attenuates 6-hydroxydopamine-induced cytotoxicity by anti-oxidation and nuclear factor-kappa B modulation in MES23.5 cells." Biochem Pharmacol **78**(2): 178-183.

Wang, L., L. Wang, W. Huang, H. Su, Y. Xue, Z. Su, B. Liao, H. Wang, X. Bao, D. Qin, J. He, W. Wu, K. F. So, G. Pan and D. Pei (2013). "Generation of integration-free neural progenitor cells from cells in human urine." Nat Methods **10**(1): 84-89.

Wang, M. S., S. Boddapati, S. Emadi and M. R. Sierks (2010). "Curcumin reduces alpha-synuclein induced cytotoxicity in Parkinson's disease cell model." BMC Neurosci **11**: 57.

Warner, T. T. and A. H. Schapira (2003). "Genetic and environmental factors in the cause of Parkinson's disease." Ann Neurol **53 Suppl 3**: S16-23; discussion S23-15.

Wisse. E., A.M. De Leeuw., Structural elements determining transport and exchange process in the liver, in: S.S. Davis, L. Illum, J.G. McVie, E. Tomlinson (Eds.), Microspheres and drug therapy, pharmaceutical, immunological and medical aspects, Elsevier, Amsterdam, 1984, pp. 1-23.

Xu, Y., B. Ku, L. Cui, X. Li, P. A. Barish, T. C. Foster and W. O. Ogle (2007). "Curcumin reverses impaired hippocampal neurogenesis and increases serotonin receptor 1A mRNA and brain-derived neurotrophic factor expression in chronically stressed rats." Brain Res **1162**: 9-18.

Yamamoto, M., T. Suhara, Y. Okubo, T. Ichimiya, Y. Sudo, M. Inoue, A. Takano, F. Yasuno, K. Yoshikawa and S. Tanada (2002). "Age-related decline of serotonin transporters in living human brain of healthy males." Life Sci **71**(7): 751-757.

Yang, F., G. P. Lim, A. N. Begum, O. J. Ubeda, M. R. Simmons, S. S. Ambegaokar, P. P. Chen, R. Kayed, C. G. Glabe, S. A. Frautschy and G. M. Cole (2005). "Curcumin inhibits formation of amyloid beta oligomers and fibrils, binds plaques, and reduces amyloid in vivo." J Biol Chem **280**(7): 5892-5901.

Yang, X., W. Li, E. D. Prescott, S. J. Burden and J. C. Wang (2000). "DNA topoisomerase IIbeta and neural development." Science **287**(5450): 131-134.

Zbarsky, V., K. P. Datla, S. Parkar, D. K. Rai, O. I. Aruoma and D. T. Dexter (2005). "Neuroprotective properties of the natural phenolic antioxidants curcumin and naringenin but not quercetin and fisetin in a 6-OHDA model of Parkinson's disease." Free Radic Res **39**(10): 1119-1125.

Zhang, G., J. Li, S. Purkayastha, Y. Tang, H. Zhang, Y. Yin, B. Li, G. Liu and D. Cai (2013). "Hypothalamic programming of systemic ageing involving IKK-beta, NF-

kappaB and GnRH." Nature **497**(7448): 211-216.

Zhang, J., G. Perry, M. A. Smith, D. Robertson, S. J. Olson, D. G. Graham and T. J. Montine (1999). "Parkinson's disease is associated with oxidative damage to cytoplasmic DNA and RNA in substantia nigra neurons." Am J Pathol **154**(5): 1423-1429.

Zhang, Y., F. Calon, C. Zhu, R. J. Boado and W. M. Pardridge (2003). "Intravenous nonviral gene therapy causes normalization of striatal tyrosine hydroxylase and reversal of motor impairment in experimental parkinsonism." Hum Gene Ther **14**(1): 1-12.

Zhu, Y. G., X. C. Chen, Z. Z. Chen, Y. Q. Zeng, G. B. Shi, Y. H. Su and X. Peng (2004). "Curcumin protects mitochondria from oxidative damage and attenuates apoptosis in cortical neurons." Acta Pharmacol Sin **25**(12): 1606-1612.

Publications from thesis

1. **Bollimpelli VS,** Kondapi AK (2015). "Enriched rat primary ventral Mesencephalic neurons as an in-vitro culture model." Neuroreport **26**(12): 728-34.
2. **Bollimpelli VS,** Kondapi AK. "Differential effects of rotenone on immature and mature ventral mesencephalic neurons in vitro." (Communicated).
3. **Bollimpelli VS,** Prashanth, Sonali D, Kondapi AK. "Neuroprotective effect of curcumin-loaded nanoparticles against rotenone induced neurotoxicity." (Communicated).

Enriched rat primary ventral mesencephalic neurons as an in-vitro culture model

Venkata S. Bollimpelli and Anand K. Kondapi

Primary ventral mesencephalic (VM) neuronal cultures are gaining importance in the study of molecular mechanisms leading to Parkinson's disease and development of treatment strategies. In practice, these neurons are cocultured with glial cells, making assessment of neuronal specific proteomic and genomic analyses difficult. Hence, development of VM neuron-enriched culture is indispensable for such analyses. In the current study, VM neurons with less than 5% of glial cells in culture were found to survive for 9 days *in vitro* (DIV), followed by a sudden death phase resulting in less than 5% of neuronal viability. Analysis of expression of precursor and mature neuronal markers, Nestin and MAP-2, respectively, has shown that these VM neurons attain maturity at the 7th DIV both in the presence and in the absence of glial cells. This VM neuron-enriched culture was shown to be rich in dopaminergic neurons from 7th DIV and survived up to 10th DIV. Reactive oxygen species and DNA damage estimated using CMH2CDFDA dye and comet assay, respectively, showed an increase in their respective levels at 9th DIV. Furthermore, expression of topoisomerase II β, a key player in neuronal development, was found to increase until 9th DIV, followed by a sudden decrease on 10th DIV. In conclusion, the above results provide a good working model of VM neurons *in vitro* along with 7th DIV as an ideal time period to study and evaluate the pro/antisurvival effects of various compounds on VM neurons. *NeuroReport* 26:728–734

NeuroReport 2015, **26**:728–734

Keywords: DNA damage, maturation, neuronal death, reactive oxygen species, topoisomerase II β, viability

Department of Biotechnology and Bioinformatics, School of Life Sciences, University of Hyderabad, Hyderabad, India

Correspondence to Anand K. Kondapi, PhD, Department of Biotechnology and Bioinformatics, University of Hyderabad, Hyderabad 500046 India
Tel: +91 40 23134571/+91 40 23000654; fax: +91 40 23010145;
e-mails: akksl@uohyd.ernet.in, akondapi@gmail.com

Received 28 May 2015 **accepted** 15 June 2015

Introduction

The hallmark feature of Parkinson's disease (PD) is the selective loss of neurons in the substantia nigra pars compacta (SNpc) region of the brain [1]. Primary neuronal culture is an in-vitro approach that is used in an attempt to reduce the inherent complexity of the brain and is being used widely as an in-vitro model [2,3]. Various culture models of ventral mesencephalic (VM) neurons reported earlier involve either the use of feeder cells or mixed cultures [4,5]. However, detailed analysis of VM neuron-enriched culture is not available. Hence, this paper presents an in-vitro evaluation of maturation of VM neuron-enriched culture. This information will be very useful in understanding VM neuron-specific molecular signaling processes that occur during differentiation, network formation, and eventually development. In case of cerebellar granule neurons, glial cell contamination was circumvented by supplementing growth media with a mitotic inhibitor that eliminates non-neuronal mitotic cells [3,6,7]. In the current study, we have used a mitotic inhibitor to obtain VM neuron-enriched culture to gain insights into VM neuron-specific cellular mechanisms.

Nestin is a neurofilament protein expressed in progenitor cells [8–10] and the lack of its immune reactivity *in vitro* was used to classify the culture as mature cells [11], whereas MAP-2 is widely accepted as a mature neuronal marker [12–14]. We used these markers to classify mature and precursor stages of in-vitro VM neuronal culture.

Markers of oxidative stress and DNA damage were reported in the VMc brain region of PD patients [15,16]. In addition, reactive oxygen species (ROS) was also implicated in neuronal death [17]. Considering this importance of ROS and DNA damage, we have studied their levels in in-vitro VM neuronal culture. As topoisomerase II β plays an important role in DNA repair, neuronal development, differentiation, and longevity [5, 7,18–20], expression of topoisomerase II β was monitored during the VM neuronal culture *in vitro*.

The aim of this study is to characterize and investigate the utility of VM neuron-enriched culture to study VM neuron-specific cellular mechanisms implicated in neurodegeneration and eventually PD etiology.

Experimental procedures

Animals

Wistar rats were obtained from the National Institute of Nutrition, Hyderabad, India, and maintained at the animal house facility according to the norms of Institutional animal ethical committee (IAEC), University of Hyderabad (Proposal number LS/IAEC/AKK/10/1).

DOI: 10.1097/WNR.0000000000000420

Primary antibodies

Mouse anti-rat MAP-2 monoclonal antibody [immunofluorescence (IF) 1 : 500] (ab11267) and rabbit anti-rat Nestin polyclonal antibody (IF 1 : 200) (ab27952) were obtained from Abcam (Cambridge, Massachusetts, USA); mouse anti-topoisomerase IIβ monoclonal antibody (IF 1 : 1000, WB 1 : 1000) (611493) was from Becton Dickinson Biosciences (Franklin Lakes, New Jersey, USA). Rabbit anti-rat tyrosine hydroxylase polyclonal antibody (IF 1 : 1000, WB 1 : 1000) (OPA1-04050) was from Thermo Scientific (Rockford, Illinois, USA).

Secondary antibodies

Goat anti-rabbit HRP-conjugated antibody (1 : 5000) (ab6721) and goat anti-mouse HRP-conjugated antibody (1 : 5000) (ab97023) were obtained from Abcam; Alexa Fluor 594 goat anti-rabbit antibody (A11037), Alexa Fluor 488, and goat anti-mouse antibody (A11029) were from Invitrogen (Grand Island, New York, USA). Alexa fluor antibodies were used at 1 : 200 dilutions.

Isolation and culture of neurons

Isolation of VM neurons was carried out according to the method described by Barker and Johnson [21]. VM tissues from embryonic (E14) rat were collected in Hanks Balanced Salt Solution (HBSS) (Gibco, Grand Island, New York, USA) at 4°C and incubated in 2 ml of 2.5 mg/ml trypsin solution (Gibco) for 15 min at 37°C. The trypsinized tissue was resuspended in 2 ml DNAse (10 μg/ml) and centrifuged at 1200 g for 4 min. The supernatant was triturated with 0.1–0.2 ml triturating solution (1 mg/ml BSA, 10 μg/ml DNAse 1, and 0.5 mg/ml soybean trypsin inhibitor in HBSS) per piece of VM tissue to obtain a suspension of single cells. VM neurons were seeded at 1×10^6 cells in 1 ml of Dulbecco's Minimum Essential Media (DMEM-F12) with 10% fetal bovine serum, 1× glutamax (35050) (2 mM L-glutamine), and 1× pen strep (15070-063) (50 units/ml pencillin, 50 μg/ml streptomycin) (Gibco) per well in a 12-well plate coated with 0.1 mg/ml poly-D-lysine (Sigma Chemical Co., St Louis, Missouri, USA). Cultures were incubated in a humidified atmosphere of 5% CO_2 at 37°C. Cultures from 2nd day *in vitro* (DIV) were supplemented with 2 μM of mitotic inhibitor arabinosylcytosine (Ara C) (Sigma Chemical Co.).

Cell viability assay

Cell viability was measured on the basis of the principle of reduction of MTT (3-(4,5-dimethylthiazol-2-yl)-2,5-diphenyltetrazolium bromide) (Sigma Chemical Co.) to purple formazan crystals, a chromogenic product of the mitochondrial dehydrogenases of viable cells [22]. Briefly, MTT at a concentration of 5 mg/ml was added to each well of 96-well plates. Each well contained 0.1×10^6 cells and were incubated in 200 μl of media for 4 h at 37°C in a 5% humidified CO_2 atmosphere. These plates were centrifuged at 1500 rpm for 20 min and the medium was aspirated. Formazan crystals were dissolved in DMSO and absorbance was measured at 570 nm using a Tecan multiplate reader-INFINITE 200 (Tecan, Mannedorf, Switzerland) with DMSO as a blank.

Immunofluorescence

Adherent VM cultures grown on poly-D-lysine-coated cover slips were washed with PBS containing 4% sucrose (PBS + sucrose). The cultures were fixed with 4% paraformaldehyde and permeabilized with 0.05% Triton X-100. These were washed thrice with PBS + sucrose and blocked with 5% fetal bovine serum in PBS + sucrose for 1 h at 37°C. The fixed cultures were incubated overnight with the primary antibody at specified dilutions mentioned above at 4°C. The following day, cells were washed thrice with PBS + sucrose and the secondary antibody at specified dilutions was added with a nuclear dye, DAPI (1 μg/ml) (Sigma Chemical Co.), and incubated for 1 h at 37°C. These cover slips were washed thrice and mounted onto glass slides with 50% glycerol and were imaged with a confocal microscope.

Alkaline comet assay

The assay was performed as described earlier [23]. Ice-cold PBS (500 μl) with 0.1 million cells was added to 1.5 ml of 0.75% low-melting agarose (BRL Inc., Gaithersburg, Maryland, USA). The agarose–cell suspension was gently layered on a 0.75% agarose-precoated frosted-glass microscopic slide. After solidification of gel on ice, it was transferred to ice-cold lysis buffer [2.5 M NaCl, 100 mM EDTA, 10 mMTris (pH 10.0), and 1% Triton X-100] and incubated for 2 h at 4 °C. Then, they were equilibrated for 1 h in electrophoresis buffer (300 mM NaOH and 1 mM EDTA, pH 13), followed by electrophoresis (1 h, 1 V/cm). After neutralization of these slides with 0.4 M Tris, pH 7.5, they were placed in 100% ethanol for 5 min and then air-dried. The DNA was then stained with 20 μg/ml of ethidium bromide (Sigma Chemical Co.) for 20 min and slides were washed twice for 5 min in TBE. To ensure random sampling, 50 images/slide were captured using a confocal microscope (Leica, Buffalo Grove, Illinois, USA). Comet parameter such as tail length describing migrated DNA, which in turn is proportional to DNA damage, was scored using CometScoreTM Freeware v1.5 (TriTek Corporation, Sumerduck, Virginia, USA).

Detection of intracellular ROS accumulation

Intracellular ROS accumulation was monitored by incubating cells with 7 μM CM-H2DCFDA (Invitrogen) for 20 min. Cells were rinsed twice with HEPES buffer and fluorescence was measured using a Tecan multiplate reader INFINITE 200 (Tecan) at excitation and emission wavelengths of 485 and 535 nm, respectively. The final values were normalized for intracellular protein in each well and expressed in terms of fluorescence/μg protein.

Statistics

Experiments were conducted in triplicate and repeated independently for three times. Data were averaged and presented as mean ± SD. Statistical comparisons were made using Student's unpaired *t*-test.

Results

To obtain VM neuron-enriched culture, growth medium of VM neurons was supplemented with mitotic inhibitor AraC on 2nd DIV. Similar to the observations made by Takeshima *et al.* [24], in the presence of 2 μM AraC, VM neuronal culture was maintained with a minimal presence of glial cells (< 5%) until 9th DIV, which followed a catastrophic phase where most of the neurons died with truncated neurites and rounded soma, resulting in viability of less than 5% of neurons.

Viability and morphological features of VM neurons in the absence of glial cells in in-vitro culture

The viability of these VM neurons over this period of 9 days in culture was measured using an MTT assay. The cells on 3rd DIV was taken as the starting point and considered to be 100% viable. Figure 1a shows the survival of VM neurons *in vitro*, which showed a gradual decrease in viability, reaching 45% by 9th DIV ($P < 0.0005$). Figure 1b shows the adherence of cells with small soma bearing no neuritic outgrowths on 2nd DIV and a visible neuritic outgrowth by 3rd DIV, which developed into an extensive network by 7th DIV, reaching its magnitude on 9th DIV and became truncated by 10th DIV, showing a beaded dendritic appearance.

Maturation of VM neurons in the presence and absence of glial cells in culture

As shown in Fig. 2a, after 6th DIV, MAP-2 expression was predominant in most of the neuronal population, whereas the Nestin expression was detected along with MAP-2 only until 6th DIV. These observations suggest that VM neuron-enriched culture *in vitro* consists of neuronal precursor cells until 6th DIV and attains maturity by 7th DIV. Surprisingly, the maturation pattern of these neurons was similar, both in the presence (absence of AraC in culture medium) and in the absence of glial cells. These observations suggest that the presence of glial cells in neuronal culture might be important in later stages of maturation rather than at initial stages. Thus, 7th DIV of VM neuronal culture can be considered a stage of maturity both in the presence and in the absence of glial cells.

Dopaminergic neurons and topoisomerase II β in VM neuron-enriched culture *in vitro*

Tyrosine hydroxylase (TH) expression was observed to assess dopaminergic (DA) neurons in the culture. The results in Fig. 2b show that DA neurons were present from 3rd DIV to 10th DIV; the maximum expression of

Fig. 1

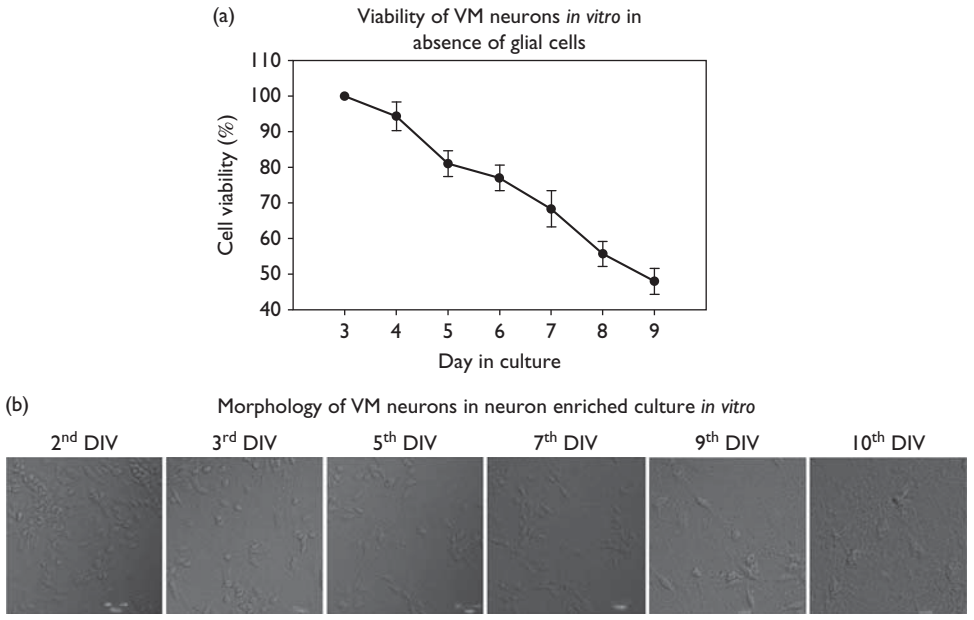

Cell viability and morphological features of VM neurons in the absence of glial cells *in vitro*. (a) Cells on 3rd DIV were taken as the starting point for the MTT viability assay and were considered to be 100% viable. The line graph in the figure shows a gradual decrease in cell viability until 9th DIV. (b) Cells on 2nd DIV had small soma and short neurites and these cell bodies became larger and more defined, whereas neurites became elongated from 3rd DIV to 9th DIV. Once they attained maturity, that is, from 7th DIV to 9th DIV, the network became more complex, with a bundled appearance. At 10th DIV, neuritic dendrites became truncated with rounded soma. DIV, day of culture *in vitro*; VM, ventral mesencephalic.

Fig. 2

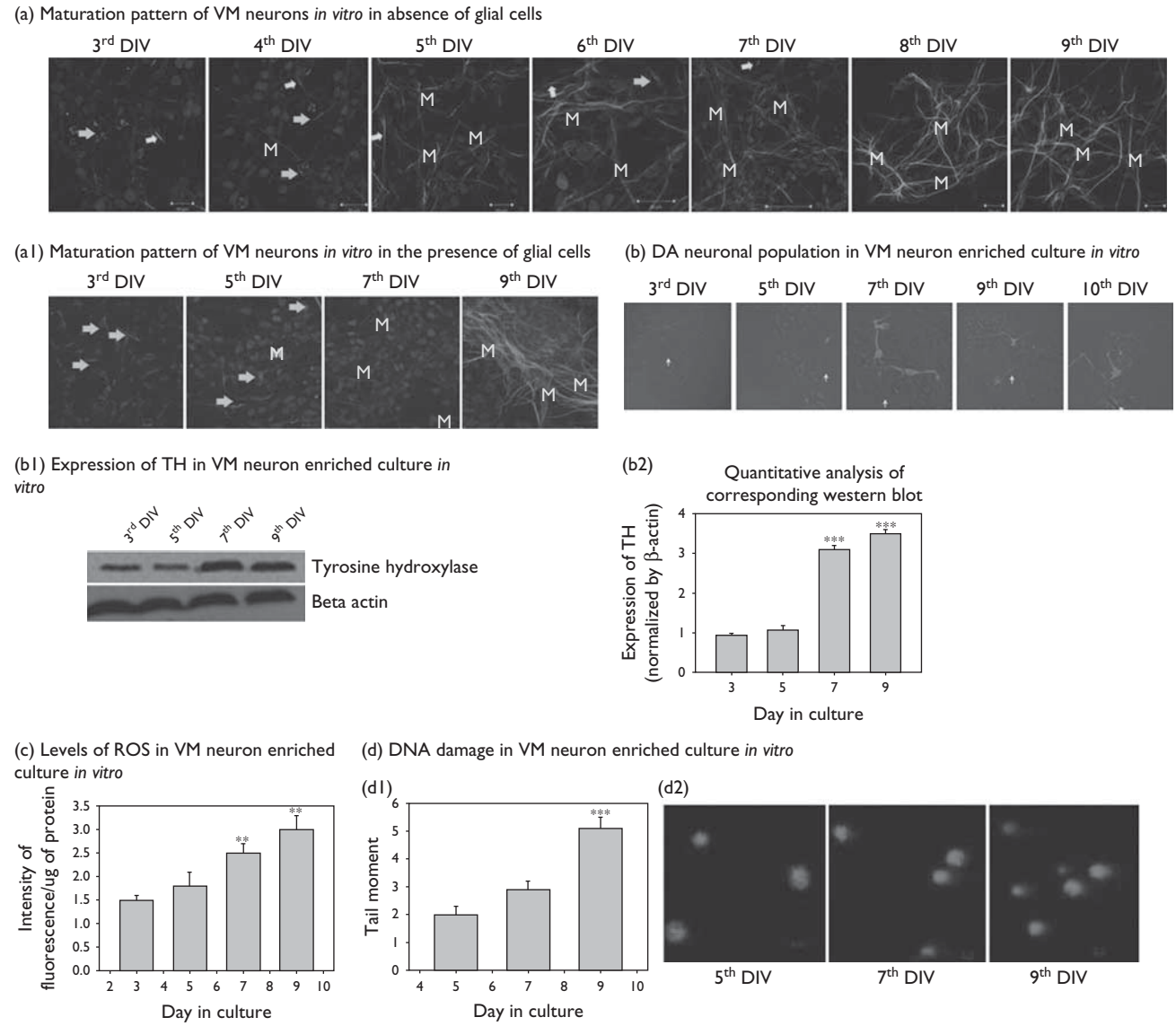

(a, a1) Maturation pattern of VM neurons in the presence and absence of glial cells *in vitro*. VM neurons, both in the presence and in the absence of glial cells, showed expression of the immature neuronal marker Nestin (stained by alexafluor 594, shown in arrow marks) on 3rd DIV, which was slightly increased by 5th DIV and completely disappeared on 7th DIV. Expression of mature neuronal marker MAP-2 (stained by alexafluor 488, shown by letter "M") was also observed on 3rd DIV, which increased till 9th DIV. Here, the nucleus was stained by DAPI. (b) DA neurons in VM neuron-enriched culture *in vitro*. (b) DA neurons stained with TH (marker for DA neurons) antibody were very few in numbers during the initial days of culture and reached maximum in number by 7th DIV and continued to 10th DIV. Most of the neurons that survived on 10th DIV were DA neurons and had a beaded appearance of dendrites. (b1) Expression of TH protein during the course of culture was estimated using western blot analysis. A significant increase in TH expression was observed from 7th DIV and continued to 10th DIV. Beta actin was taken as a loading control. (b2) Densitometric analysis of bands representing the expression of TH, obtained through western blot analysis, showed an increase from 7th DIV. Averages and SDs from three experiments are shown. Statistical significance was estimated using an unpaired *t*-test: ***$P < 0.0005$. (c) ROS levels in VM neuron-enriched culture *in vitro* (c) Levels of ROS in in-vitro VM neurons showed a gradual increase during the culture period. There was a marked increase on 7th DIV and 9th DIV. Averages and SDs from three experiments are shown. Statistical significance was estimated using an unpaired *t*-test: **$P < 0.005$. (d) DNA damage in VM neuron-enriched culture *in vitro*. (d1) The degree of DNA damage was assessed by measurement of the extent of tail movement, which is the product of tail length and fraction of DNA in the comet tail as presented in the bar graph. This shows an increase in DNA damage levels on 9th DIV of VM neuronal culture. Averages and SDs from three experiments are shown. Statistical significance was estimated using an unpaired *t*-test: ***$P < 0.0005$. (d2) Comet tail movement is a measure of DNA damage. There was no comet tail movement on 5th DIV, whereas on 7th DIV, there was a visible tail movement that became further elongated on 9th DIV, suggesting DNA damage on 9th DIV in VM neuron-enriched culture *in vitro*. DA, dopaminergic; DIV, day of culture *in vitro*; ROS, reactive oxygen species; TH, tyrosine hydroxylase; VM, ventral mesencephalic.

TH was present from 7th DIV to 10th DIV ($P < 0.0005$). An interesting feature noted here was that only DA neurons survived until 10th DIV. These observations were corroborated by western blot analysis of TH protein in VM neuron-enriched culture (Fig. 2b1). As the number of neurons was significantly low on 10th DIV, expression levels of TH could not be analyzed using western blot analysis. These observations establish that 7th DIV is a suitable time period to study DA neurons in VM neuron-enriched culture.

ROS and DNA damage in VM neuron-enriched culture *in vitro*

The representative bar graphs in Fig. 2c and d1 show an increase in ROS levels (using CM-H_2DCFDA dye) and DNA damage (estimated by an alkaline comet assay), respectively, during the period of culture of VM neurons *in vitro*. Results of the representative comet tail lengths analyzed by fluorescent microscopy showed a slight DNA damage at 7th DIV, which increased significantly by 9th DIV ($P < 0.0005$) (Fig. 2d2). The plausible cause for this increase in DNA damage could be the presence of increased ROS levels. These results together shows the presence of low level of ROS and DNA damage at 7th DIV, which should be considered while evaluating any compound for oxidative stress and DNA damage.

Topoisomerase II β in VM neuron-enriched culture *in vitro*

There was an increase in the expression of topoisomerase II β until 9th DIV as shown through confocal microscopy and western blot analysis (Fig. 3a and b), corroborating its key role in neuronal protection during development. Moreover, the sudden decrease in the expression of topoisomerase II β on 10th DIV (Fig. 3a) raises curiosity over the role of this protein in the sudden death of neurons.

Discussion

We have characterized VM neuron-enriched culture in terms of maturation, oxidative stress, and DNA damage to establish them as an in-vitro culture model. Neuronal progenitor cells differentiate into specific cellular lineages such as neurons, glial cells, etc. This differentiation process involves activation/expression of various intracellular and extracellular factors. Each neuronal type has distinct characteristics and is associated with a specific function in the brain. As maturation is a process of progenitor cells differentiating into post mitotic neurons, study of these events would shed light on neuron-specific developmental mechanisms.

In the present study, we observed a complete absence of the expression of precursor cell marker nestin and the concomitant expression of mature neuronal marker MAP-2 by 7th DIV of VM neuronal culture both in the presence and in the absence of glial cells. This indicates that VM neurons attain maturity at 7th DIV both in the presence and in the absence of glial cells and thus suggests the role of glial cells at later stages of neuronal maturation. Although TH expression was evident from 3rd DIV, there was a marked increase in its expression from 7th DIV, indicating the presence of a higher number of DA neurons. Thus, 7th DIV is a suitable time period to gain insights into cellular mechanisms, particularly of DA neurons in VM neuron-enriched culture. These VM neurons in the absence of glial cells were viable for 9 days, followed by a sudden death of neurons, corroborating an earlier report of Takeshima *et al.* [24].

The results of the present study showed a marginal increase in ROS and DNA damage during this time period, which peaked at the 9th DIV. At physiological levels, ROS serve as signaling species and only an excessive amount of these molecules leads to oxidative stress [25]. The present study indicates an increase in ROS levels, which in turn might have led to increased DNA damage assessed by an alkaline comet assay on 9th DIV. ROS levels can initially be considered to be at near-basal levels as there was no significant DNA damage until 9th DIV. It was observed through the alkaline comet assay that there was no significant DNA damage on 7th DIV and so this period of culture can be used to evaluate the effect of ROS and DNA-damaging agents on VM neurons, which have gained prominence recently.

Aging is associated with increased oxidative stress and its influence on neurodegeneration and unscheduled cell cycle re entry was also reported [26]. Hence, the present study hypothesizes that ROS and DNA damage at 9th DIV of VM neuron-enriched culture might be one of the factors leading to neuronal death.

Topoisomerase II β was reported to be highly expressed when neuronal cells become postmitotic from the progenitor phase [19]. Western blot analysis and IF observations showed an increase in topoisomerase II β expression on 7th DIV to 9th DIV, suggesting the entry of VM neurons into the postmitotic phase from the progenitor phase. A decreased expression of topoisomerase II β on 10th DIV from a much more concentrated pattern on 9th DIV suggests a crucial role of topoisomerase II β in the catastrophe after 9th DIV. This is strengthened by a recent report, where topoisomerase II β deficiency led to premature death of postmitotic neurons because of its impaired regulation in the transcriptional process [19].

Conclusion

These 9 days of neuronal culture can offer a good platform to study the molecular mechanisms associated with VM neurons. Near-basal levels of ROS, DNA damage, and abundance of DA neurons on 7th DIV make it an ideal time period to understand epigenetics and signaling modifications that occur in these neurons. Further, they

Fig. 3

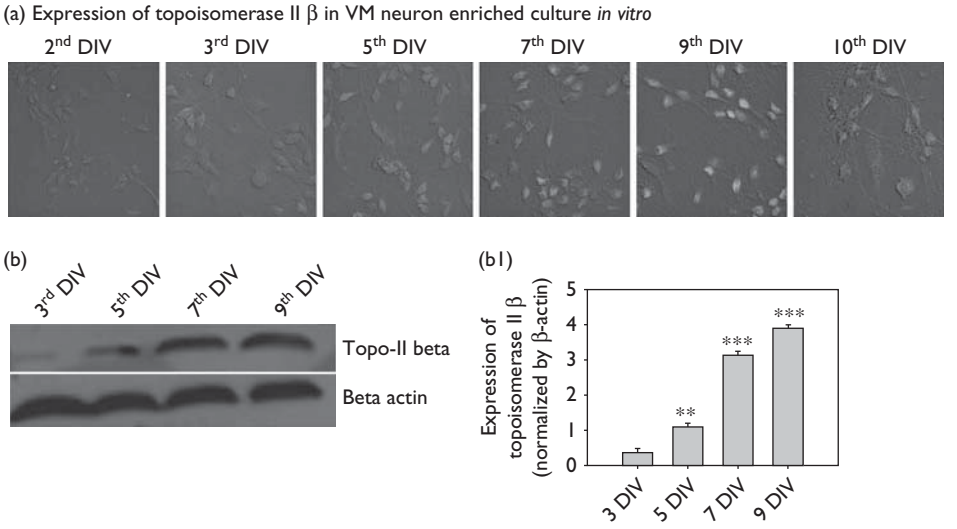

Expression of topoisomerase II β in VM neuron-enriched culture *in vitro*. (a) Topoisomerase II β showed a sparse expression during the initial days of culture and its expression increased gradually by 9th DIV. Tenth DIV culture showed a decrease in its expression concomitant with cellular death. (b) Expression of topoisomerase II β was estimated using western blot analysis. Its expression increased gradually till 9th DIV. (b1) Densitometric analysis of bands representing the expression of topoisomerase II β, obtained through western blot analysis, showed a significant increase from 5th DIV. Averages and SDs from three experiments are shown. Statistical significance was estimated using an unpaired *t*-test: $^{**}P < 0.005$; $^{***}P < 0.0005$. DIV, day of culture *in vitro*; VM, ventral mesencephalic.

can serve as a development and aging model *in vitro*. Also, this model can be used to evaluate prosurvival and antisurvival activities of various bioactive molecules on VM neurons.

This study documents the suitability and utility of a VM neuron-enriched culture system as it can be used for proteomic and genomic analysis to gain deeper insights into VM neuronal-specific neurodegenerative mechanisms. This model can also be used for developmental studies of VM neurons as the immature neuronal precursor stage and the mature post mitotic phase were clearly established.

Acknowledgements

The authors thank the council for scientific and industrial research, Government of India, for providing a doctoral fellowship to B.V.S. This work was carried out under a Department of Biotechnology-funded project and UGC FRPS BSR one-time grant to A.K.K.

Author contributions: A.K.K. conceived the project plan. B.V.S. planned and conducted the experiments. A.K.K. and B.V.S. wrote the manuscript.

This research work was supported by the Department of Biotechnology (DBT), Government of India, under R&D project under Medical Biotechnology Taskforce (Sanction No. BT/PR14285/Med/30/456/10). The sponsors did not play any role in the study, design, collection, and interpretation of data.

Conflicts of interest

There are no conflicts of interest.

References

1 Lang AE, Lozano AM. Parkinson's disease. *N Engl J Med* 1998; **339**:1130–1143.
2 Aksenova MV, Aksenov MY, Mactutus CF, Booze RM. Cell culture models of oxidative stress and injury in the central nervous system. *Curr Neurovasc Res* 2005; **2**:73–89.
3 Bhanu MU, Mandraju RK, Bhaskar C, Kondapi AK. Cultured cerebellar granule neurons as an in vitro aging model: topoisomerase IIβ as an additional biomarker in DNA repair and aging. *Toxicol In Vitro* 2010; **24**:1935–1945.
4 Ahmadi FA, Linseman DA, Grammatopoulos TN, Jones SM, Bouchard RJ, Freed CR, *et al*. The pesticide rotenone induces caspase-3-mediated apoptosis in ventral mesencephalic dopaminergic neurons. *J Neurochem* 2003; **87**:914–921.
5 Tolosa A, Zhou X, Spittau B, Krieglstein K. Establishment of a survival and toxic cellular model for Parkinson's disease from chicken mesencephalon. *Neurotox Res* 2013; **24**:119–129.
6 Bilimoria PM, Bonni A. Cultures of cerebellar granule neurons. *CSH Protoc* 2008; **13**:5107.
7 Gupta KP, Swain U, Rao KS, Kondapi AK. Topoisomerase II β regulates base excision repair capacity of neurons. *Mech Ageing Dev* 2012; **133**:203–213.
8 Paek SH, Shin HY, Kim JW, Park SH, Son JH, Kim DG. Primary culture of central neurocytoma: a case report. *J Korean Med Sci* 2010; **25**:798–803.
9 Palm K, Salin-Nordström T, Levesque MF, Neuman T. Fetal and adult human CNS stem cells have similar molecular characteristics and developmental potential. *Brain Res Mol Brain Res* 2000; **78**:192–195.
10 Varghese K, Das M, Bhargava N, Stancescu M, Molnar P, Kindy MS, Hickman JJ. Regeneration and characterization of adult mouse hippocampal neurons in a defined in vitro system. *J Neurosci Methods* 2009; **177**:51–59.
11 Bertrand SJ, Aksenova MV, Aksenov MY, Mactutus CF, Booze RM. Endogenous amyloidogenesis in long-term rat hippocampal cell cultures. *BMC Neurosci* 2011; **12**:38.
12 Cossette M, Lévesque D, Parent A. Neurochemical characterization of dopaminergic neurons in human striatum. *Parkinsonism Relat Disord* 2005; **11**:277–286.

13 Cavallaro M, Mariani J, Lancini C, Latorre E, Caccia R, Gullo F, *et al.* Impaired generation of mature neurons by neural stem cells from hypomorphic Sox2 mutants. *Development* 2008; **135**:541–557.
14 Wang L, Wang L, Huang W, Su H, Xue Y, Su Z, *et al.* Generation of integration-free neural progenitor cells from cells in human urine. *Nat Methods* 2013; **10**:84–89.
15 Jenner P, Olanow CW. Oxidative stress and the pathogenesis of Parkinson's disease. *Neurology* 1996; **47** (Suppl 3):S161–S170.
16 Zhang J, Perry G, Smith MA, Robertson D, Olson SJ, Graham DG, Montine TJ. Parkinson's disease is associated with oxidative damage to cytoplasmic DNA and RNA in substantia nigra neurons. *Am J Pathol* 1999; **154**:1423–1429.
17 Leonardi ET, Mytilineou C. Cell culture models of neuronal degeneration and neuroprotection. Implications for Parkinson's disease. *Adv Exp Med Biol* 1998; **446**:203–222.
18 Yang X, Li W, Prescott ED, Burden SJ, Wang JC. DNA topoisomerase II beta and neural development. *Science* 2000; **287**:131–134.
19 Tiwari VK, Burger L, Nikoletopoulou V, Deogracias R, Thakurela S, Wirbelauer C, *et al.* Target genes of topoisomerase IIβ regulate neuronal survival and are defined by their chromatin state. *Proc Natl Acad Sci USA* 2012; **109**:E934–E943.
20 Mandraju RK, Chekuri A, Bhaskar C, Duning K, Kremerskothen J, Kondapi AK. Topoisomerase II β associates with Ku70 and PARP-1 during double strand break repair of DNA in neurons. *Arch Biochem Biophys* 2011; **516**:128–137.
21 Barker R, Johnson A. *Neural cell culture: a practical approach, Nigral and striatal neurons.* New York: IRL Press at Oxford University Press; 1995.
22 Mosmann T. Rapid colorimetric assay for cellular growth and survival: application to proliferation and cytotoxicity assays. *J Immunol Methods* 1983; **65**:55–63.
23 Singh NP, McCoy MT, Tice RR, Schneider EL. A simple technique for quantitation of low levels of DNA damage in individual cells. *Exp Cell Res* 1988; **175**:184–191.
24 Takeshima T, Shimoda K, Sauve Y, Commissiong JW. Astrocyte-dependent and -independent phases of the development and survival of rat embryonic day 14 mesencephalic, dopaminergic neurons in culture. *Neuroscience* 1994; **60**:809–823.
25 D'Autréaux B, Toledano MB. ROS as signalling molecules: mechanisms that generate specificity in ROS homeostasis. *Nat Rev Mol Cell Biol* 2007; **8**:813–824.
26 Klein JA, Ackerman SL. Oxidative stress, cell cycle, and neurodegeneration. *J Clin Invest* 2003; **111**:785–793.